

**Development of Multiple Probe Microdialysis Sampling Techniques
for Site-Specific Monitoring in the Stomach**

by

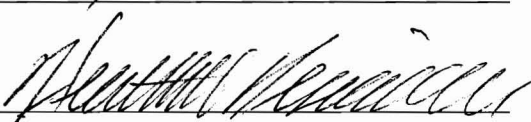
Kristin Lindsey Woo
B.S., Rockhurst University,
Kansas City, MO, 2002

Submitted to the Department of Chemistry and the Faculty of the
Graduate School of the University of Kansas in partial fulfillment of
the requirements for the degree of Doctor of Philosophy



(Committee Chair)









(Committee Members)

Date defended: 12/11/2007

The Dissertation Committee for Kristin Lindsey Woo certifies
that this is the approved version of the following dissertation:

**Development of Multiple Probe Microdialysis Sampling Techniques
for Site-Specific Monitoring in the Stomach**

(Committee Chair)

(Committee Members)

Date approved: _____

ABSTRACT

Kristin Lindsey Woo, Ph.D.
R.N. Adams Institute for Bioanalytical Chemistry
Department of Chemistry, December 2007
University of Kansas

Microdialysis sampling is a technique used extensively to monitor analytes within numerous tissues. Although the capability of implanting multiple probes into a single animal exists, typical experiments are performed using a single probe. When sampling from heterogeneous tissues (*e.g.* the stomach), differences between each tissue layer cannot be determined by sampling from one probe. Microdialysis probes implanted into each layer would better represent sampling in the stomach.

The focus of this research was to develop multiple probe microdialysis sampling techniques to simultaneously sample different tissue layers of the stomach. Furthermore, to augment the application of this approach, multiple probe microdialysis sampling was developed to compare different tissue types (*i.e.* diseased and healthy tissue in the same stomach).

Initially, methods of probe implantation simultaneously in the lumen, mucosa, submucosa and the blood of a rat were developed. Histology confirmed that microdialysis probes were successfully implanted in both the mucosa and submucosa. Alternatively, to compare normal and ulcerated tissue, methods of multiple probe microdialysis sampling in the lumen, submucosa of ulcerated and normal tissue and in blood were developed. Methods of gastric ulcer induction were optimized and

probes were successfully implanted into the ulcerated and normal tissue, with probe location confirmed through histology.

To determine the significance of a multiple probe approach, this method was used to monitor drug absorption in both normal and ulcerated stomachs. Concentration-time curves and pharmacokinetics analyses were performed to determine differences in drug concentrations from each probe location. Results from dosed test compounds were determined to be comparable with predicted absorption rates. Differences in drug concentration were observed between the mucosa and submucosa and increased concentrations were determined in ulcerated relative to normal tissue.

Overall, the research presented illustrates that microdialysis probes can be successfully implanted in different stomach tissue layers simultaneously and that this approach can be used to monitor different tissue layers in the stomach as well as directly compare ulcerated and normal tissue. A multiple probe approach serves as improvements to current uses of microdialysis sampling in the stomach as well as traditional sampling methods to measure drug absorption in the GI tract.

DEDICATION

For two very special and extraordinary ladies in my life that I love and miss everyday

Connie J. Woo
My Mother
(1947 – 2003)

and

Anita F. Woo
My Grandmother
(1914 – 2003)

ACKNOWLEDGEMENTS

I would initially like to thank my graduate advisor, Craig Lunte. I have been extremely fortunate to be mentored by you. I am truly appreciative of every opportunity to allow me to grow as a scientist. I am grateful for your support, guidance and that little nudge to stay in graduate school when I thought I needed some time off. I would not be where I am today without that nudge. Of course, I need to say one last thing, “Go Cubs!”

To the past and present members of the Lunte Lab, I have been grateful to work with you. Kim, Stacy and Eric, thank you so much for “babysitting” Danie and for your help starting out in the lab. Kristin, Sara and Swetha, I really enjoyed getting to know you. Thank you for all of the chats, your friendship and the encouraging words when probes were not in correct locations or when ulcers broke. Sarah, I am happy we became friends during my internship. Thank you for allowing me to have that valuable experience. Gill and Blánaid, I thank you both for your advice and encouragement during every step of the dissertation writing process. More importantly, I am happy to have two fabulous transatlantic friends!

I would like to thank the University of Kansas, Department of Chemistry and the R. N. Adams Institute for Bioanalytical Chemistry. A special thanks to my committee members: Cory Berkland, Cindy Berrie, Heather Desaire and Mario Rivera for their input and support.

I would like to acknowledge the University of Kansas Animal Care Unit, especially Dr. James Bresnahan and Jodi Troup, for all of the help with animal housing and care and for their advice on animal surgeries. Additionally, thanks to Dr. Mike Thompson and the pathology lab at Lawrence Memorial Hospital for processing the histology slides.

To my entire family, your continual love and support not just through school, but also throughout my entire life has been more than I could have ever hoped for. Dad, I am very honored to be your daughter. I will always be your Little Bo. Annette and Justin, I am so lucky to have you both in my life. I am very blessed to have a brother and sister that I am so close to. Additionally, thank you to my aunts and uncles and my mother-in-law, Eileen, for their support and prayers. Natalie, thank you for putting up with a sister-in-law and roommate like me. I am so fortunate to have so many amazing people in my life. I love you all.

To my husband, Daniel, thank you for your patience, encouragement and especially your love. You are my touchstone. I would have never imaged meeting my counterpart and best friend at an animal care orientation! Thank you for your endless support and for picking up the slack...now it's my turn! I love you and truly believe that I am "The Luckiest".

TABLE OF CONTENTS

Chapter One: Introduction to Microdialysis Sampling and Drug Absorption in the Gastrointestinal (GI) Tract

1.1. Drug Development and Delivery-----	1
1.1.1. Routes of Administration -----	2
1.1.2. Drug Administration by Oral Dosing-----	7
1.2. Drug Absorption in the GI Tract -----	7
1.2.1. Anatomy of the GI Tract -----	7
1.2.2. GI Disease: Ulcers -----	11
1.2.3. Mechanisms of Drug Absorption -----	13
1.2.4. Factors Affecting GI Drug Absorption-----	16
1.2.4.1. Normal Anatomical and Physiological Factors -----	16
1.2.4.2. Physicochemical Properties and Drug Formulation -----	18
1.2.4.3. GI Disease Effects -----	21
1.3. Methods to Study GI Tract Drug Absorption-----	22
1.3.1. <i>In Vitro</i> Permeability Studies-----	22
1.3.1.1. Cell Culture Models -----	22
1.3.1.2. Everted Intestinal Sacs -----	23
1.3.1.3. Excised Tissue Permeability Studies: Ussing Chamber -----	24
1.3.2. <i>In Vivo</i> Absorption Studies -----	25
1.3.2.1. Blood Sampling -----	25

1.3.2.2.	<i>In Situ</i> Closed Loop Animal Studies -----	27
1.3.2.3.	Tissue Homogenate Studies -----	27
1.4.	Microdialysis Sampling -----	28
1.4.1.	Theory and Principles of Microdialysis Sampling -----	28
1.4.1.1.	Microdialysis Probe Designs -----	29
1.4.1.2.	Implantation of Microdialysis Probes -----	32
1.4.2.	Microdialysis Probe Extraction Efficiency -----	34
1.4.2.1.	<i>In Vitro</i> Methods -----	34
1.4.2.2.	No-Net-Flux -----	35
1.4.2.3.	Retrodialysis -----	35
1.4.2.4.	Calibration by Delivery of Analyte -----	36
1.4.3.	Advantages to Microdialysis Sampling -----	37
1.4.4.	Disadvantages to Microdialysis Sampling -----	37
1.4.5.	Microdialysis Sample Analysis -----	38
1.5.	Scope of This Research -----	39
1.6.	References -----	41

Chapter Two: Implantation of Multiple Microdialysis Probes in the Rat Stomach

2.1.	Introduction -----	51
2.2.	Specific Aims of This Research -----	54
2.3.	Chemicals and Reagents -----	55
2.4.	Microdialysis Probe Construction -----	55

2.4.1. Linear Probe -----	56
2.4.2. Vascular Probe -----	59
2.5. Fasting Procedures -----	64
2.6. Designs for Multiple Probe Microdialysis Sampling in the Stomach -----	65
2.6.1. Probe Implantation in the Normal Rat Stomach -----	65
2.6.1.1. Linear Probe Implantation -----	67
2.6.1.1.1. Determination of Implantation Method-----	67
2.6.1.1.2. Stomach Ligation and Gavage Tube Insertion-----	70
2.6.1.1.3. Submucosa Implantation -----	75
2.6.1.1.4. Mucosa Implantation-----	78
2.6.1.1.5. Lumen Implantation-----	81
2.6.1.2. Vascular Probe Implantation -----	84
2.6.1.3. Tissue Response to Probe Implantation-----	88
2.6.1.4. Optimization of Linear Probe Membrane Length -----	91
2.6.2. Probe Implantation in the Ulcerated Rat Stomach-----	92
2.6.2.1. Chemical Ulcer Induction -----	93
2.6.2.2. Probe Implantation in Ulcerated Submucosa-----	98
2.6.2.3. Verification of Probe Location-----	102
2.7. Conclusions -----	102
2.8. References-----	106

Chapter Three: Monitoring Drug Absorption in the Stomach by Multiple Probe Microdialysis Sampling

3.1. Introduction -----	110
3.2. Specific Aims of This Research -----	111
3.3. Materials and Methods -----	113
3.3.1. Chemicals and Reagents -----	113
3.3.2. Microdialysis Probes -----	114
3.3.3. Surgical Procedures-----	114
3.3.4. Microdialysis System-----	115
3.3.5. Experimental Design -----	115
3.3.6. Sample Analysis by HPLC-UV -----	118
3.3.6.1. Analysis of Salicylic Acid (SA)-----	119
3.3.6.2. Analysis of Caffeine-----	119
3.3.6.3. Analysis of Metoprolol-----	119
3.3.7. Data Analysis-----	120
3.3.7.1. Determination of Tissue Concentration from Dialysate Samples ----	120
3.3.7.2. Concentration-time Curves -----	120
3.3.7.3. Pharmacokinetics Modeling-----	120
3.4. Microdialysis Sampling to Monitor Absorption in the Stomach-----	123
3.4.1. HPLC-UV Method Validation -----	123
3.4.2. Normal Stomach Absorption Studies-----	125
3.4.2.1. <i>In Vivo</i> Extraction Efficiency -----	125

3.4.2.2. Salicylic Acid -----	126
3.4.2.3. Caffeine -----	128
3.4.2.4. Metoprolol -----	130
3.4.2.5. Pharmacokinetics Analysis -----	130
3.4.3. Ulcerated Stomach Absorption Studies -----	134
3.4.3.1. <i>In Vivo</i> Extraction Efficiency -----	135
3.4.3.2. Salicylic Acid -----	136
3.4.3.3. Caffeine -----	139
3.4.3.4. Metoprolol -----	145
3.4.3.5. Pharmacokinetics Analysis -----	150
3.4.4. Submucosal Probe Implantation Effects on Absorption -----	153
3.4.5. Bi-directional Flow of Analyte Through the Tissue-----	155
3.4.6. Advantages and Disadvantages to This Approach-----	157
3.4.6.1. Advantages -----	157
3.4.6.2. Disadvantages -----	158
3.5. Conclusions -----	159
3.6. References-----	161

Chapter Four: Summary and Future Directions of Multiple Probe Microdialysis Sampling in the Stomach

4.1. Summary of the Presented Research-----	163
4.1.1. Implantation of Multiple Microdialysis Probes in the Rat Stomach-----	164

4.1.2. Multiple Probe Microdialysis Sampling to Monitor Drug Absorption in the Stomach -----	165
4.2. Future Directions of This Research -----	168
4.2.1. Continuation of Drug Absorption Studies in the Stomach-----	168
4.2.2. Extension of a Multiple Probe Approach in the Intestines -----	169
4.2.3. Utilization of Multiple Probe Microdialysis Sampling in Awake Animals-----	169
4.2.4. Enhancement of the Current Uses of Microdialysis Sampling in the Stomach -----	170
4.2.5. Examination of Endogenous Compounds in Relation to GI Disease-----	170
4.3. References-----	172

LIST OF FIGURES

Figure 1.1. Schematic of drug concentration in plasma versus time-----	3
Figure 1.2. Plot of drug concentration in plasma versus time for intravenous and oral routes of drug administration -----	6
Figure 1.3. Schematic of the GI tract -----	8
Figure 1.4. Tissue layers of the stomach -----	10
Figure 1.5. Schematic of a gastric ulcer -----	12
Figure 1.6. Mechanisms of transport across gastric mucous cells -----	15
Figure 1.7. Microdialysis probe designs -----	31
Figure 2.1. Linear microdialysis probe construction -----	57
Figure 2.2. Vascular microdialysis probe construction-----	61
Figure 2.3. HPLC-UV chromatograms of luminal dialysate after fasting -----	66
Figure 2.4. Histology image of normal stomach tissue-----	69
Figure 2.5. Pyloric sphincter ligation -----	72
Figure 2.6. Gavage tube insertion and cardiac sphincter ligation -----	73
Figure 2.7. Stomach ligated at the cardiac and pyloric sphincters with 3 mL of artificial gastric solution injected into the stomach via gavage tube -----	74
Figure 2.8. Microdialysis probe implantation in the stomach submucosa -----	76
Figure 2.9. Microdialysis probe implantation in the stomach mucosa -----	79
Figure 2.10. Microdialysis probe implantation in the stomach lumen -----	82
Figure 2.11. Linear microdialysis probes simultaneously implanted in the lumen, mucosa and submucosa of the rat stomach-----	83
Figure 2.12. Isolation of the jugular vein -----	85

Figure 2.13. Microdialysis probe implantation in the jugular vein -----	86
Figure 2.14. Histology images of linear probe implantation-----	90
Figure 2.15. Gastric ulcer formed by injection of 20% acetic acid into the submucosa-----	95
Figure 2.16. Histology from the injection of (a) 10% acetic acid, (b) absolute ethanol and (c) 7 mM indomethacin in ethanol-----	97
Figure 2.17. Microdialysis probe implantation in the submucosa of ulcerated tissue -----	100
Figure 2.18. Linear microdialysis probes simultaneously implanted in the lumen and submucosa of both ulcerated and normal tissue -----	101
Figure 2.19. Histology of a linear microdialysis probe implanted in the stomach submucosa of ulcerated tissue -----	103
Figure 3.1. Microdialysis sampling setup -----	116
Figure 3.2. Catenary compartmental modeling to describe the transport of drug from the lumen, across the stomach tissue and into the blood after an oral dose -----	121
Figure 3.3. Representative chromatogram of SA in mucosa dialysate prior to and 15 minutes after a 5 mM oral dose of SA-----	124
Figure 3.4. Salicylic acid determined from microdialysis sampling in the normal stomach-----	127
Figure 3.5. Caffeine determined from microdialysis sampling in the normal stomach-----	129
Figure 3.6. Metoprolol determined from microdialysis sampling in the normal stomach-----	131
Figure 3.7. Salicylic acid determined from microdialysis sampling in the large ulcerated stomach-----	137
Figure 3.8. Salicylic acid determined from microdialysis sampling in the small ulcerated stomach-----	138

Figure 3.9. Caffeine determined from microdialysis sampling in the large ulcerated stomach-----	140
Figure 3.10. Caffeine determined from microdialysis samplig in the small ulcerated stomach -----	141
Figure 3.11. Individual curves of caffeine concentrations determined in the ulcerated submucosa in the small ulcer stomach -----	143
Figure 3.12. Histology slides of two different ulcers -----	144
Figure 3.13. Metoprolol determined from microdialysis sampling in the large ulcerated stomach -----	146
Figure 3.14. Metoprolol determined from microdialysis sampling in the small ulcerated stomach -----	147
Figure 3.15. Histology image showing the proximity of a normal submucosal probe to ulcerated tissue -----	149
Figure 3.16. Submucosal probe implantation effects on drug absorption-----	154

LIST OF TABLES

Table 1.1. Transit times and pH values for the different segments in the GI tract---	17
Table 2.1. Rat stomach layer thickness-----	68
Table 2.2. Comparison of <i>in vivo</i> extraction efficiencies in the stomach layers from 10 mm and 5 mm linear microdialysis probes-----	92
Table 2.3. Ulcer index values for large ulcers (no lubricant used) and small ulcers (lubricant used)-----	98
Table 3.1. Properties of the chosen analytes representing various degrees of drug absorption in the rat stomach -----	112
Table 3.2. EE_d values for multiple probes in the normal rat stomach -----	125
Table 3.3. Pharmacokinetics parameters for the results of microdialysis sampling in the lumen, mucosa, submucosa and blood-----	132
Table 3.4. EE_d values for multiple probes in the ulcerated rat stomach-----	135
Table 3.5. Pharmacokinetics parameters from the results of microdialysis sampling from the lumen, submucosa of normal and ulcerated tissue and blood in large ulcer studies -----	151
Table 3.6. Pharmacokinetics parameters from the results of microdialysis sampling from the lumen, submucosa of normal and ulcerated tissue and blood in small ulcer studies-----	152
Table 3.7. Microdialysis sampling study of bi-directional flow of SA across the stomach tissue after a 20 mg/kg i.v. bolus dose -----	156

CHAPTER ONE

Introduction to Microdialysis Sampling and Drug Absorption in the Gastrointestinal (GI) Tract

1.1 Drug Development and Delivery

The 2006 National Center for Health Statistics Report stated that an average of 1.7 drugs were ordered or provided to patients per physician visit and that collectively, 1.6 billion drugs were ordered or provided by physicians offices in 2004 [1]. With this high demand for medications, development of new and existing pharmaceuticals continues to be an ongoing and important aspect for pharmaceutical companies. However, the development of pharmaceuticals is an arduous task. Not only does the drug need to have the chemical properties necessary to interact with specific receptors at the site of action and create a therapeutic effect, the drug must also be able to reach the target site when introduced into the body [2]. The amount of drug, typically measured by the extent of absorption into the systemic circulation, that is accessible for a therapeutic effect is called drug bioavailability [3]. Plots of drug

concentration in the plasma with respect to time are generated to assess bioavailability. Figure 1.1 is a representation of a plot of concentration versus time [2]. Bioavailability is determined by measuring the area under the curve (AUC) of the concentration versus time plot [2]. These plots are also useful to determine the time of drug onset in the plasma and the duration of drug concentration in the therapeutic range (*i.e.* concentrations above the minimum effective concentration (MEC) and below the minimum toxic concentration (MTC)).

Blood sampling is carried out to determine drug bioavailability since measurements of drug concentration at the target site are not practical in a clinical setting. It is generally assumed that the drug concentration at the target site is in equilibrium with the blood since the bloodstream is the carrier of drug to the target site [3]. Although blood sampling is useful in the determination of overall absorption into the bloodstream, drug concentrations at the site of absorption and at the target site of action cannot be assessed from blood sampling alone. Several methods have been developed in attempts to further monitor the site of absorption and drug concentrations at the target site, which will be discussed further in this chapter.

1.1.1 Routes of Administration

The formulation of the drug and the route of drug administration are key components that can alter drug distribution, the onset of drug appearance systemically, the concentration of drug available and the duration of the drug in the therapeutic range [2]. The route of administration is the method in which a drug is

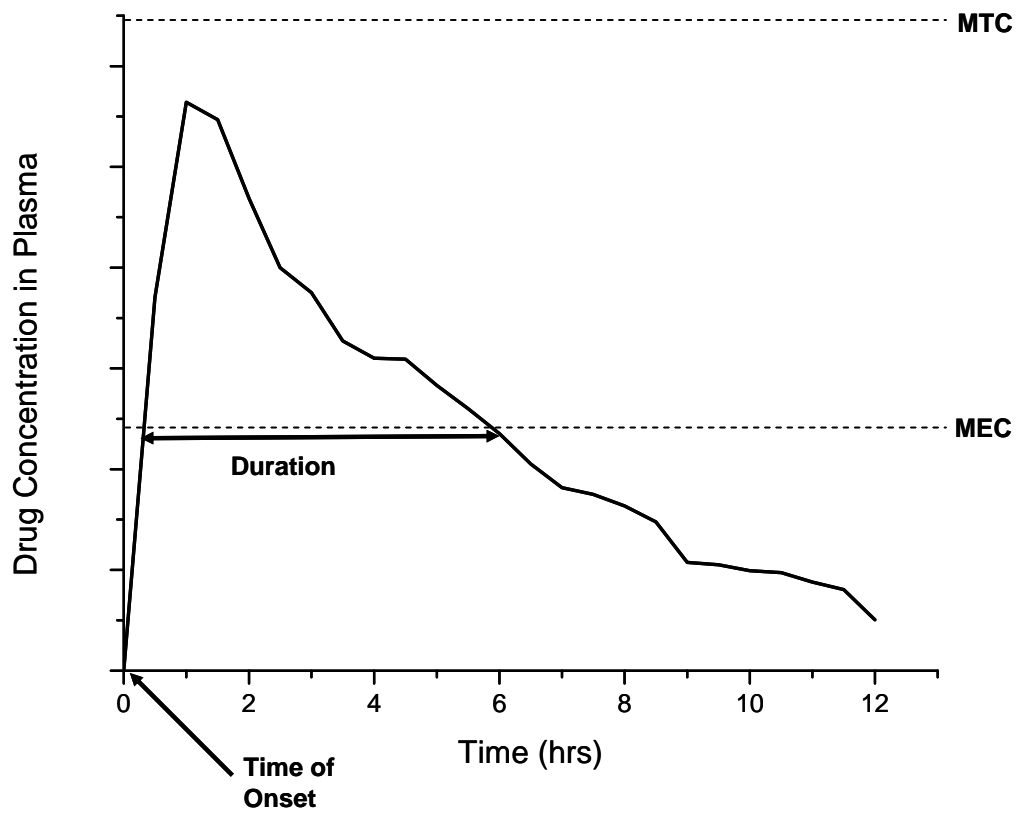


Figure 1.1. Schematic of drug concentration in plasma versus time. MEC is the minimum effective concentration and MTC is the minimum toxic concentration [2].

introduced to the body. There are numerous ways to administer a drug, which can be grouped into two categories: invasive and non-invasive.

Invasive techniques are parenteral routes of administration, including intravenous, intramuscular and subcutaneous. Drugs delivered by these routes are directly injected into the blood, muscle or subcutaneous layer. Intravenous administration has complete bioavailability since it is directly injected into the bloodstream and no absorption needs to occur. In intramuscular or subcutaneous administration, drug must diffuse through the muscle layer or connective and adipose tissues, respectively. However, neither needs to cross a biological barrier to be bioavailable. As drug diffuses across these tissue layers, some drug may be subjected to metabolism and degradation. Therefore, intramuscular and subcutaneous injections have a later onset than intravenous administration and may have lower bioavailability. Moreover, parenteral routes are not only invasive, but injection of drugs via a hypodermic needle punctured through the skin is unfavorable for most patients. This is the basis of trypanophobia (*i.e.* needle phobia), which can result in patient avoidance of crucial medical treatments completely [4]. In addition to this route of administration resulting in poor patient compliance, it typically requires a skilled person for dosing to ensure the injection is made to the correct area, especially for intravenous administration [3].

Non-invasive techniques are any route of administration that does not involve injection of the drug. These are routes such as enteral (*e.g.* oral, sublingual and suppositories), transdermal and pulmonary routes. Dosing by these routes of

administration can be more difficult because drugs must cross a biological barrier in order to be bioavailable [3]. In the case of enteral routes, the gastrointestinal (GI) tract poses a barrier to drug delivery, while the skin is the barrier for transdermal delivery and the lungs create a barrier for pulmonary delivery of drugs. There are several formulations and routes to administer a drug to the body that need to be considered during drug development in order to achieve higher bioavailability.

Figure 1.2 shows the concentration-time curves for invasive and non-invasive routes of administration, intravenous and oral, respectively [3]. These two routes have distinct curves corresponding to different times of onset, intensity and duration in the therapeutic range. Due to complete bioavailability (no absorption phase) with intravenous administration, the intensity of the drug in the therapeutic range is higher than the oral route of administration. Intravenous administration also has a fast time of onset, whereas delays may be observed due to slow absorption from oral dosing. These curves are typical results expected from comparing routes of administration. For example, studies of the effects of route of administration of aspirin show a 68% decrease in bioavailability in oral dosing relative to intravenous dosing in the rabbit [5] and a 57% decrease from oral dosing in comparison to intravenous administration in humans [6]. In addition, the bioavailability of an intramuscular dose of aspirin was 89% that of an intravenous dose in humans [7]. Bioavailability from the oral and intramuscular dose in these studies was determined by comparison of plasma concentrations to the equivalent intravenous dose, which is assumed to be complete since the drug is administered directly to the bloodstream. This is the common

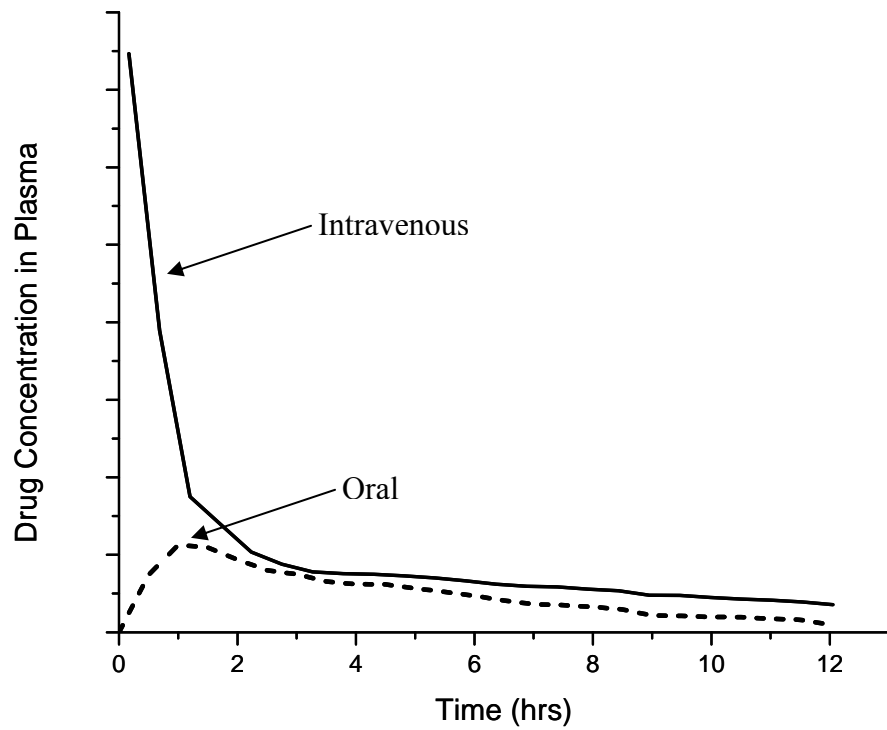


Figure 1.2. Plot of drug concentration in plasma versus time for intravenous (—) and oral (----) routes of drug administration [3].

method to quantify relative bioavailability for routes of administration other than intravenous [2].

1.1.2 Drug Administration by Oral Dosing

Despite the documented difficulties of drug absorption and the decreased bioavailability from oral dosing, this route of administration continues to be the preferred route by both physicians and patients because of the non-invasive nature of administration and good patient compliance. An estimated 90% of medications are given as oral doses, making oral formulations a major focus in drug development [3]. However, as will be discussed in the next section, the GI tract has many unfavorable conditions for drug absorption making oral drug delivery very challenging.

1.2 Drug Absorption in the GI Tract

1.2.1 Anatomy of the GI Tract

The GI tract starts at the mouth and ends at the rectum with several segments in-between as shown in Figure 1.3 [8]. Each segment of the GI tract serves a different function. The primary function of the mouth is to start digestion by breaking materials into smaller pieces. The esophagus connects the mouth to the stomach; however, because of the fast transit time of materials through the esophagus, the esophagus is not involved in the digestive process itself. The stomach is mainly a digestive organ, but for oral dosing, the stomach is the first area of possible

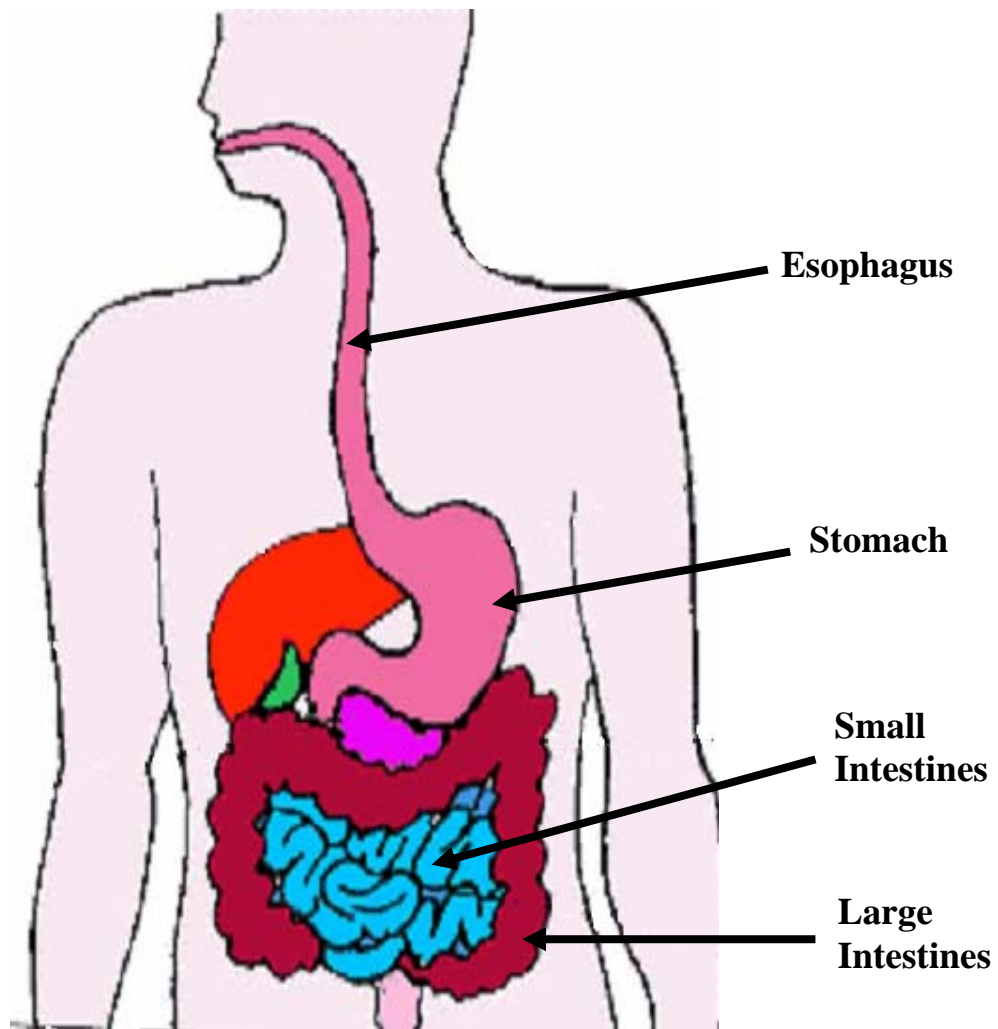


Figure 1.3. Schematic of the GI tract. Reproduced from www.gicancertrials.org.au/GENERAL/images/stomach.gif

significant drug absorption [9,10]. The reasons for this will be discussed in Section 1.2.4. The stomach is connected to the duodenum, the first part of the small intestines, where most absorption occurs. Absorption continues through the jejunum and the ileum, the remaining sections of the small intestines. The small intestines connect to the large intestines, where material is prepared for excretion from the rectum.

The tissue of the GI tract is heterogeneous with several layers. Figure 1.4 shows the tissue layers of the stomach [3,8]. Although there are differences in cell type and organization within the different segments of the GI tract, there are four basic layers common to all segments of the GI tract [8]. The lumen is the inner cavity, which holds unabsorbed material, mucus and GI solution. The mucosa is the innermost tissue layer throughout the GI tract. It consists of a monolayer of cells supported by the lamina propria and muscularis mucosa. The next layer is the submucosa, a layer of connective tissue, which houses the major blood vessels, lymphatics and nerves in the GI tract and, therefore, is the site of the majority of systemic absorption. The muscularis externa is a muscle layer that acts as an outer supporting wall and contributes to peristalsis throughout the GI tract. The serosa (not shown in Figure 1.4) is the outermost layer and is a thin sheath comprised of connective tissue [8,11].

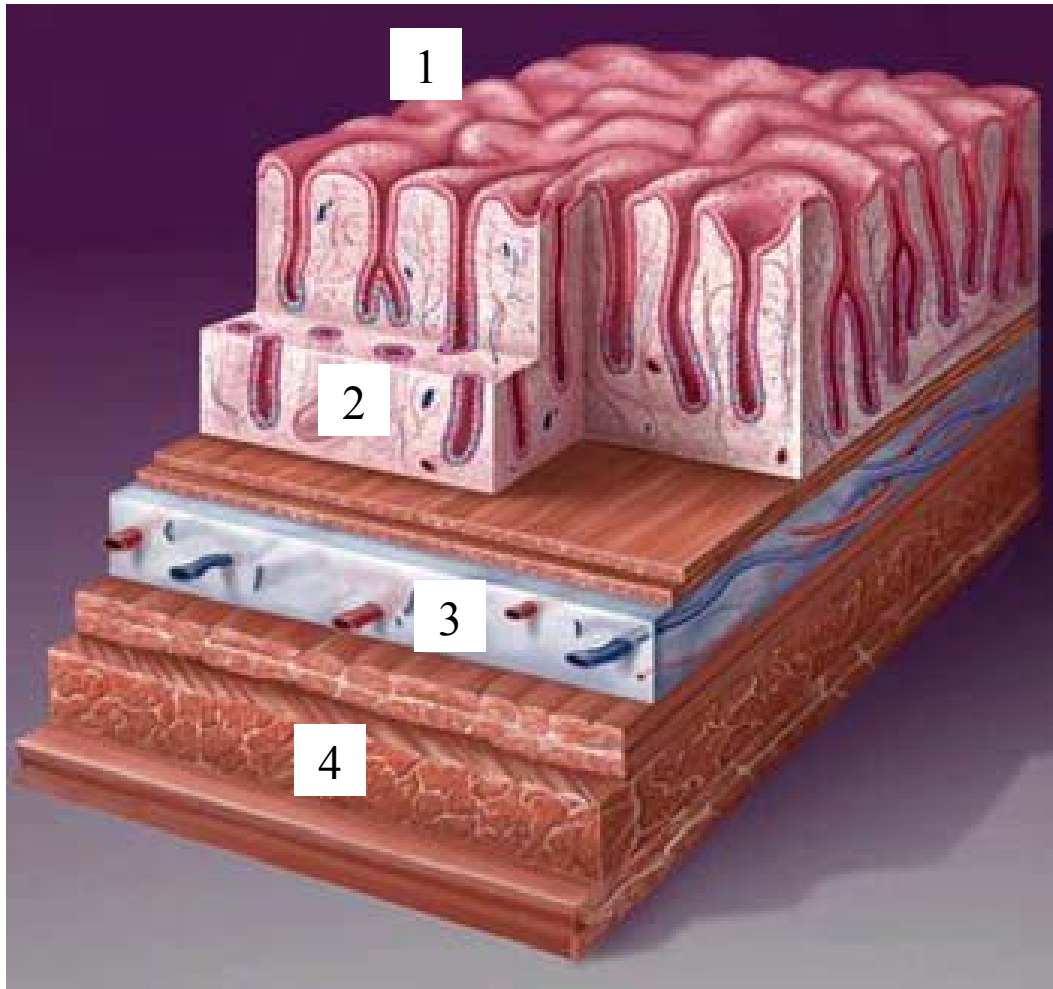


Figure 1.4. Tissue layers of the stomach. 1- Lumen; 2- Mucosa; 3- Submucosa and 4- Muscularis Externa. Reproduced from www.echomedicalmedia.com/anat07.html

1.2.2 GI Disease: Ulcers

Affecting approximately 15% of the population in the United States, ulcers are one of the most prevalent diseases of the stomach and duodenum [12]. Variable frequencies of ulceration have been reported for other countries with a high prevalence in developing countries [12,13]. Ulcers are formed by the erosion of the mucosa layer [14]. Commonly, this erosion is ≥ 3 mm in length in humans [12]. Without the protective mucosa layer present, the underlying submucosa is subjected to the harsh environment of the lumen. For instance, in the stomach, the low pH and luminal flora in the lumen cause further damage to the stomach tissue once the mucosa is compromised. The continued degradation of the mucosa and submucosa can result in perforation of the GI tissue, leading to more serious, life-threatening conditions such as peritonitis [14]. Typically, multiple ulcers form concurrently adding to the severity of the disease. Figure 1.5 is a schematic of a gastric (stomach) ulcer.

Helicobacter pylori and non-steroidal anti-inflammatory drugs (NSAIDs) have been identified as the two main ulcer causing agents [14,15]. *H. pylori* infection has been the reported source of 75% of gastric ulcers and 90% of duodenal ulcers [12,16]. However, ulceration has been shown to be further aggravated by other factors such as stress, smoking, alcohol and coffee beverages, delayed gastric emptying and bile reflux [12,15]. Successful eradication of *H. pylori*, most commonly achieved by proton pump inhibitors (PPIs) based therapy, has been shown to be effective in the majority of ulcer treatments [17]. However, ulcer relapse and

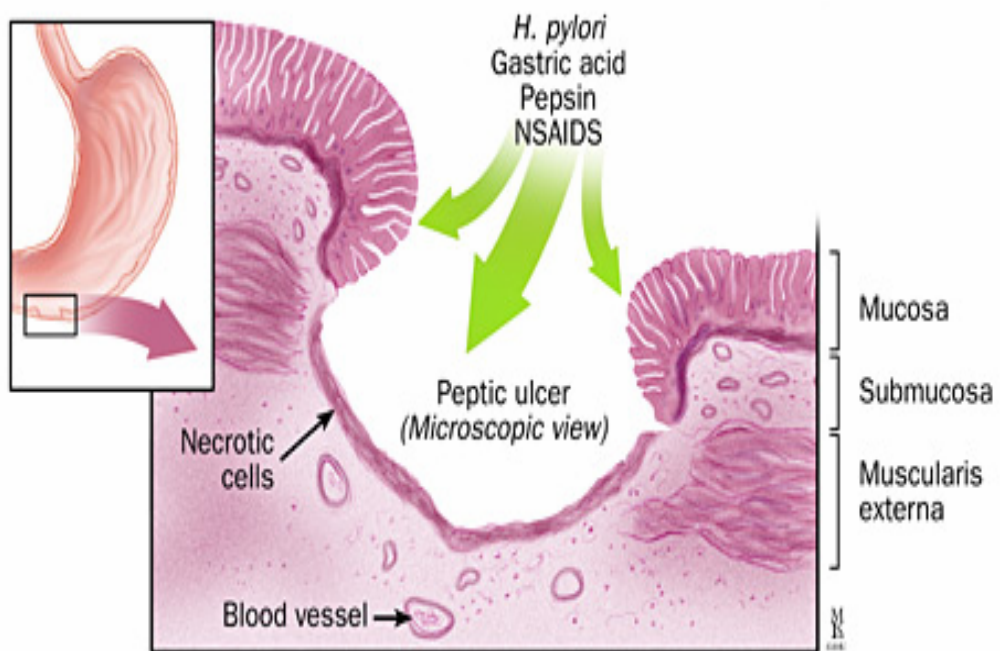


Figure 1.5. Schematic of a gastric ulcer. Reproduced from http://hopkinsgi.nts.jhu.edu/images/shared/disease/database/shared_327_PU-04.jpg

exacerbation has been reported, especially in patients on long-term low-dose aspirin or other NSAIDs for treatment of arthritis, for cardiovascular protection, or for general pain and inflammation reduction [18,19].

1.2.3 Mechanisms of Drug Absorption

The general theory on absorption through the GI tissue is that the majority of absorption occurs by passive diffusion [3]. By passive diffusion, drug uptake through the mucosa layer is driven by a concentration gradient. The rate of passive diffusion can be described by Fick's First Law:

$$J_x = -D \frac{dC}{dx} \quad (1)$$

where J_x is the flux, D is the diffusion coefficient and dC/dx is the concentration change over a distance x [2,3]. This equation illustrates that diffusion across a membrane is based on a concentration gradient, and so continued diffusion will depend upon the rate at which the diffused drug is transported away from the membrane, as well as drug concentration on both sides of the membrane. There are two mechanisms of passive diffusion, transcellular (through the cell) and paracellular (between adjacent cells). Molecules taken up transcellularly are limited by the lipid cell membrane and the lipid/water interface on the surface of the membrane. Therefore, only small, lipophilic compounds will typically transport across the mucosa cells through a transcellular pathway [2,3]. Paracellular transport can be

hindered by junction complexes between the cells. These junction complexes, made of binding proteins and filamentous matter, basically bind the cells near the apical side and protect luminal contents from entering in-between the cells and limiting transport to small, hydrophilic molecules transport [2,3]. Although passive diffusion is mostly limited to small molecules (< 500 Da), several reports have suggested that paracellular transport of some polypeptides (4000 Da) across the intestinal epithelium is possible [20].

Besides passive diffusion, transport across the GI mucosa can occur by carrier-mediated processes. In this type of transport, membrane proteins, either on the cell surface or that span the entire membrane, can complex with molecules and transport them across the cell membrane [2,3]. Carrier-mediated processes can occur with (facilitated transport) or against (active transport) a concentration gradient. Both facilitated and active transport requires energy from ATP hydrolysis in order to transport molecules across cellular membranes [2,3,21].

Figure 1.6 shows a schematic of the major different modes of transport across a cell membrane in the stomach [3,8]. Normally, transport across the cell occurs from the apical (top of the cell) surface to the basolateral (bottom of the cell) surface. In normal cellular processes, both passive diffusion and carrier-mediated modes transport drugs across cellular membranes, with modes of passive transport being the primary ones since they do not require energy to transport molecules. Typically transport occurs by a primary mechanism; however, alternative mechanisms can act in conjunction with the primary mode [11,22].

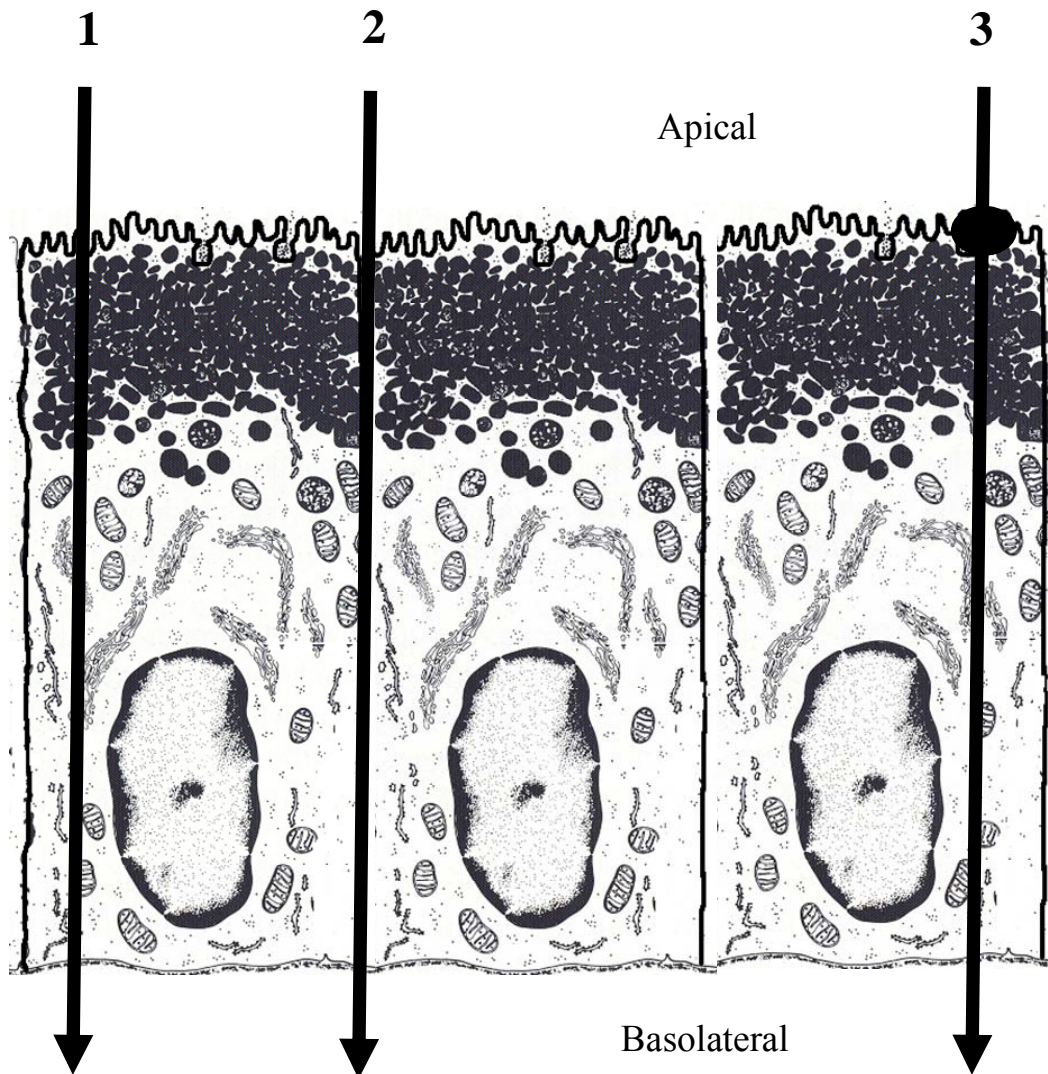


Figure 1.6. Mechanisms of transport across gastric mucous cells.
1- Transcellular passive transport; 2-Paracellular passive transport and
3-Carrier-mediated active transport [3,8].

1.2.4 Factors Affecting GI Drug Absorption

1.2.4.1 Normal Anatomical and Physiological Factors

There are many factors that affect when and where drugs will be absorbed in the GI tract. Anatomical and physiological factors of the GI tract greatly influence absorption and make oral drug delivery an extremely variable route of administration [21]. Most segments of the GI tract have folds in the mucosa layer to increase surface area and to make room for passing materials. The majority of absorption occurs in the small intestines because it has the most folds in the mucosa layer and also because the mucosa has microvilli. The mobility of passing material and transit time, in addition to the amount of time the materials are exposed to the surface of each segment in the GI tract, will affect the absorption. Table 1.1 lists the typical transit times in the human GI tract [23].

Bacteria, enzymes and food present in the lumen alter absorption, making prediction of the location of drug absorption more problematic. Bacteria and enzymes can act on drugs and degrade them before they are absorbed. The presence of food in the stomach creates changes including in pH, viscosity of luminal solution and, especially, changes in gastric emptying [24]. In general, food has been shown to increase gastric emptying, decreasing drug exposure to the stomach surface and ultimately decreasing drug absorption [11,23]. Studies have reported that oral drug administration in fed states has been shown to cause a decrease in drug absorption relative to fasted states [25-27]. However, increases [27] or no change in absorption [27-29] have also been observed for several drugs despite the expected trend that food

causes decreased absorption. In addition to altering gastric emptying, drugs can adsorb to food in the lumen, which can further delay or decrease drug bioavailability [21].

The pH is different in each segment of the GI tract. There is a pH gradient from the stomach to the large intestines, which is illustrated in Table 1.1 [11]. The effects of the different pH levels on drug absorption will be further discussed in the next section.

	Transit Time	pH
Esophagus	5-15 seconds	5-6
Stomach	0.5-1 hour	1-3
Small Intestines	3-5 hours	5-6
Large Intestines	5-7 hours	7

Table 1.1. Transit times and pH values for the different segments in the GI tract.

Along with transit times, pH levels and luminal flora, the mucosa is lined with a stagnant, aqueous layer adjacent to the epithelial cells that can impede uptake of drugs [21]. This viscous layer consists mostly of water, mucus and mucins where, in particular, drugs of large molecular weight or poor aqueous solubility have limited permeability into the mucosa [11]. The function of this layer is to protect the GI tissue

from destructive components (*i.e.* luminal pH, food, alcohol, microorganisms) and also to hydrate the GI tissue. In addition to selectively impeding large molecular weight and highly lipophilic compounds, drugs can complex with stagnant layer matrix components further prohibiting uptake of drugs [21]. As mentioned above, one of the functions of this aqueous layer is to protect the GI tissue from the luminal pH. This is particularly important in the stomach, where the pH is very low, as was shown in Table 1.1. The stagnant aqueous layer impedes movement of hydrogen cations to the mucosa layer. At the same time, the mucous epithelial cells of the mucosa secrete bicarbonate into the stagnant layer. This creates a pH gradient within the stagnant layer with low pH closer to the luminal side of the stagnant layer and near neutral pH next to the mucosa [21]. For drug absorption, the microclimate of the stagnant aqueous layer needs to be considered. Studies have indicated that for most compounds, the layer is insignificant for overall absorption [30,31]; however, some dependence of this layer on absorption has been reported (*e.g.* for digoxin and quinidine) [32,33].

1.2.4.2 Physicochemical Properties and Drug Formulation

Physicochemical properties of the drug and its formulation are important factors in affecting the extent and location of drug absorption. The conventional formulations for oral drug delivery include: solutions, suspensions, capsules, and tablets [11]. Dissolution of the drug is required prior to absorption for all of the formulations except solutions. The dissolution rate of the drug is typically the rate-

limiting step for oral dosing and is described by the Noyes Whitney equation:

$$\frac{dC}{dt} = \frac{DA}{h}(C_s - C) \quad (2)$$

where dC/dt is the rate of dissolution, D is the diffusion rate constant, A is the particle surface area, h is the stagnant layer thickness and C_s and C are the concentrations of drug in the stagnant layer and the bulk solution, respectively [2]. The stagnant layer results from the saturation of drug in solution at the surface of the drug particle during dissolution. The drug diffuses to bulk solution once it passes the stagnant layer adjacent to the particle. Along with a concentration gradient, this equation describes that dissolution is driven by surface area. Smaller particles have more surface area to the dissolving solution, which results in a faster dissolution rate [11].

The drug not only needs to have good aqueous solubility for dissolution, the compound also needs good lipid solubility to permeate the mucosa barrier. Lipid solubility is predicted from the drug partition coefficient (P):

$$P = \frac{C_{oil}}{C_{water}} \quad (3)$$

where the concentration of drug (C) is measured in two immiscible liquids at equilibrium to determine the partitioning of drug between the lipophilic and aqueous phases [3]. Drugs with positive log P values have higher lipid solubility and are more

likely to permeate the mucosa barrier in comparison to compounds with negative log P values, which exhibit lower lipid solubility. For ionizable compounds, log P is affected by pH. Therefore, the distribution coefficient (D) is used to determine drug lipophilicity for ionizable compounds. Partition coefficients and distribution coefficients are related by the equation:

$$D = P(1 - \alpha) \quad (4)$$

where α is the degree of ionization. This equation indicates that the distribution coefficient is the partition coefficient of the fraction of unionized drug at a given pH [3].

According to the pH partition hypothesis, drugs in an unionized form will passively diffuse through the mucosal barrier [11,21]. The degree of ionization is described by the Henderson-Hasselbach equation, which relates pH, pK_a and the ratio of the concentrations of the ionized form of the drug to the unionized form [3,21].

For weak acids:
$$pH = pK_a + \log \frac{[A^-]}{[HA]} \quad (5)$$

For weak bases:
$$pH = pK_a + \log \frac{[B]}{[BH^+]} \quad (6)$$

As shown above in Table 1.1, in the stomach, the luminal pH is around 1-3. In general, weakly acidic drugs will be neutral and weakly basic drugs will be charged when protonated in this acidic environment. Therefore, based on the pH-partition hypothesis, weakly acidic drugs can be absorbed in the stomach whereas most weakly basic drugs would not be absorbed.

Overall, the physicochemical properties of the drug in combination with the anatomical and physiological factors can make drug absorption in the GI tract difficult to predict. Therefore, methods to monitor the location and extent of absorption would be useful for drug development studies.

1.2.4.3 GI Disease Effects

Diseases in the GI tract can alter the anatomy and physiology of the GI tissue by affecting mobility, pH levels and mucosal tissue integrity caused by atrophy [34,35]. Therefore, bioavailability of orally dosed drugs may be altered as a result of disease. In the case of ulcerated tissues, as described earlier in Section 1.2.2, the mucosa barrier that is normally selective for absorption is absent. Therefore, increased and non-selective absorption through the GI tissue occurs. For example, Tur *et al.* studied the absorption of phenol red, normally a non-absorbed compound in the rat stomach, in both normal and ulcerated rat stomach after oral administration. Urine analysis for phenol red showed a 3-fold increase in overall absorption of phenol red in ulcerated relative to normal stomach [36]. The results from this study are an example of both drug absorption enhancement and decreased selectivity in absorption in ulcerated tissue.

Even though overall bioavailability has been shown to be enhanced in diseased states, most studies of drug absorption and bioavailability are performed on healthy, normal subjects [37]. Dose adjustments may be needed to account for this increased bioavailability in patients with GI diseases. Methods to understand drug absorption in diseased states and also the biological mechanisms that change in disease will help the development of dose adjustments of pharmaceuticals.

1.3 Methods to Study GI Tract Drug Absorption

1.3.1 *In Vitro* Permeability Studies

Drug absorption in the GI tract has been studied by several *in vitro* and *in vivo* methods. *In vitro* methods can be easily performed in place of *in vivo* models to rapidly screen GI absorption of potential drug candidates or in order to study specific events that can be difficult to monitor due to the complexity of biological systems. Three commonly used *in vitro* models for GI drug absorption are described below.

1.3.1.1 Cell Culture Models

Cell culture models are widely used to rapidly screen potential candidates in drug development. The most commonly used system for studies in the GI tract is Caco-2 cell monolayers [22,38,39]. These cells are derived from the human colorectal carcinoma cell line [39]. Although from the colon by nature, Caco-2 cells have been shown to exhibit the morphological and physiological behaviors of intestinal absorptive cells [38]. Of particular importance is the ability of these cells to

form tight junctions between cells [38,39]. Tight junctions are a component of the junctional complex, described in Section 1.2.3, which are the main barrier in paracellular transport. Therefore, mechanisms of transport other than transcellular passive diffusion can be studied with Caco-2 monolayers. For this method, cells are grown on a semi-permeable membrane. Interestingly, these cells have been shown to polarize and form a confluent layer on the membrane [39]. This membrane is placed in a diffusion cell with a donor and a receiver chamber. Drug is applied to the donor chamber, typically the apical side of the monolayer, and permeability studies are performed by monitoring drug concentrations from both chambers [38,39]. The use of cell models such as the Caco-2 line is advantageous as an *in vitro* technique since the cells are derived from human; however, Caco-2 cells have a tumor origin and require at least a 2-3 week period for full morphological and functional differentiation [38,39]. Other cell lines, such as HT-29 or MDCK cells, have been used as alternative monolayers or have been co-cultured with Caco-2 cells for study specialization [38]. For instance, HT-29-H and HT-29-MTX cells have been co-cultured with Caco-2 cells to monitor mucus secretion and to mimic carrier-mediated uptake, respectively [38,40].

1.3.1.2 Everted Intestinal Sacs

The everted intestinal sac has been commonly used as a relatively inexpensive and rapid procedure for drug permeability studies in the intestines [39,41,42]. For this procedure, the intestines are harvested from the euthanized animal and everted so that the mucosa becomes the outer surface of the intestines. The intestines are

clamped at both ends and then filled with solution. The tissue is then suspended in an oxygenated tissue culture. The drug of interest is dissolved and added to the tissue culture. At the end of the experiment, the tissue is removed from the culture and the inner solution is analyzed for drug content. The drug in this solution represents the amount of drug that permeated the intestines. Variations to this technique have been made that include methods of serial sampling and the use of non-everted intestinal sacs [42,43]. The everted intestinal sac is a technique to look at absorption through an actual segment of the intestines where all cell types are present on the mucosa, which is not the case when using cultured cell lines to monitor absorption. The major disadvantages to this method are that there is no blood perfusion to the tissue and that drug absorption must occur across the entire tissue, even the muscularis externa and serosa. However, for fast semi-quantitative results, the everted intestinal sac is a useful method over other *in vitro* techniques.

1.3.1.3 Excised Tissue Permeability Studies: Ussing Chamber

The two previously described *in vitro* techniques of using cell cultured monolayers and everted intestinal sacs are limited to studying drug absorption in the intestines. To study absorption in the stomach by *in vitro* models, excised stomach tissue can be mounted into a diffusion chamber by the Ussing Chamber technique [44]. The Ussing Chamber was originally designed to monitor ion transport across membranes, but variations to this technique have been made to extend its use in drug absorption studies [39]. Similar in concept to the cell cultured monolayers, a small section of tissue is mounted between two chambers, a donor chamber and receiver

chamber. Drug is placed in the donor chamber and samples are taken from the receiving chamber and analyzed for drug permeation across the tissue [38,39]. Like the everted intestinal sac method, using excised tissue is advantageous because actual tissue that includes the different cell types of the mucosa. As previously mentioned, most tissues can be mounted in the chamber and because of the small sample size needed for the chamber ($\sim 9 \text{ cm}^2$), Caco-2 monolayers and human tissue biopsies have been used as well [39,45,46]. As with the everted intestinal sacs, a disadvantage of the Ussing Chamber is that it is used to monitor drug absorption across the entire tissue, even through the muscularis externa and serosa. Another drawback is the time required to prepare the chamber and perform the procedure, therefore, it is not recommended as a rapid screening technique [39,45].

1.3.2 *In Vivo* Absorption Studies

The disadvantage to *in vitro* studies is that they do not take into account the aforementioned physiological factors that affect drug absorption in the GI tract. Therefore, *in vivo* models are used for a more complete understanding of drug absorption in the GI tract. A number of *in vivo* models are discussed below.

1.3.2.1 Blood Sampling

Venous blood sampling at timed intervals is by far the most common method to monitor drug absorption after an oral dose for *in vivo* studies [47-51]. This involves giving an oral dose to the animal and drawing blood samples post dose. However, blood sampling results in overall fluid loss, which can perturb the system

under study. Rodent blood typically takes up to 2 weeks to fully regenerate and it is suggested that only 1% of the circulating blood volume (which is 20-25 mL in the rat) can be safely removed every 24 hours [52,53]. This limits the temporal resolution possible before the volume of blood in the system changes. For most studies involving blood sampling in the rat, volumes of 150-400 μ L are withdrawn for each time point, exceeding the recommended sampling rate [47,50,51]. Whole blood samples have many components that are not amenable with analytical systems and need to be removed prior to analysis, resulting in increased analysis time. A conventional sample clean-up procedure for analysis is to collect blood samples into heparinized vials to prevent blood clotting. The vial is centrifuged down and the supernatant is drawn up, which is the plasma [47,49,51]. The plasma is further prepped for analysis by methods including protein precipitation, solid-phase extraction or liquid-liquid extraction [47-49,54]. Efforts to decrease preparation time, such as direct injection of plasma samples for analysis by column switching or turbulent flow chromatography (TFC), have been developed [54,55]. Although decreased temporal resolution and sample pre-treatment are big disadvantages, more importantly, results from blood sampling only reflect that the compound was absorbed. Sampling in this manner gives no indication of the location in the GI tract from which the drug was absorbed or what concentration of drug is present in the tissue. Tissue homogenate studies by Choi *et al.* which suggest that salicylic acid accumulates in the gut tissue of the intestines after an oral dose is just one example of why a more tissue-specific technique is needed [56]. Blood sampling is not sufficient

to allow for the site of drug absorption to be located or for the assessment of tissue accumulation.

1.3.2.2 *In Situ* Closed Loop Animal Studies

An *in situ* closed loop method is another way to monitor drug absorption in the GI tract that is more site-specific than blood sampling alone [56,57]. For this method, drug in solution is dosed through a cannula to a closed portion of the GI tract and absorption is determined by extracting solution from the lumen. This method gives a direct measurement of the lumen, but assumes that any amount of drug not present in the lumen was absorbed and does not account for events such as degradation nor does it assess what is happening in the tissue of the GI tract. Also, because this method relies on a section of the GI tract to be closed off, this method is not capable of further development in conscious animals for extended periods of time. *In situ* closed loop animal studies are therefore very limited both in their application and in terms of the information that can be gained from them. Methods to site-specifically monitor the location and the extent of absorption in the GI tract would serve as an improvement for drug development studies.

1.3.2.3 Tissue Homogenate Studies

Excised tissue studies have been performed to look at the gut tissue directly for tissue distribution studies [56,58,59]. At a certain time point post dose, the animal is sacrificed and the gut tissue is removed and processed for drug concentration as a tissue homogenate. The concentration determined from the tissue is the total drug concentration (protein bound + free, unbound drug). Typically, the fraction of

interest is the free, unbound drug since it is the therapeutically active portion. Further analysis is needed to determine the unbound drug concentration. For a complete study, multiple animals are used to monitor drug absorption. This use of several animals in one study causes larger biological variability and therefore, subtle changes are more difficult to assess. Methods to reduce the number of animals used would lower biological variability within the study.

1.4 Microdialysis Sampling

Microdialysis sampling is a tissue-specific technique that has been used for decades to monitor drug concentrations directly in targeted tissues for pharmacokinetics (PK) studies [60-66]. Microdialysis sampling has been shown to be suitable to overcome the shortcomings of the *in vivo* techniques outlined above. Extension of this technique to monitor drug absorption in the GI tract could prove beneficial for a more complete understanding of absorption in both normal and diseased GI tissues.

1.4.1 Theory and Principles of Microdialysis Sampling

Microdialysis sampling is a site-specific technique typically used to sample low molecular weight compounds in the extracellular space at a site of interest [67,68]. A microdialysis probe consists of a small semi-permeable membrane that is implanted into a tissue or site of interest (*e.g.* the blood) where the probe acts

similarly to a blood vessel. A perfusion fluid, that is isotonic and at the same pH as the surrounding environment, is continuously pumped through the probe inlet. Typical flow rates through the probe are 1-5 $\mu\text{L}/\text{min}$ although lower flow rates can be achieved. Low molecular weight compounds diffuse into and out of the probe based on a concentration gradient and are carried by the perfusion fluid to the probe outlet for collection. The collected samples are termed dialysate samples.

Microdialysis was first used as a sampling technique in the brain to monitor dopamine [69] and the brain has continued to be the most widely studied organ with microdialysis. In addition, implantation of microdialysis probes has been extended to basically every tissue [60,62,64-66,70]. Microdialysis sampling has been used to look at endogenous compounds before and after an event such as drug dosing as in pharmacodynamics (PD) studies and also to look at exogenous compounds for PK studies, as previously mentioned. This technique has been used for *in vitro* and *in vivo* studies mainly in animal studies including anesthetized and awake animals, but recently, the use of microdialysis sampling in humans has grown [71-74].

1.4.1.1 Microdialysis Probe Designs

There are many different probe designs and configurations based on the target sampling site. The main components of a microdialysis probe are inlet and outlet tubing and a semi-permeable membrane. Several materials have been used for the semi-membrane. Some of the most commonly used membrane types are polyacrylonitrile, polycarbonate, regenerated cellulose and cellulose acetate [75]. The choice of membrane is based on membrane composition (charge and

hydrophobicity) and on the molecular weight cut off (MWCO) [76]. There are two main configurations of microdialysis probes: cannula style and linear.

A cannula style probe can be in a concentric or side-by-side fashion. The membrane is slid over the probe inlet and the inlet is placed inside the outlet (concentric) or directly next to the outlet (side by side). These probes are used for tissues where increased spatial resolution is needed, such as the brain. Moreover, because of the rigidity of the probe, this style probe is robust enough for awake animal studies in the brain. Although this style probe can be used in other tissues, tissue tearing is possible due to the rigidity of the probe [76]. A more flexible cannula style probe was designed to implant in tissues, which is used mostly for sampling from the blood [77]. Figure 1.7a is a schematic of a flexible cannula style probe. A more in-depth discussion of the flexible style probe construction will be presented in the next chapter.

Linear probe configurations were designed for use in peripheral tissues [76]. The inlet and the outlet are connected to the membrane in a successive fashion. Linear probes are flexible and are used for sampling when a cannula style is not necessary (*i.e.* when spatial resolution is not crucial). Figure 1.7b is a schematic of a linear probe. The construction of linear probes will be discussed in more depth in the next chapter.

Another design, the shunt probe, has been developed for sampling in moving fluids, mostly the bile [76]. The design of the probe is similar to a linear probe, but the probe is placed inside a larger tube and the tube is implanted (*i.e.* into the bile

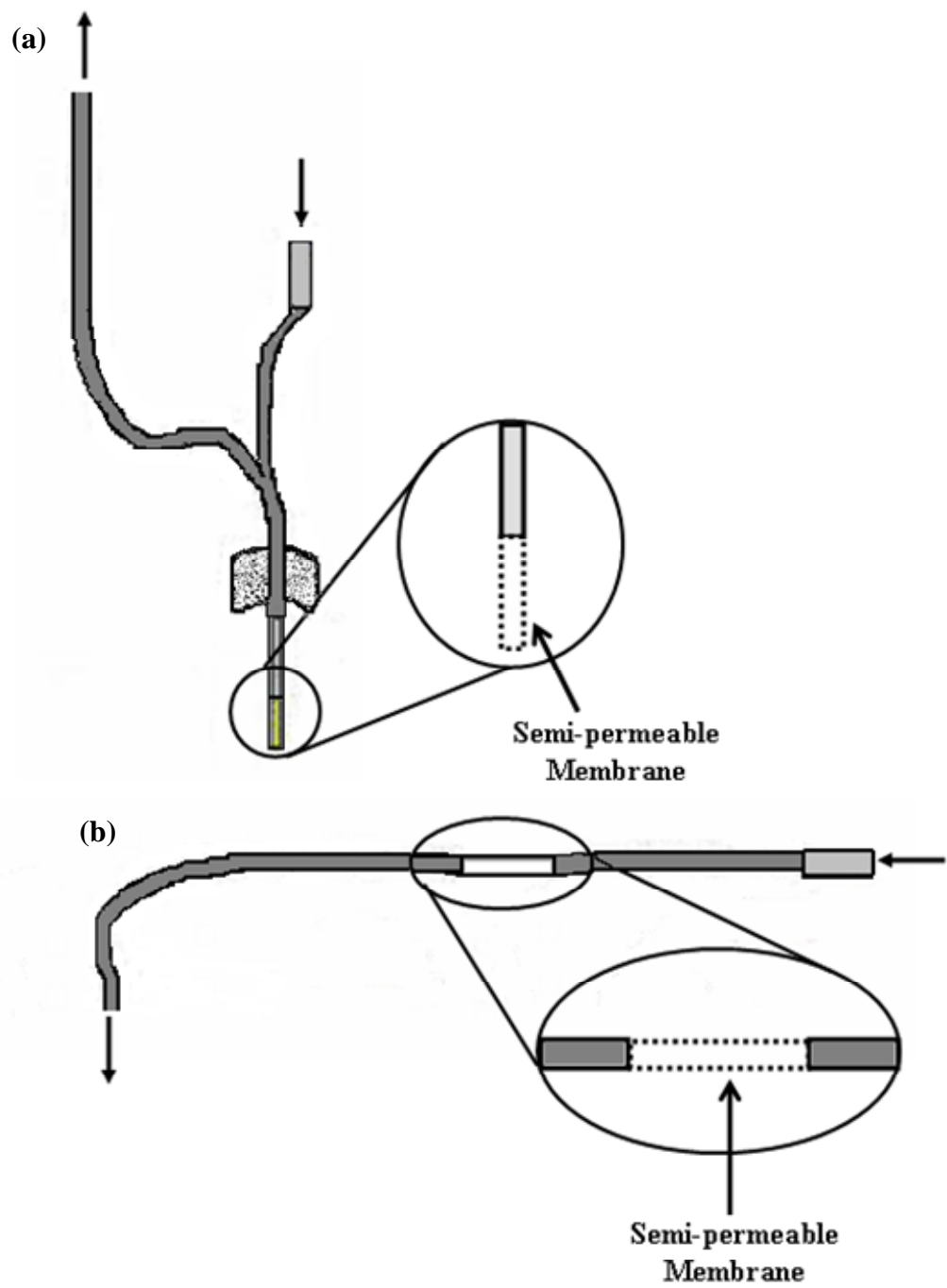


Figure 1.7. Microdialysis probe designs (a) flexible cannula and (b) linear probe designs. Arrows indicate direction of perfusion fluid flow. Adapted from www.bioanalytical.com.

duct of the liver). The bile flows freely inside the larger tube where it can be readily sampled by the probe [76].

1.4.1.2 Implantation of Microdialysis Probes

Successful microdialysis sampling experimentation is dependent on the probe recovery, which in turn, is a factor of several factors including membrane type and length, probe geometry, perfusate flow rate and the analyte properties and transport across the probe membrane [76]. Furthermore, for successful *in vivo* microdialysis sampling, proper probe implantation techniques are important. Improper probe implantation can cause damage to the microdialysis probe as well as to the target tissue. The required criterion for successful microdialysis probe implantation includes a small outer diameter microdialysis probe that will minimize damage to the tissue and the probe upon implantation and also surgical procedures that are minimally invasive for proper probe implantation [77].

The conventional method of implantation is by use of some type of cannula or introducer, which guides the probe into the tissue and serves to protect the probe during implantation into the tissue [67]. The guide cannula is initially inserted into the tissue and the microdialysis probe is inserted into the guide cannula. The cannula is subsequently removed, leaving the microdialysis probe in the tissue. The cannula needs to be large enough to house the probe but not too big to cause extensive damage to the tissue [77]. Alternately, implantation of a cannula style microdialysis probe into peripheral tissue can be achieved by puncturing the tissue with a needle. The probe is then inserted into the hole created by the needle [78-80]. Ideally,

implantation by this method would cause less damage to the tissue relative to using a guide cannula since the guide cannula needs to have a larger diameter than the probe. However, this method could result in damage to the probe during implantation due to tissue resistance. This method is not feasible for linear probe implantation since an entrance and exit site are needed for probe implantation.

Implantation of the probe with minimal tissue perturbation is necessary; however, another crucial factor is the controlling of the location of probe implantation. Microdialysis probe implantation into the brain is conventionally performed with the use of a stereotaxic frame [63,81]. Because of the precision of the stereotaxic frame, highly reproducible implantation procedures can be achieved [82]. For implantation in peripheral tissues; however, equipment to accurately and reproducibly implant guide cannulas into peripheral tissues have not been designed. Therefore, implantation into the tissue relies on the precision of the surgeon who is implanting the probe. Implantation into a homogenous tissue, such as the liver, is not surgically complicated since the tissue type is the same throughout [83]. When the tissue is heterogeneous (*i.e.* has several tissue layers within the tissue) implantation into separate layers is more difficult to control and reproduce because of the limitations that the tissue layer thickness imposes. As described in Section 1.2.1, the stomach tissue is heterogeneous mainly consisting of a mucosa, submucosa and muscularis externa layer. Proper microdialysis probe implantation is crucial in order to keep the probe from penetrating into the adjacent tissue layer. For example, improper probe implantation in the stomach mucosa could result in the probe

penetrating into the submucosa, which results in sampling from two layers collectively instead of the intended single layer.

1.4.2 Microdialysis Probe Extraction Efficiency

Microdialysis sampling is carried out under non-equilibrium conditions since the perfusion fluid is continuously pumped through the probe. Therefore, the probe recovery must be known in order to use microdialysis sampling as a quantitative sampling tool [67,76]. The general equation to determine microdialysis probe extraction efficiency (EE) by the ratio of concentration (C) of analyte in the dialysate and the sample is as follows [84]:

$$EE = \frac{C_{perfusate} - C_{dialysate}}{C_{perfusate} - C_{sample}} \quad (7)$$

In vivo, the C_{sample} cannot be determined directly, so the use of microdialysis sampling as a quantitative tool relies on the determination of the EE. A number of literature methods have been used previously to calculate the EE of the individual probe. These methods are discussed in the following sections.

1.4.2.1 *In Vitro* Methods

Methods to determine the probe EE have been carried out through *in vitro* methods [75]. However, if the probe is to be implanted *in vivo*, the EE determined *in vitro* is not the same as it would be *in vivo*. The environment around the probe in the *in vitro* study is in a more hydrodynamic environment. A probe implanted in a tissue

has different diffusion properties resulting in a decrease in EE *in vivo*. Therefore, probes that are used for *in vivo* quantitative studies must be calibrated as such.

1.4.2.2 No-Net-Flux

The no-net-flux method is used to look at transport across the probe membrane as a function of varying the analyte concentration in the perfusate [85,86]. The analyte is added to the perfusate at different concentrations. When the concentration of analyte is greater in the perfusate than the surrounding environment, the analyte will be delivered from the probe. When the analyte concentration in the surrounding environment is greater than the concentration in the perfusate, the analyte will diffuse into the probe. The transport of the analyte into and out of the probe is reflected in the resulting dialysate concentrations. When the concentration in the perfusate and the surrounding environment are equal, there will be no net flux of analyte. A plot of the change in the dialysate concentration versus the initial perfusate concentration is made, where the slope is the EE and the x-axis is the determined concentration in the surrounding extracellular fluid [85,86]. The main disadvantage is that this method of calibration is very time consuming, taking over 8 hours to have a sufficient number of different concentrations to plot against [85].

1.4.2.3 Retrodialysis

The determination of microdialysis probe EE by adding a marker to the perfusate solution and monitoring any changes in that marker over time is called retrodialysis [61,64,65]. The chosen marker must be chemically similar and have almost identical transport through the probe and diffusion through the studied site as

the analyte. However, the marker must be analytically distinguishable from the analyte to monitor both compounds. Finding a compound with analogous properties of transport through the probe makes retrodialysis a difficult method for probe calibration. Radiolabeled forms of analytes can be used as markers, but labeling the compound and having the analytical tools to measure the labeled compound can be expensive [61,87].

1.4.2.4 Calibration by Delivery of Analyte

A modification to retrodialysis to determine the EE of the microdialysis probe is by delivery of actual analyte through the probe [60,66,85]. A low concentration of the analyte is perfused through the probe. Samples are analyzed once a steady state of delivery is achieved, as monitored through the dialysate concentration. The extraction efficiency by delivery (EE_d) is derived from Equation 7. For delivery studies, there is no initial concentration of analyte in the sample so the equation becomes

$$EE_d = \frac{C_{perfusate} - C_{dialysate}}{C_{dialysate}} \quad (8)$$

For recovery studies, there is no analyte in the perfusate so the EE, derived from Equation 7, becomes:

$$EE_r = \frac{C_{dialysate}}{C_{sample}} \quad (9)$$

Transport across the probe should be independent of direction, therefore, equal for both the delivery and recovery [75]. By this assumption, the EE_d value equals the EE_r . Therefore, the analyte concentration in the sample or tissue of interest (C_{sample}), can be calculated by determining the concentration in the dialysate ($C_{\text{dialysate}}$) and substituting the EE_d for EE_r in Equation 9.

1.4.3 Advantages to Microdialysis Sampling

Microdialysis sampling as a site-specific technique is an improvement over traditional sampling techniques. Because of the MWCO of the membrane, only small molecules readily diffuse through the probe. Proteins and large molecules are excluded from the dialysate, making sample pretreatment typically unnecessary for analysis. The perfusion fluid is continuously pumped through the probe resulting in no net fluid loss from the system under study, which maintains equilibrium in the system during sampling. Multiple samples are taken from the same probe, which reduces variability in the study and for *in vivo* studies also reduces the number of animals used for the study. In addition, the animal can serve as its own control, further reducing variability [77].

1.4.4 Disadvantages of Microdialysis Sampling

Microdialysis sampling is not an all-inclusive sampling technique. The probes must be continuously infused with the perfusion fluid. The most common way to deliver the perfusion fluid is by a syringe pump, which requires the animal to be

tethered so the probe inlets and outlets do not get tangled as the animal moves. However, a solution to this problem is the commonly used BASi RaturTM system (West Lafayette, IN) where the animal can move freely without tangling and breaking the probe tubing [77]. Another disadvantage is that microdialysis probes are fragile by nature, especially linear, vascular and shunt probes. Care must be taken to not damage the membrane or the tubing for the probe inlet and outlet. A further drawback to microdialysis is that it is a time consuming technique since probes have to be calibrated in addition to the actual sampling experiment when microdialysis is used for quantitative sampling. Moreover, probe implantation procedures are difficult in areas of heterogeneous tissues, such as the GI tract and the skin, where implantation of the probe within a certain region of the tissue is more difficult in comparison to homogenous tissues, such as the liver. Probe implantation techniques will be discussed in-depth in Chapter Two. Nonetheless, microdialysis sampling offers an unparalleled opportunity for site-specific tissue sampling.

1.4.5 Microdialysis Sample Analysis

The most common analytical techniques to analyze dialysate samples are by liquid chromatography (LC) or capillary electrophoresis (CE) with an appropriate detection scheme [61-65,76,81]. Dialysate samples contain high salts from the perfusion fluid, which can present a challenge for detection with some analytical systems such as mass spectrometry (MS) where high salt samples can impede the ionization source and create high background noise [76]. Methods to improve

detection limits of LC-MS, such as the use of capillary LC or online desalting techniques (*e.g.* desalting columns or solid phase extraction (SPE)) have been developed [88-92]. Microdialysis sampling itself is continuous, but fractions are collected and analyzed, which is a limiting factor in the temporal resolution achieved. The flow rate of the perfusion fluid through the probe can be increased, but results in less recovery from the probe and dilution of the analyte below detectable limits. Decreasing the flow rate through the probe, increases recovery through the probe, but results in smaller sample volumes. On-line capillary electrophoretic and microchip separation based methods have been developed to analyze small sample volumes and have been used for microdialysis sampling experiments with rapid sampling intervals [81,93,94].

1.5 Scope of This Research

This research focuses on extending the use of microdialysis sampling with the development of a multiple probe approach to simultaneously implant probes in different layers of the rat stomach. Initially, methods for a four-probe design in the stomach lumen, mucosa, submucosa and in blood were developed in the normal rat stomach. This design was further extended to developing a multiple-probe approach of implanting probes to compare both normal and ulcerated tissue of the same rat stomach. The significance of this multiple probe approach was determined by studying drug absorption through both the normal and ulcerated stomach.

The hypothesis is that since the stomach tissue is heterogeneous, different analyte concentrations would be expected between the tissue layers. A difference would also be expected when comparing tissue types (*i.e.* healthy versus diseased tissue). Probe implantation methods developed within the different layers or into different tissue types would improve sampling methods in the stomach. The significance of sampling by this approach was determined by monitoring drug concentration in each of the studied sites after three test compounds with differing degrees of absorption in the rat stomach were dosed. The ultimate aim of this research was to extend this technique to implant multiple probes within the intestines. Multiple probes implanted in several points throughout the GI tract can be used as a technique to determine the location and extent of absorption in the GI tract drug development studies. Currently, this cannot fully be assessed by the techniques mentioned in Section 1.3. The stomach is the first possible segment of the GI tract for significant absorption to occur, so methods of probe implantation were developed in the stomach for this research.

Development of the multiple-probe design of microdialysis sampling in both the normal and ulcerated rat stomach is discussed in Chapter Two. Results of using this design to study drug absorption in both the normal and ulcerated stomach are presented in Chapter Three. The summary and future goals for this research are described in Chapter Four.

1.6 References

- [1] Hing, E.; Cherry, D. A.; Woodwell, D. A., National Ambulatory Medical Care Survey: 2004 Summary. *Advance data from vital and health statistics* **2006**, (374).
- [2] Shargel, L.; Yu, A. B. C., *Applied Biopharmaceutics & Pharmacokinetics*. New York, 1999.
- [3] Hillery, A. M., Drug delivery: the basic concepts. In *Drug Delivery and Targeting for Pharmacists and Pharmaceutical Scientists*, Hillery, A. M.; Lloyd, A. W.; Swarbrick, J., Eds. Taylor & Francis, Inc.: New York, 2001; pp 1-48.
- [4] Fernandes, P. P., Rapid desensitization for needle phobia. *Psychosomatics* **2003**, 44, (3), 253-254.
- [5] Kergueris, M. F.; Bourin, M.; Larousse, C.; Lasserre, M. P.; Ortega, A., Effects of administration route on pharmacokinetics of aspirin in the rabbit. *Methods and Finding in Experimental and Clinical Pharmacology* **1988**, 10, (3), 171-175.
- [6] Bochner, F.; Williams, D. B.; Morris, P. M. A.; Siebert, D. M.; Lloyd, J. V., Pharmacokinetics of low-dose oral modified release, soluble and intravenous aspirin in man, and effects on platelet function. *European Journal of Clinical Pharmacology* **1988**, 35, 287-294.
- [7] Aarons, L.; Hopkins, K.; Rowland, M.; Brossel, S.; Thiercelin, J.-F., Route of administration and sex differences in the pharmacokinetics of aspirin, administered as its lysine salt. *Pharmaceutical Research* **1989**, 6, (8), 660-666.
- [8] Magee, D. F.; Dalley II, A. F., *Digestion and the Structure and Function of the Gut*. Karger: Basel, 1986; Vol. 8.
- [9] Konishi, Y.; Zhao, Z.; Shimizu, M., Phenolic acids are absorbed from the rat stomach with different absorption rates. *Journal of Agricultural and Food Chemistry* **2006**, 54, (20), 7539-7543.
- [10] Vanzo, A.; Cecotti, R.; Vrhovsek, U.; Torres, A. M.; Mattivi, F.; Passamonti, S., The fate of trans-caftaric acid administered into the rat stomach. *Journal of Agricultural and Food Chemistry* **2007**, 55, (4), 1604-1611.

- [11] Lee, V. H. L.; Yang, J. J., Oral drug delivery. In *Drug Delivery and Targeting for Pharmacists and Pharmaceutical Scientists*, Hillery, A. M.; Lloyd, A. W.; Swarbrick, J., Eds. Taylor & Francis: New York, 2001; pp 145-183.
- [12] Levine, M. S., Peptic Ulcers. In *Textbook of Gastrointestinal Radiology*, 2nd ed.; Gore, R. M.; Levine, M. S.; Bralow, L., Eds. WB Saunders: Philadelphia, 2000; pp 511-545.
- [13] Makola, D.; Peura, D. A.; Crowe, S. E., Helicobacter pylori infection and related gastrointestinal diseases. *Journal of Clinical Gastroenterology* **2007**, 41, (6), 548-558.
- [14] Thompson, W. G., *The Ulcer Story: The Authoritative Guide to Ulcers, Dyspepsia, and Heartburn*. Plenum Press: New York, 1996.
- [15] Caldwell, S. H.; McCallum, R. W., Hypothesis of peptic ulcer: a modern classification of a multifactorial disease. In *Pharmacology of Peptic Ulcer Disease*, Collen, M. J.; Benjamin, S. B., Eds. Springer-Verlag: New York, 1991; pp 189-228.
- [16] Yuan, Y.; Padol, I. T.; Hunt, R. H., Peptic ulcer disease today. *Nature Clinical Practice Gastroenterology & Hepatology* **2006**, 3, (2), 80-89.
- [17] Vergara, M.; Vallve, M.; Gisbert, J. P.; Calvet, X., Meta-analysis: comparative efficacy of different proton-pump inhibitors in triple therapy for Helicobacter pylori eradication. *Alimentary Pharmacology & Therapeutics* **2003**, 18, (6), 647-654.
- [18] Goldstein, J. L.; Huang, B.; Amer, F.; Christopoulos, N. G., Ulcer recurrence in high-risk patients receiving nonsteroidal anti-inflammatory drugs plus low-dose aspirin: results of a post HOC subanalysis. *Clinical Therapeutics* **2004**, 26, (10), 1637-1643.
- [19] Wang, G. Z.; Huang, G. P.; Yin, G. L.; Zhou, G.; Guo, C. J.; Xie, C. G.; Jia, B. B.; Wang, J. F., Aspirin can elicit the recurrence of gastric ulcer induced with acetic acid in rats. *Cellular Physiology and Biochemistry* **2007**, 20, (1-4), 205-212.
- [20] Salamat-Miller, N.; Johnston, T. P., Current strategies used to enhance the paracellular transport of therapeutic polypeptides across the intestinal epithelium. *International Journal of Pharmaceutics* **2005**, 294, (1-2), 201-216.
- [21] Macheras, P.; Reppas, C.; Dressman, J. B., *Biopharmaceutics of orally administered drugs*. Ellis Horwood Limited: New York, 1995.

- [22] Waterbeemd, H. v. d., Intestinal permeability: prediction from theory. In *Oral Drug Absorption Prediction and Assessment*, Dressman, J. B.; Lennernäs, H., Eds. Marcel Dekker, Inc.: New York, 2000; Vol. 106, pp 31-49.
- [23] Wilson, C. G., Gastrointestinal transit and drug absorption. In *Oral Drug Absorption Prediction and Assessment*, Dressman, J. B.; Lennernäs, H., Eds. Marcel Dekker, Inc.: New York, 2000; Vol. 106, pp 1-10.
- [24] Abrahamsson, B., Dissolution testing in the development of oral drug products. In *Oral Drug Absorption Prediction and Assessment*, Dressman, J. B.; Lennernäs, H., Eds. Marcel Dekker, Inc.: New York, 2000; Vol. 106, pp 197-228.
- [25] Kimura, T.; Higaki, K., Gastrointestinal transit and drug absorption. *Biological & Pharmaceutical Bulletin* **2002**, 25, (2), 149-164.
- [26] Purkins, L.; Wood, N.; Kleinermans, D.; Greenhalgh, K.; Nichols, D., Effect of food on the pharmacokinetics of multiple-dose oral voriconazole. *British Journal of Clinical Pharmacology* **2003**, 56 Suppl 1, 17-23.
- [27] Singh, B. N.; Malhotra, B. K., Effects of food on the clinical pharmacokinetics of anticancer agents: underlying mechanisms and implications for oral chemotherapy. *Clinical Pharmacokinetics* **2004**, 43, (15), 1127-1156.
- [28] Corey, A. E.; Agnew, J. R.; Valentine, S. N.; Nesbitt, J. D.; Wagner, D. L.; Powell, J. H.; Thompson, G. A., Comparative oral bioavailability of azimilide dihydrochloride in the fed and fasted states. *British Journal of Clinical Pharmacology* **2000**, 49, (3), 279-282.
- [29] Yap, S. P.; Yuen, K. H.; Wong, J. W., Pharmacokinetics and bioavailability of alpha-, gamma- and delta-tocotrienols under different food status. *Journal of Pharmacy and Pharmacology* **2001**, 53, (1), 67-71.
- [30] Fagerholm, U.; Lennernaes, H., Experimental estimation of the effective unstirred water layer thickness in the human jejunum, and its importance in oral drug absorption. *European Journal of Pharmaceutical Sciences* **1995**, 3, (5), 247-253.
- [31] Wils, P.; Warnery, A.; Phung-Ba, V.; Legrain, S.; Scherman, D., High lipophilicity decreases drug transport across intestinal epithelial cells. *Journal of Pharmacology and Experimental Therapeutics* **1994**, 269, (2), 654-658.

- [32] Huang, J. D., Role of unstirred water layer in the exsorption of quinidine. *Journal of Pharmacy and Pharmacology* **1990**, 42, (6), 435-437.
- [33] Liu, S.; Tam, D.; Chen, X.; Pang, K. S., P-glycoprotein and an unstirred water layer barring digoxin absorption in the vascularly perfused rat small intestine preparation: induction studies with pregnenolone-16alpha-carbonitrile. *Drug Metabolism and Disposition* **2006**, 34, (9), 1468-1479.
- [34] Langman, M. J. S., Disease affecting drug delivery. In *Drug Delivery to the Gastrointestinal Tract*, Hardy, J. G.; Davis, S. S.; Wilson, C. G., Eds. Ellis Horwood Limited: New York, 1989; pp 221-228.
- [35] Gubbins, P. O.; Bertch, K. E., Drug absorption in gastrointestinal disease and surgery. Clinical pharmacokinetic and therapeutic implications. *Clinical Pharmacokinetics* **1991**, 21, (6), 431-447.
- [36] Tur, K. M.; Ch'ng, H.-S.; Baie, S., Effect of bioadhesive polymer on phenol red absorption in normal and ulcer rats. *International Journal of Pharmaceutics* **1997**, 156, 59-65.
- [37] Milovic, V.; Stein, J., Gastrointestinal disease and dosage form performance. In *Oral Drug Absorption Prediction and Assessment*, Dressman, J. B.; Lennernäs, H., Eds. Marcel Dekker, Inc.: New York, 2000; Vol. 106, pp 17-30.
- [38] Hamalainen, M. D.; Frostell-Karlsson, A., Predicting the intestinal absorption potential of hits and leads. *Drug Discovery Today: Technologies* **2004**, 1, (4), 397-405.
- [39] Tukker, J. J., In vitro methods for the assessment of permeability. In *Oral Drug Absorption: Prediction and Assessment*, Dressman, J. B.; Lennernas, H., Eds. Marcel Dekker, Inc.: New York, 2000; Vol. 106, pp 51-72.
- [40] Hilgendorf, C.; Spahn-Langguth, H.; Regardh, C. G.; Lipka, E.; Amidon, G. L.; Langguth, P., Caco-2 versus Caco-2/HT29-MTX co-cultured cell lines: permeabilities via diffusion, inside- and outside-directed carrier-mediated transport. *Journal of Pharmaceutical Sciences* **2000**, 89, (1), 63-75.
- [41] Mahomoodally, M. F.; Gurib-Fakim, A.; Subratty, A. H., Effect of exogenous ATP on *Momordica charantia* Linn. (Cucurbitaceae) induced inhibition of D-glucose, L-tyrosine and fluid transport across rat everted intestinal sacs in vitro. *Journal of Ethnopharmacology* **2007**, 110, (2), 257-263.

- [42] Sharma, P.; Chawla, H.; Panchagnula, R., Analytical method for monitoring concentrations of cyclosporin and lovastatin in vitro in an everted rat intestinal sac absorption model. *Journal of Chromatography B Analytical Technologies in the Biomedical and Life Sciences* **2002**, 768, (2), 349-359.
- [43] Ruan, L. P.; Chen, S.; Yu, B. Y.; Zhu, D. N.; Cordell, G. A.; Qiu, S. X., Prediction of human absorption of natural compounds by the non-everted rat intestinal sac model. *European Journal of Medicinal Chemistry* **2006**, 41, (5), 605-610.
- [44] Moazed, B.; Hiebert, L. M., An in vitro study with an Ussing chamber showing that unfractionated heparin crosses rat gastric mucosa. *Journal of Pharmacology and Experimental Therapeutics* **2007**, 322, (1), 299-305.
- [45] Gotoh, Y.; Kamada, N.; Momose, D., The advantages of the Ussing chamber in drug absorption studies. *Journal of Biomolecular Screening* **2005**, 10, (5), 517-523.
- [46] Kouritas, V. K.; Hatzoglou, C.; Foroulis, C. N.; Hevas, A.; Gourgoulisanis, K. I.; Molyvdas, P. A., Low glucose level and low pH alter the electrochemical function of human parietal pleura. *European Respiratory Journal* **2007**, 30, (2), 354-357.
- [47] Iwanaga, K.; Kushibiki, T.; Miyazaki, M.; Kakemi, M., Disposition of lipid-based formulation in the intestinal tract affects the absorption of poorly water-soluble drugs. *Biological and Pharmaceutical Bulletin* **2006**, 29, (3), 508-512.
- [48] Marier, J. F.; Pope, L. E.; Yakatan, G. J.; Berg, J. E.; Stiles, M.; Vachon, P., Influence of concomitant quinidine administration on dextromethorphan disposition in rats. *Journal of Veterinary Pharmacology Therapeutics* **2004**, 27, (2), 111-114.
- [49] Park, J. H.; Jhee, O. H.; Park, S. H.; Lee, J. S.; Lee, M. H.; Shaw, L. M.; Kim, K. H.; Lee, J. H.; Kim, Y. S.; Kang, J. S., Validated LC-MS/MS method for quantification of gabapentin in human plasma: application to pharmacokinetic and bioequivalence studies in Korean volunteers. *Biomedical Chromatography* **2007**, 21, (8), 829-835.
- [50] Sepehr, E.; Cooke, G.; Robertson, P.; Gilani, G. S., Bioavailability of soy isoflavones in rats Part I: application of accurate methodology for studying the effects of gender and source of isoflavones. *Molecular Nutrition & Food Research* **2007**, 51, (7), 799-812.

- [51] Shyr, M.-H.; Lin, L.-C.; Lin, T.-Y.; Tsai, T.-H., Determination and pharmacokinetics of evodiamine in the plasma and feces of conscious rats. *Analytica Chimica Acta* **2006**, 558, 16-21.
- [52] Guidelines for survival bleeding of mice and rats. <http://oacu.od.nih.gov/> (May 20, 2007).
- [53] Hoff, J., Methods of blood collection in the mouse. *Lab Animal* **2000**, 29, (10), 47-53.
- [54] Calderoli, S.; Frigerio, E.; James, C. A., Comparison of protein precipitation, turbulent flow and automated on-line solid phase extraction, as plasma sample preparation techniques for the determination of compound I by LC-MS-MS. *Chromatographia* **2004**, 59, (Supplement 2), S183-186.
- [55] Souverain, S.; Mottaz, M.; Cherkaoui, S.; Veuthey, J. L., Rapid analysis of fluoxetine and its metabolite in plasma by LC-MS with column-switching approach. *Analytical and Bioanalytical Chemistry* **2003**, 377, (5), 880-885.
- [56] Choi, Y., M.; Chung, S. M.; Chiou, W. L., First-pass accumulation of salicylic acid in gut tissue after absorption in anesthetized rat. *Pharmaceutical Research* **1995**, 12, (9), 1323-1327.
- [57] Shen, Q.; Lin, Y.; Handa, T.; Doi, M.; Sugie, M.; Wakayama, K.; Okada, N.; Fujita, T.; Yamamoto, A., Modulation of intestinal P-glycoprotein function by polyethylene glycols and their derivatives by in vitro transport and in situ absorption studies. *International Journal of Pharmaceutics* **2006**, 313, (1-2), 49-56.
- [58] Chung, S. Y.; Han, K. S.; Shon, S. K.; Chang, M. S.; Lee, M. G., Pharmacokinetics of a new proton-pump inhibitor, YJA-20379-8, after intravenous and oral administration to rats with streptozotocin-induced diabetes mellitus. *Journal of Pharmacy and Pharmacology* **1999**, 51, (8), 929-34.
- [59] Kaddoumi, A.; Fleisher, D.; Heimbach, T.; Li, L. Y.; Cole, S., Factors influencing regional differences in intestinal absorption of UK-343,664 in rat: possible role in dose-dependent pharmacokinetics. *Journal of Pharmaceutical Sciences* **2006**, 95, (2), 435-45.
- [60] Aggarwal, D.; Pal, D.; Mitra, A. K.; Kaur, I. P., Study of the extent of ocular absorption of acetazolamide from a developed niosomal formulation, by microdialysis sampling of aqueous humor. *International Journal of Pharmaceutics* **2007**, 338, (1-2), 21-26.

- [61] Bostrom, E.; Simonsson, U. S.; Hammarlund-Udenaes, M., In vivo blood-brain barrier transport of oxycodone in the rat: indications for active influx and implications for pharmacokinetics/pharmacodynamics. *Drug Metabolism and Disposition* **2006**, 34, (9), 1624-1631.
- [62] Brunner, M.; Dehghanyar, P.; Seigfried, B.; Martin, W.; Menke, G.; Muller, M., Favourable dermal penetration of diclofenac after administration to the skin using a novel spray gel formulation. *British Journal of Clinical Pharmacology* **2005**, 60, (5), 573-577.
- [63] Groenendaal, D.; Blom-Roosemalen, M. C.; Danhof, M.; Lange, E. C., High-performance liquid chromatography of nalbuphine, butorphanol and morphine in blood and brain microdialysate samples: application to pharmacokinetic/pharmacodynamic studies in rats. *Journal of Chromatography B Analytical Technologies in the Biomedical and Life Sciences* **2005**, 822, (1-2), 230-237.
- [64] Marchand, S.; Chenel, M.; Lamarche, I.; Couet, W., Pharmacokinetic modeling of free amoxicillin concentrations in rat muscle extracellular fluids determined by microdialysis. *Antimicrobial Agents and Chemotherapy* **2005**, 49, (9), 3702-3706.
- [65] Mathy, F. X.; Ntivunwa, D.; Verbeeck, R. K.; Preat, V., Fluconazole distribution in rat dermis following intravenous and topical application: a microdialysis study. *Journal of Pharmaceutical Sciences* **2005**, 94, (4), 770-780.
- [66] Tsai, P.; Tsai, T. H., Simultaneous determination of berberine in rat blood, liver and bile using microdialysis coupled to high-performance liquid chromatography. *Journal of Chromatography A* **2002**, 961, (1), 125-130.
- [67] Joukhadar, C.; Muller, M., Microdialysis: current applications in clinical pharmacokinetic studies and its potential role in the future. *Clinical Pharmacokinetics* **2005**, 44, (9), 895-913.
- [68] Weiss, D. J.; Lunte, C. E.; Lunte, S. M., In vivo microdialysis as a tool for monitoring pharmacokinetics. *Trends in Analytical Chemistry* **2000**, 19, (10), 606-615.
- [69] Ungerstedt, U.; Pycock, C., Functional correlates of dopamine neurotransmission. *Bulletin der Schweizerischen Akademie der Medizinischen Wissenschaften* **1974**, 30, (1-3), 44-55.

- [70] Rizell, M.; Naredi, P.; Lindner, P.; Hellstrand, K.; Sarno, M.; Jansson, P. A., Histamine pharmacokinetics in tumor and host tissues after bolus-dose administration in the rat. *Life Sciences* **2002**, 70, (8), 969-976.
- [71] Benfeldt, E.; Hansen, S. H.; Volund, A.; Menne, T.; Shah, V. P., Bioequivalence of topical formulations in humans: evaluation by dermal microdialysis sampling and the dermatopharmacokinetic method. *Journal of Investigative Dermatology* **2007**, 127, (1), 170-178.
- [72] Dabrosin, C., Increased extracellular local levels of estradiol in normal breast in vivo during the luteal phase of the menstrual cycle. *Journal of Endocrinology* **2005**, 187, (1), 103-108.
- [73] Ederoth, P.; Tunblad, K.; Bouw, R.; Lundberg, C. J.; Ungerstedt, U.; Nordstrom, C. H.; Hammarlund-Udenaes, M., Blood-brain barrier transport of morphine in patients with severe brain trauma. *British Journal of Clinical Pharmacology* **2004**, 57, (4), 427-435.
- [74] Richards, D. A.; Silva, M. A.; Murphy, N.; Wigmore, S. J.; Mirza, D. F., Extracellular amino acid levels in the human liver during transplantation: a microdialysis study from donor to recipient. *Amino Acids* **2007**, 33, (3), 429-437.
- [75] Zhao, Y.; Liang, X.; Lunte, C. E., Comparison of recovery and delivery in vitro for calibration of microdialysis probes. *Analytica Chimica Acta* **1995**, 316, 403-410.
- [76] Davies, M. I.; Cooper, J. D.; Desmond, S. S.; Lunte, C. E.; Lunte, S. M., Analytical considerations for microdialysis sampling. *Advanced Drug Delivery Reviews* **2000**, 45, 169-188.
- [77] Hansen, D. K.; Davies, M. I.; Lunte, S. M.; Lunte, C. E., Pharmacokinetic and metabolism studies using microdialysis sampling. *Journal of Pharmaceutical Sciences* **1999**, 88, (1), 14-27.
- [78] Rittenhouse, K. D.; Peiffer, R. L., Jr.; Pollack, G. M., Evaluation of microdialysis sampling of aqueous humor for in vivo models of ocular absorption and disposition. *Journal of Pharmaceutical and Biomedical Analysis* **1998**, 16, (6), 951-959.
- [79] Sorg, B. S.; Peltz, C. D.; Klitzman, B.; Dewhirst, M. W., Method for improved accuracy in endogenous urea recovery marker calibrations for microdialysis in tumors. *Journal of Pharmacological and Toxicological Methods* **2005**, 52, (3), 341-349.

- [80] Stenken, J. A.; Lunte, C. E.; Southard, M. Z.; Stahle, L., Factors that influence microdialysis recovery. Comparison of experimental and theoretical microdialysis recoveries in rat liver. *Journal of Pharmaceutical Sciences* **1997**, 86, (8), 958-966.
- [81] Shou, M.; Ferrario, C. R.; Schultz, K. N.; Robinson, T. E.; Kennedy, R. T., Monitoring dopamine in vivo by microdialysis sampling and on-line CE-laser-induced fluorescence. *Analytical Chemistry* **2006**, 78, (19), 6717-6725.
- [82] Bjartmarz, H.; Rehncrona, S., Comparison of Accuracy and Precision between Frame-Based and Frameless Stereotactic Navigation for Deep Brain Stimulation Electrode Implantation. *Stereotactic and Functional Neurosurgery* **2007**, 85, (5), 235-242.
- [83] Hebel, R.; Stromberg, M. W., *Anatomy of the Laboratory Rat*. The Williams & Wilkins Company: Baltimore, 1976.
- [84] Song, Y.; Lunte, C. E., Calibration methods for microdialysis sampling in vivo: muscle and adipose tissue. *Analytica Chimica Acta* **1999**, 400, 143-152.
- [85] Song, Y.; Lunte, C. E., Comparison of calibration by delivery versus no net flux for quantitative in vivo microdialysis sampling. *Analytica Chimica Acta* **1999**, 379, 251-262.
- [86] Lönnroth, P.; Jansson, P. A.; Smith, U., A microdialysis method allowing characterization of intercellular water space in humans. *American Journal of Physiology* **1987**, 253, (16), E228-E231.
- [87] Scheller, D.; Kolb, J., The internal reference technique in microdialysis: a practical approach to monitoring dialysis efficiency and to calculating tissue concentration from dialysate samples. *Journal of Neuroscience Methods* **1991**, 40, 31-38.
- [88] Lanckmans, K.; Van Eeckhaut, A.; Sarre, S.; Smolders, I.; Michotte, Y., Capillary and nano-liquid chromatography-tandem mass spectrometry for the quantification of small molecules in microdialysis samples: comparison with microbore dimensions. *Journal of Chromatography A* **2006**, 1131, (1-2), 166-175.
- [89] Shackman, H. M.; Shou, M.; Cellar, N. A.; Watson, C. J.; Kennedy, R. T., Microdialysis coupled on-line to capillary liquid chromatography with tandem mass spectrometry for monitoring acetylcholine in vivo. *Journal of Neuroscience Methods* **2007**, 159, (1), 86-92.

- [90] Bengtsson, J.; Jansson, B.; Hammarlund-Udenaes, M., On-line desalting and determination of morphine, morphine-3-glucuronide and morphine-6-glucuronide in microdialysis and plasma samples using column switching and liquid chromatography/tandem mass spectrometry. *Rapid Communications in Mass Spectrometry* **2005**, 19, (15), 2116-2122.
- [91] Pickl, K. E.; Magnes, C.; Bodenlenz, M.; Pieber, T. R.; Sinner, F. M., Rapid online-SPE-MS/MS method for ketoprofen determination in dermal interstitial fluid samples from rats obtained by microdialysis or open-flow microperfusion. *Journal of Chromatography B* **2007**, 850, (1-2), 432-439.
- [92] Zang, X.; Luo, R.; Song, N.; Chen, T. K.; Bozigian, H., A novel on-line solid-phase extraction approach integrated with a monolithic column and tandem mass spectrometry for direct plasma analysis of multiple drugs and metabolites. *Rapid Communications in Mass Spectrometry* **2005**, 19, (22), 3259-3268.
- [93] Hogan, B. L.; Lunte, S. M., On-line coupling of in vivo microdialysis sampling with capillary electrophoresis. *Analytical Chemistry* **1994**, 66, (5), 596-602.
- [94] Huynh, B. H.; Fogarty, B. A.; Nandi, P.; Lunte, S. M., A microchip electrophoresis device with on-line microdialysis sampling and on-chip sample derivatization by naphthalene 2,3-dicarboxaldehyde/2-mercaptoethanol for amino acid and peptide analysis. *Journal of Pharmaceutical and Biomedical Analysis* **2006**, 42, (5), 529-534.

CHAPTER TWO

Implantation of Multiple Microdialysis Probes in the Rat Stomach

2.1 Introduction

Microdialysis sampling is a well-established technique to monitor analyte concentrations in several tissues *in vivo*. An in-depth discussion of this sampling technique was presented in Section 1.4. Among the various uses of this technique, microdialysis probes have been implanted in the stomach submucosa to monitor endogenous analytes. Originally, Bunnett *et al.* implanted a bundle of 20 dialysis fibers in the submucosa of the dog stomach [1]. In order to implant the fibers in the submucosa, a long incision was made on the muscularis externa and the bundle was placed into this incision. The wound was then sutured closed over the bundle to encapsulate the fibers in the submucosal space. In other studies, this technique was extended to rabbits and rats by reducing the number of dialysis fibers in the bundle to 10 and 6 fibers, respectively [2,3]. However, this method of a long incision and suturing on the stomach was determined to be too surgically invasive. Surgical

procedures that minimize perturbation to the system under study are an important aspect of *in vivo* sampling. In 1997, Iversen *et al.* placed a rigid, concentric cannula-style microdialysis probe, discussed in Section 1.4.1.1, into the rabbit stomach submucosa [4]. The probe was implanted by puncturing the serosal surface with a needle then the probe was inserted tangentially into the antrum of the stomach. This method was successful for probe implantation in the submucosa; however, because the mucosa is a more dense tissue layer, implantation into the mucosa by this procedure would most likely damage the probe membrane, which is inserted first into the tissue. Furthermore, the use of a rigid probe in the stomach could cause tissue tearing during peristalsis or general animal movement during *in vivo* sampling. A more flexible probe would be more suitable for sampling in the stomach. Kitano *et al.* developed methods of implanting a flexible microdialysis probe in the rat stomach submucosa [5]. A 22-gauge needle was used as a guide cannula to tunnel along the submucosa. The use of a flexible probe minimized tissue tearing due to animal movement; however, the use of such a big guide needle during implantation can cause damage to the tissue upon insertion of the guide. This method of implanting probes in the stomach submucosa has been used for several other studies to monitor endogenous compounds such as histamine release from enterochromaffin-like (ECL) cells [5-9]. ECL cells; however, are located in the mucosa layer while the probes were implanted in the submucosa layer. Kitano *et al.* stated that sampling in the submucosa may not accurately represent the amount of histamine released since degradation can occur as histamine diffuses from the mucosa to the submucosa and

subsequently to the microdialysis probe [5]. The addition of sampling in the mucosa would enhance previous studies of microdialysis sampling in the stomach.

Furthermore, the ability to implant microdialysis probes simultaneously in both the mucosa and submucosa would significantly improve sampling from the stomach tissue. Even though the possibility of implanting several microdialysis probes simultaneously into one animal exists, for most studies, sampling is performed by a single or dual probe approach where a probe is implanted in the target tissue and, in some cases, also in the blood for comparison [10-13]. Microdialysis sampling from a single probe in a well-perfused, homogeneous tissue, such as the liver, results in a good representation of concentrations from the whole tissue. However, in tissues that consist of different layers (*i.e.* heterogeneous tissues) microdialysis sampling by a multiple probe approach in each layer is a more accurate approach to monitoring tissue concentrations. In a study by Mathy *et al.*, for example, microdialysis probes were implanted simultaneously in the skin dermal and subcutaneous layers to monitor skin concentrations from iontophoretically applied flurbiprofen [11]. This study reported a concentration gradient observed in the tissue with C_{\max} values of 8.7 $\mu\text{g/mL}$ and 0.5 $\mu\text{g/mL}$ flurbiprofen in the dermis and subcutaneous layers, respectively. The use of a dual-probe approach in the skin was useful to assess the differences in concentrations of these two tissue layers. Like the skin, the stomach is a heterogeneous tissue where a multiple probe approach to microdialysis sampling to monitor both the mucosa and submucosa layers would enhance the current uses of microdialysis sampling in the stomach [6,8,9].

2.2 Specific Aims of This Research

The purpose of this research was to develop a multiple probe microdialysis sampling design of implanting microdialysis probes in different regions of the stomach. A multiple probe approach to monitor several layers in the same stomach has not been reported and would be an improvement to the current uses of gastric microdialysis sampling. In the normal, healthy rat stomach, a four-probe microdialysis sampling design that targets simultaneous monitoring in the stomach lumen, mucosa, submucosa and in the blood was developed. For further application, a multiple probe approach was also utilized to implant probes simultaneously in both normal and ulcerated stomach tissue to compare healthy and diseased tissue. In this model, probes were implanted in the stomach lumen, submucosa of both normal and ulcerated tissue and in the blood. The significance of this multiple probe approach was tested by monitoring drug absorption in both normal and in ulcerated stomach models. The results from drug absorption studies will be discussed in Chapter Three.

The studies presented in this chapter pertain to the design and implantation of microdialysis probes in both the normal and ulcerated tissue. Particularly, methods of probe implantation in the mucosa and ulcer were developed since implantation in these tissues has not previously reported in the literature. In addition, determination of an appropriate ulcer model, tissue response to probe implantation and fasting methods are discussed.

2.3 Chemicals and Reagents

Ringer's solution consisted of 145 mM NaCl, 2.8 mM KCl, 1.2 mM CaCl₂ and 1.2 mM MgCl₂. Artificial gastric solution (pH 2.5-3.0) consisted of 87.4 mM NaCl, 4.0 mM KCl, 0.8 mM MgSO₄, 2.1 mM Na₂SO₄ and 19.3 mM mannitol. All chemicals for Ringer's and artificial gastric solution were purchased from Sigma (St. Louis, MO, USA) or from Fisher Scientific (Fair Lawn, NJ, USA). Water for Ringer's solution and artificial gastric solution preparation was processed through a Labconco WaterPro Plus water purification system (18 MΩ/cm) (Kansas City, MO, USA) and filtered through a 47 mm, 0.22 μm nylon filter prior to use. Isoflurane was purchased from Fort Dodge Animal Health (Fort Dodge, IA, USA). Xylazine was purchased from Lloyd Laboratories (Shenandoah, IA, USA). Acepromazine was purchased from Boehringer Ingelheim Vetmedica, Inc. (St. Joseph, MO, USA). VetBond tissue glue was purchased from 3M (St. Paul, MN, USA). Lactated Ringer's and 5% dextrose in lactated Ringer's were purchased from B Braun Medical Inc. (Irvine, CA, USA).

2.4 Microdialysis Probe Construction

Due to the flexibility of the linear microdialysis probe, this probe geometry was used for probe implantation in the stomach lumen, mucosa and submucosa. The flexible cannula style probe has been used for microdialysis sampling in the blood

and therefore, was used for implantation in the jugular vein for these studies. The procedures for probe construction for both the linear and flexible cannula probe (vascular probe) are discussed in the following sections.

2.4.1 Linear Probe

Linear microdialysis probes were fabricated in-house with modification from a previously described technique [14]. These probes were designed for implantation in the stomach lumen, mucosa and submucosa of normal and ulcerated tissue. This probe was designed in a successive fashion so the probe inlet connected to the membrane and the membrane further connected to the outlet. The components for probe fabrication were polyacrylonitrile (PAN) dialysis fiber (molecular weight cut-off (MWCO) 40 kDa, 350 μm outer diameter (o.d.) and 250 μm inner diameter (i.d.)) (Hospal Industrie, Meyzleu, France), polyimide tubing (223 μm o.d., 175 μm i.d.) (Microlumen, Inc., Tampa, FL, USA) and tygon microbore tubing (1520 μm o.d., 508 μm i.d.) (Norton Performance Plastics, Akron, OH, USA). Figure 2.1 represents linear probe construction in a stepwise manner. A six-inch piece of polyimide tubing was cut for the probe inlet and a 10-15 mm piece of PAN dialysis fiber was used for the probe membrane. As shown in Figures 2.1a and 2.1b, the inlet tubing and the membrane were joined by sliding the inlet tubing into the lumen of the membrane (≥ 2.5 mm into the membrane). A thin layer of UV glue (Ultraviolet Exposure Systems, Sunnyvale, CA, USA) coated the tubing/membrane junction. A short piece of fused silica capillary tubing (363 μm o.d., 50 μm i.d.) (Polymicro Technologies, Phoenix,

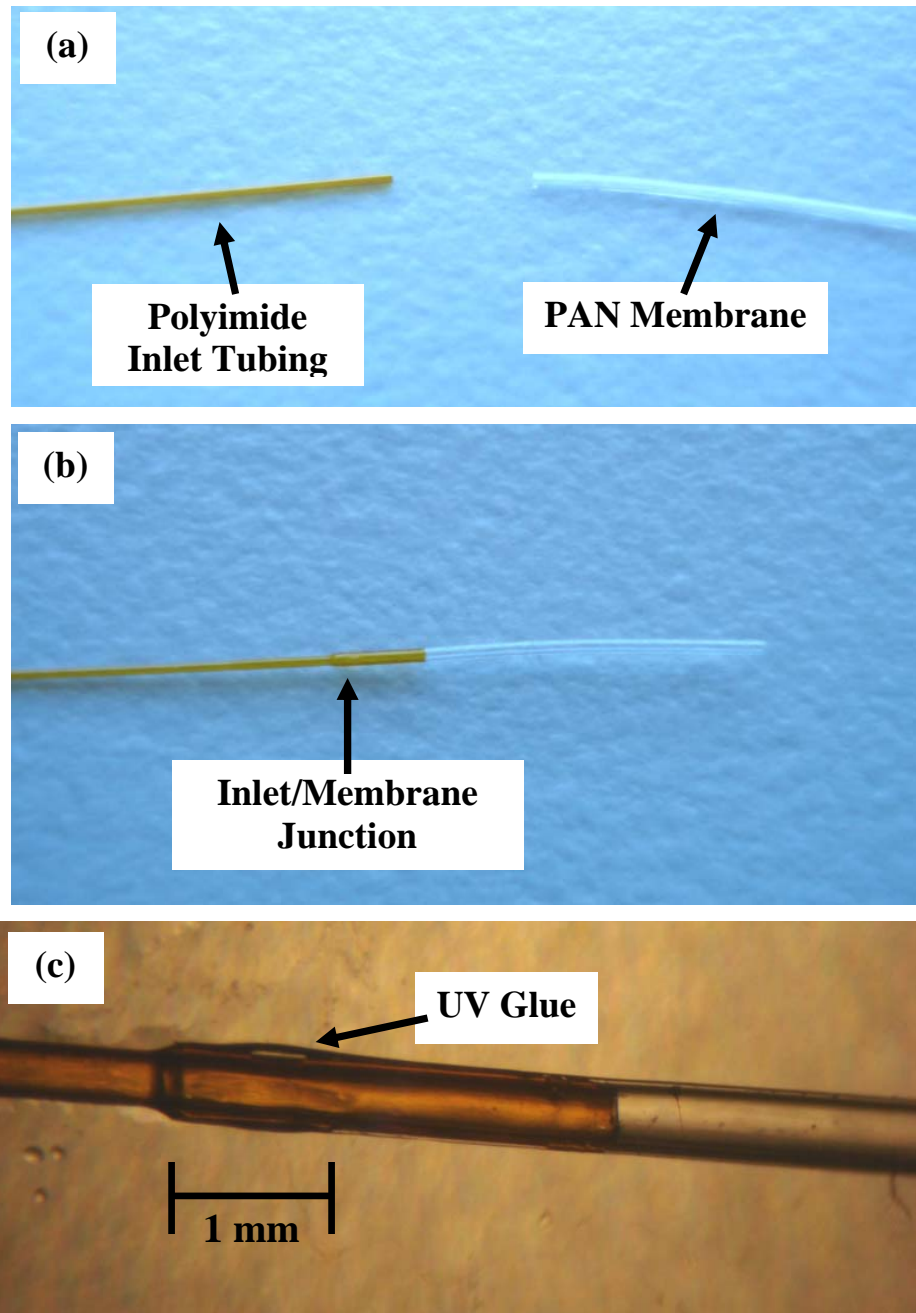


Figure 2.1. Linear microdialysis probe construction. (a) Inlet tubing and membrane, (b) inlet and membrane joined and (c) microscopic view of inlet tubing and membrane glued by UV curing (20x magnification). Figures 2.1d-f on the following page.

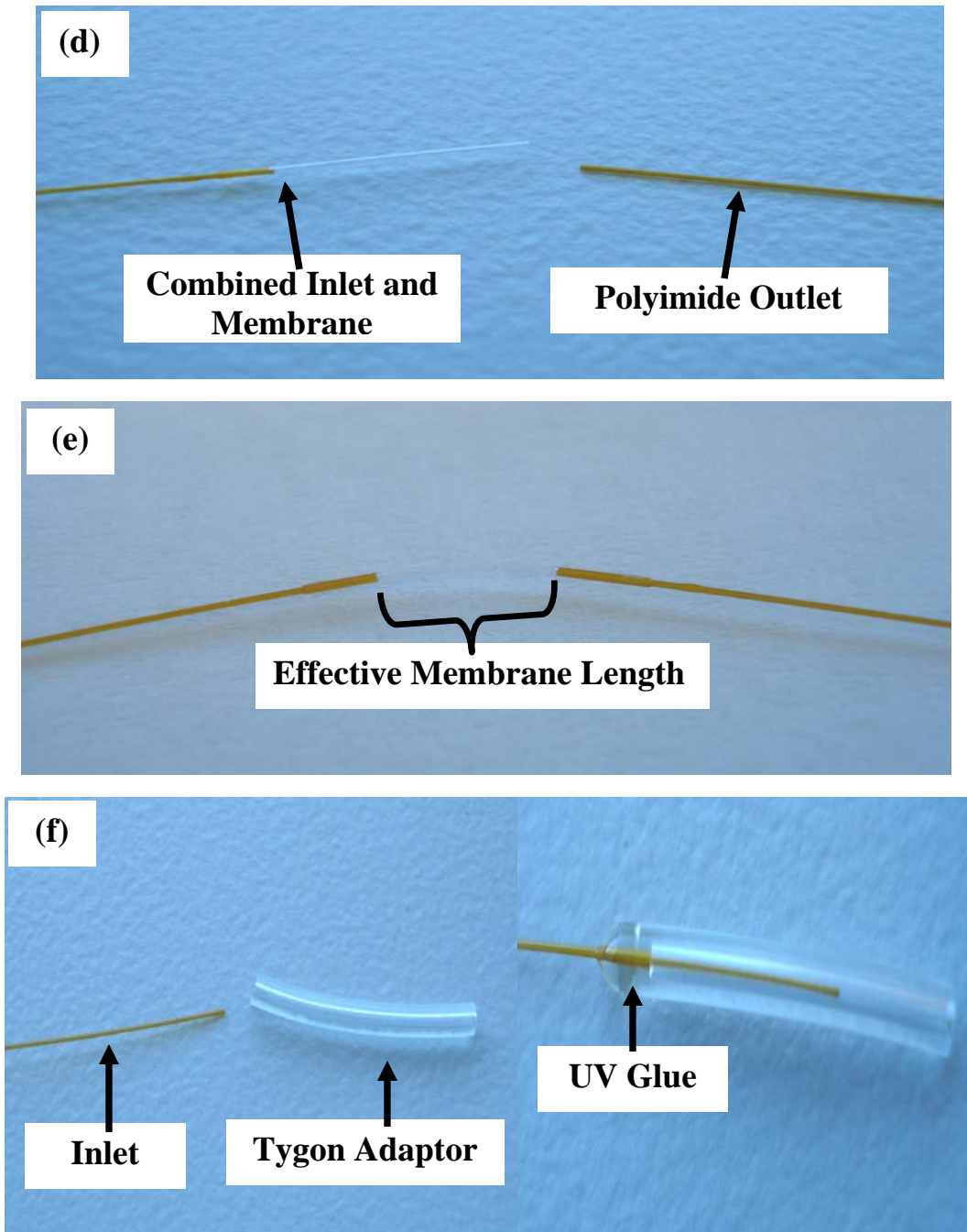


Figure 2.1 continued. Linear microdialysis probe construction. (d) Probe from Figure 2.1b and outlet tubing, (e) completed probe and (f) connection of tygon adaptor to probe inlet. Figures 2.1a-c are on the previous page.

AZ, USA) was used to apply the glue to the probe. The UV glue was set by curing with an ELC-450 UV light system (Electrolite Corporation, Bethel, CT, USA). Figure 2.1c is a view of the applied glue on the junction. A twelve-inch piece of polyimide tubing was used for the probe outlet. The probe outlet was joined to the membrane by sliding the outlet tubing into the lumen of the membrane until the effective membrane length of 5 mm was reached, shown in Figures 2.1d and 2.1e. The outlet tubing and membrane were connected at the tubing/membrane junction by UV curing as described above and shown in Figure 2.1c. To introduce perfusion fluid through the probe, an adaptor was connected to the probe inlet that could connect to a syringe of perfusion fluid. A small piece of tygon microbore tubing was slid over a small section of the probe inlet and UV glue was used to connect the two pieces, as shown in Figure 2.1f. All linear probes were stored in a sealed plastic bag and used within one week of construction.

2.4.2 Vascular Probe

Vascular microdialysis probes were fabricated in-house for implantation in the jugular vein with modification from a previously reported procedure [15]. The probe was a flexible side-by-side cannula-style probe. In this type of probe, perfusion fluid is introduced to the membrane through the probe inlet. The perfusion flows through the membrane and into an outlet chamber where the probe outlet carries the perfusion fluid out of the probe. The components for probe fabrication were PAN dialysis fiber (MWCO 40 kDa, 350 μm o.d., 250 μm i.d.) (Hospal Industrie, Meyzleu, France),

polyimide tubing (163 μm o.d., 122 μm i.d.) (Microlumen, Inc., Tampa, FL, USA), MicroRenathane® MRE-033 tubing (838 μm o.d.; 356 μm i.d.) (Braintree Scientific, Braintree, MA, USA), polyethylene tubing (PE-50) (965 μm o.d., 580 μm i.d.) (Fisher Scientific, Fair Lawn, NJ, USA) and tygon microbore tubing (1520 μm o.d., 508 μm i.d.) (Norton Performance Plastics, Akron, OH, USA). Figure 2.2 represents vascular probe construction in a stepwise manner. One end of a 15 mm piece of PAN membrane was glued closed by UV curing with an ELC-450 UV light system and UV glue. The glue was dabbed at the end of the membrane using a small piece of fused silica capillary tubing. Figure 2.2a shows the membrane before and after application of UV glue. The excessive amount of glue on the tip of the UV glued membrane was cut away with a straight edge blade. A six-inch piece of polyimide tubing was used for the probe inlet. The inlet was slid into the lumen of the membrane piece leaving a small gap between the tubing and the closed side of the membrane, as illustrated in Figures 2.2b and 2.2c. A 10 mm piece of MRE-033 tubing was used as the outlet chamber. The outlet chamber was slid over the probe inlet and was connected to the membrane piece, exposing only the effective membrane length (10 mm). This junction was joined by a small amount of UV glue, as shown in Figure 2.2d. A twelve-inch piece of polyimide tubing was used for the probe outlet and was inserted into the MRE-033 outlet chamber. As shown in Figure 2.2e, a small gap was made between the outlet tubing and the membrane in the outlet chamber. UV glue was used to close the outlet chamber, as shown in Figure 2.2f. To add extra support to the probe, a 20 mm piece of PE-50 was slid over the inlet and outlet tubing and was

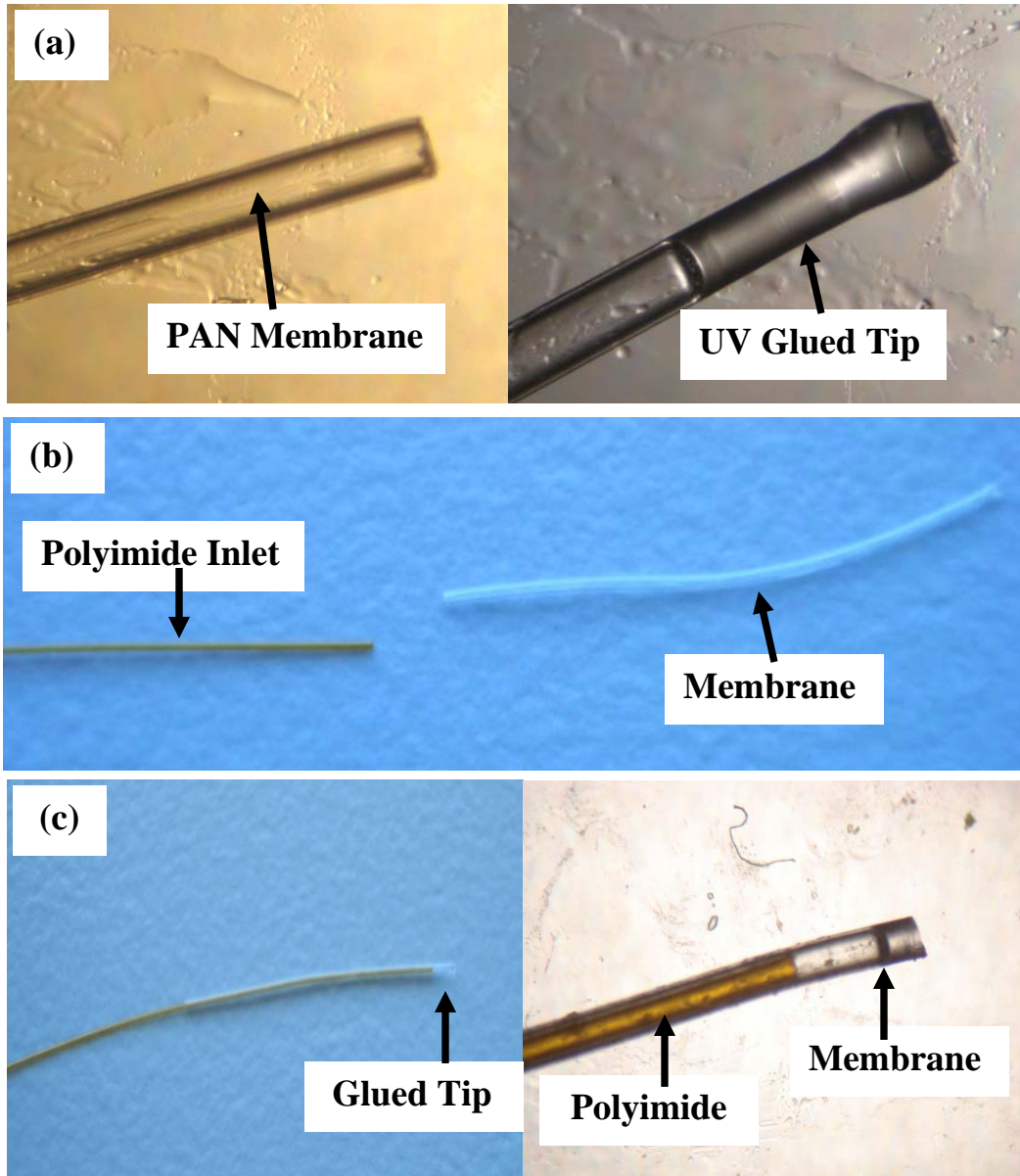


Figure 2.2. Vascular microdialysis probe construction. (a) Membrane glued closed at one end (20x magnification), (b) inlet tubing and membrane and (c) inlet slid into membrane lumen, portion of figure 20x magnification. Figures 2.2d-h are on the following pages.

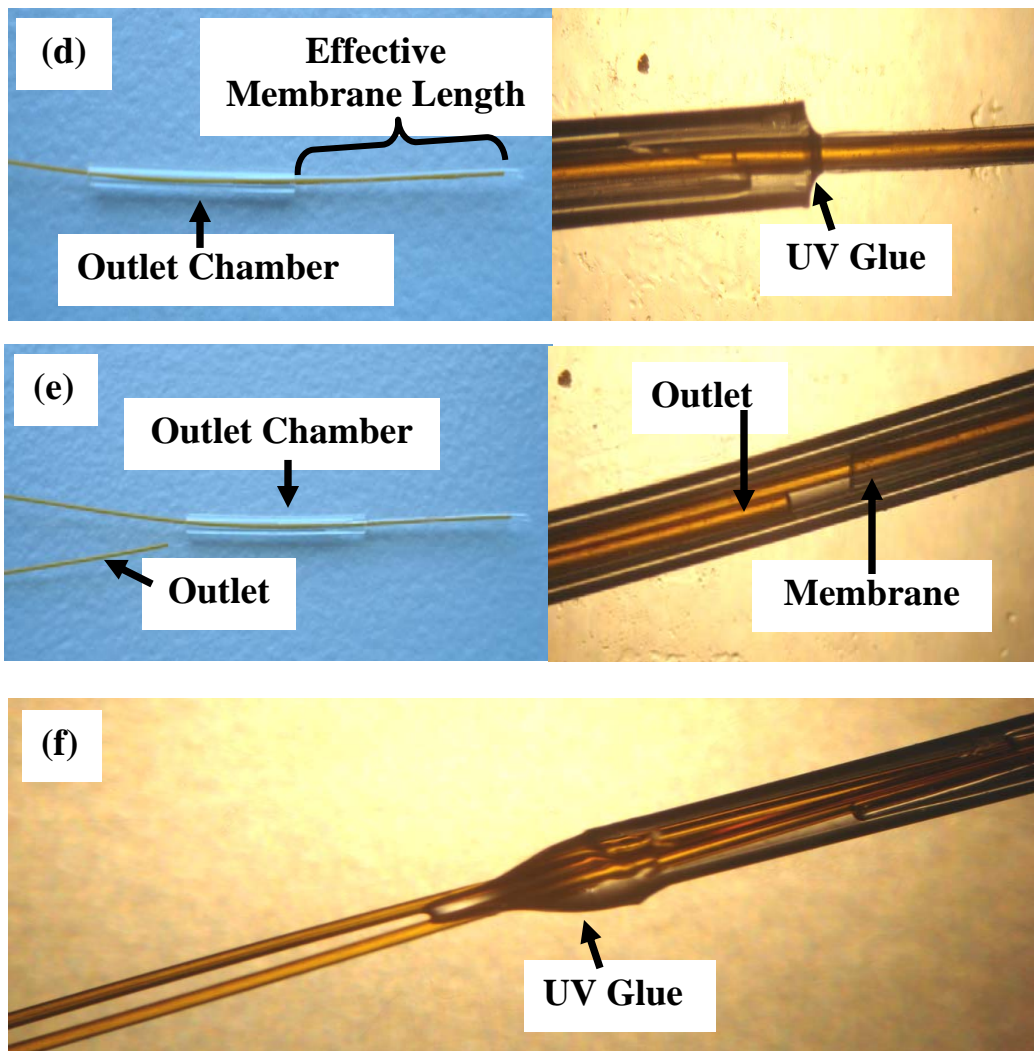


Figure 2.2 continued. Vascular microdialysis probe construction. (d) Connection of membrane to the outlet chamber, (e) insertion of probe outlet tubing into the outlet chamber and (f) closing off of the outlet chamber with UV glue. Figure 2.2f and portions of 2.2d and 2.2e at 20x magnification. Figures 2.2a-c are on the previous page and 2.2g-h are on the following page.

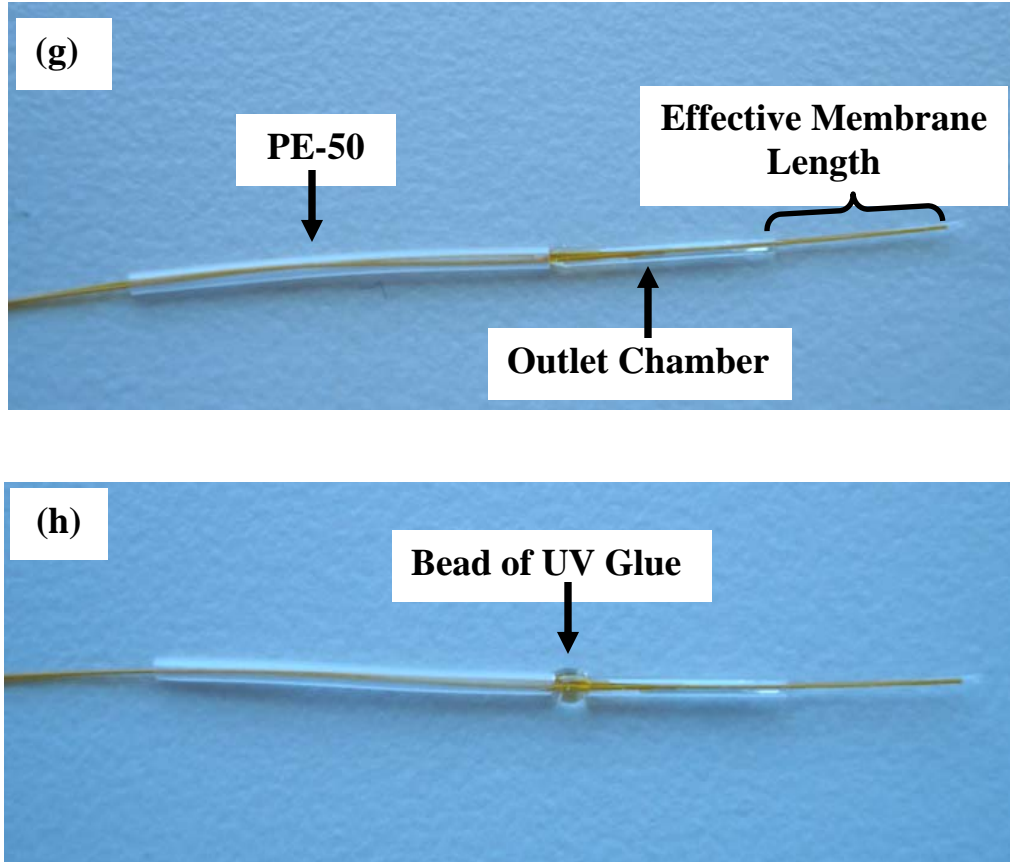


Figure 2.2 continued. Vascular microdialysis probe construction. (g) Connection of PE-50 support tubing to the outlet chamber and (h) bead of UV glue to connect the PE-50 support to the outlet chamber. Figures 2.2 a-f are on the previous pages.

connected to the outlet chamber as shown in Figure 2.2g. A bead of UV glue was added at the outlet chamber/PE-50 junction to join the pieces and also to create a stopping point for the probe when inserted into the jugular vein. A short tygon microbore tubing piece was used as an adaptor to connect the probe inlet to a syringe containing perfusion fluid. As previously described above, a small piece of tygon microbore tubing was slid over a small section of the probe inlet and UV glue was used to connect the two pieces, shown in Figure 2.1f. All vascular probes were stored in a sealed plastic bag and used within one week of construction.

2.5 Fasting Procedures

Because food and stomach particulates would interfere with microdialysis sampling in the stomach lumen, the rats were fasted prior to experimentation. From literature, a common method of fasting is to simply remove food from the animal cage for an extended period of time (24-48 hours) prior to experimentation while giving water *ad libitum* [7-9]. When this fasting procedure was performed, removal of food alone was found to not prevent coprophagy. Therefore, particulates including feces, cage bedding and hair, were found in the stomach. Several reports have utilized mesh wire bottom cages (metabolism cages) in addition to removal of food for 24-48 hours for fasting methods [6,16,17]. When using a metabolism cage for fasting, particulates and hair were still present in the stomach, indicating this fasting method was not successful in the prevention of coprophagy or self-grooming. In

addition to the physical appearance of particulates in the stomach, basal lumen dialysate samples resulted in several large unidentified peaks chromatographically as shown in Figure 2.3a.

Elizabethan collars (or cones) have been placed around the neck of animals for the prevention of self-grooming after surgery or topical application of pharmaceuticals [18-21]. Incorporation of an Elizabethan collar was added to the fasting procedure to prevent coprophagy and self-grooming. With the addition of an Elizabethan collar to fasting procedures in a metabolism cage, the previously seen interfering peaks in the lumen dialysate chromatograms were absent, as shown in Figure 2.3b. Furthermore, a complete fasting with no particulate matter or hair present in the stomach lumen was observed. Therefore, the optimized fasting procedure was to place the rat in a metabolism cage with a rodent Elizabethan collar affixed around their neck for 15-20 hours.

2.6 Designs for Multiple Probe Microdialysis Sampling in the Stomach

2.6.1 Probe Implantation in Normal Rat Stomach

To simultaneously monitor different stomach tissue layers, multiple microdialysis probes were implanted in the stomach lumen, mucosa, submucosa and also in the blood of the same rat. Female Sprague Dawley rats (225-300 grams) (Charles Rivers Laboratories, Inc., Wilmington, MA, USA) were initially housed

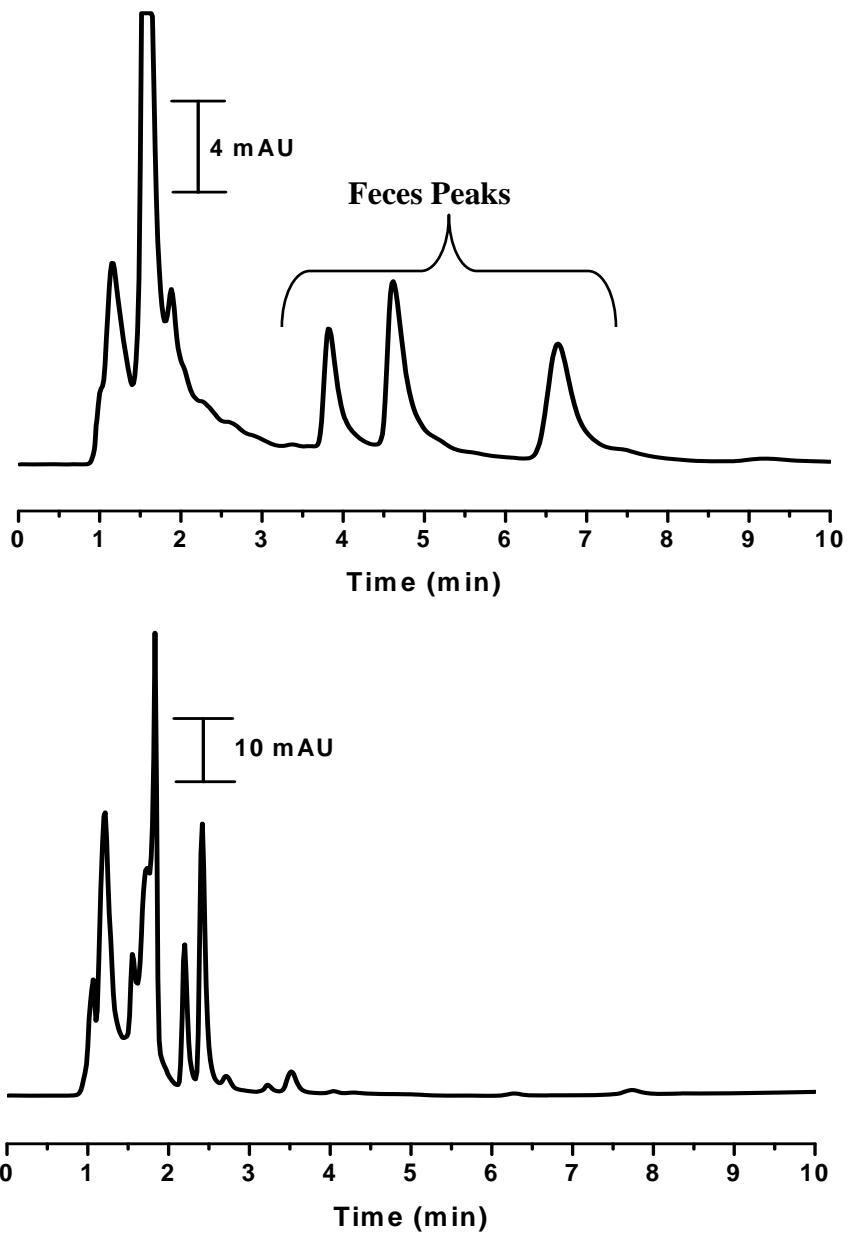


Figure 2.3. HPLC- UV chromatograms of luminal dialysate after fasting by (a) removal of food for 24 hours in a metabolism cage and (b) removal of food for 15 hours in a metabolism cage with an Elizabethan collar around the neck. Conditions: Phenomenex Synergi Polar-RP C₁₈ column (150 x 2.0 mm); 50 mM sodium phosphate (pH = 2.5) with 25% acetonitrile at 0.35 mL/min; 10 μ L injected into a 25 μ L PEEK loop; detection at 228 nm.

with access to food and water in temperature and humidity controlled rooms on a 12-hour light/dark cycle.

All experiments were in accordance with the *Principles of Laboratory Animal Care* (NIH Publication no. 85-23, revised 1985) and approved by the University of Kansas Institutional Animal Care and Use Committee (IACUC).

2.6.1.1 Linear Probe Implantation

2.6.1.1.1 Determination of Implantation Method

Because of the flexibility of the linear microdialysis probe, some type of introducer is typically used for implantation of microdialysis probe to protect it from damage during implantation. As described in Section 1.4.1.2, many studies reported implantation of linear probes in peripheral tissues with the use of a guide cannula. The guide was initially inserted into the tissue and the probe was inserted into the inside of the needle. Once the guide was removed, the probe remained implanted in the tissue. In addition, this same method was used in previous reports to implant probes in the stomach submucosa [7-9]. To protect the probe from damage during implantation, a guide needle was chosen for this research. The guide needle used for this research needed to be rigid enough to puncture into the tissue, small enough to tunnel into one tissue layer separately and also needed to have an inner diameter large enough to slide the probe into the needle lumen once the guide was implanted. Initially, the thickness of the stomach layers needed to be determined to choose the appropriate diameter guide needle.

To measure the stomach tissue layer thickness, stomach tissue with no prior perturbation to the tissue was harvested and placed in approximately 20 mL of 10% neutral buffered formalin for at least 24 hours. The specimens were taken to the pathology lab at Lawrence Memorial Hospital (Lawrence, KS, USA) where the tissue was embedded into paraffin wax blocks and tissue slices were mounted onto microscope slides. For tissue visualization, the slides were stained with hematoxylin and eosin (H and E) dyes. Under a light microscope, the stomach layer thickness was measured. Figure 2.4 shows a microscopic view of a representative histology slide of the stomach tissue and Table 2.1 shows the determined thickness of the layers of the female Sprague-Dawley rat stomach.

Rat Stomach Tissue Layer	Thickness of Layer (mm) (n = 15)
Mucosa	0.69 ± 0.28
Submucosa	0.50 ± 0.42
Muscularis Externa	0.21 ± 0.21
Entire Stomach	1.40 ± 0.49

Table 2.1. Rat stomach layer thickness

The results show that the entire stomach tissue was nearly 1.5 mm thick with approximately 50% of the tissue as mucosa and 35% of the tissue as submucosa.

The outer diameter of the linear microdialysis probes used for this research was 350 μm. Therefore, a proper size guide needle to maintain a 350 μm probe

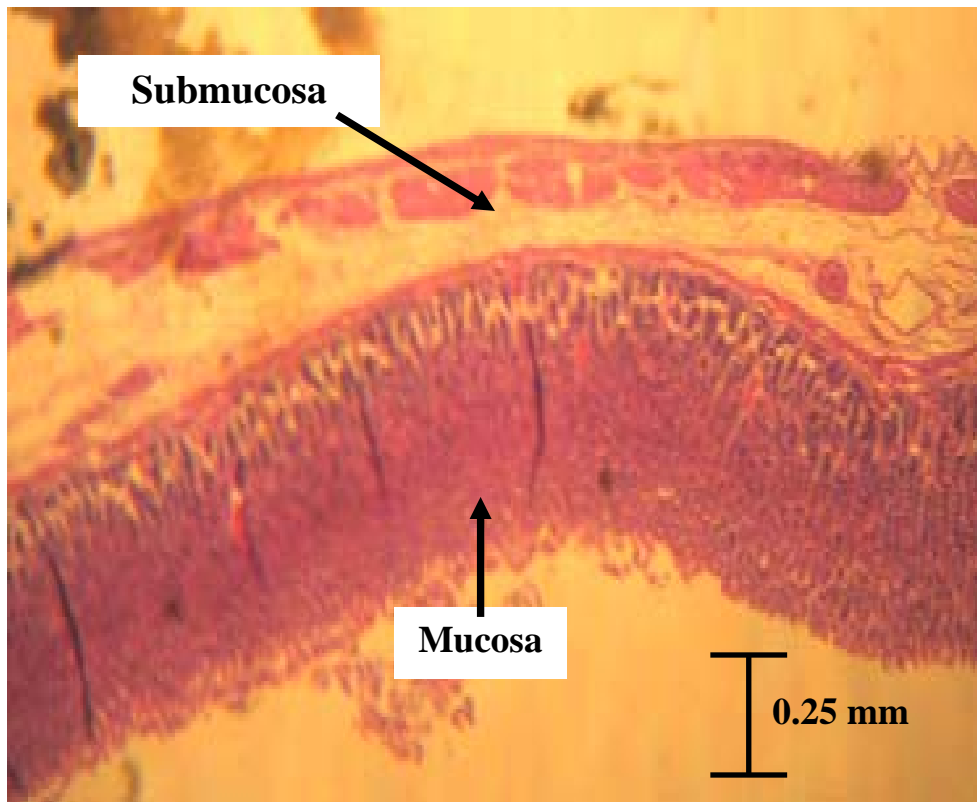


Figure 2.4. Histology image of normal stomach tissue at 40x magnification.

correctly in the mucosa layer (690 μm) and in the submucosa (500 μm) was needed. A 25-gauge needle (500 μm o.d.; 260 μm i.d.; 1.5 inch length), was found to be of a suitable diameter to implant in both the mucosa and submucosa separately and to thread the polyimide of the probe inside the needle and was chosen for implantation of linear probes in the stomach.

2.6.1.1.2 Stomach Ligation and Gavage Tube Insertion

The rats were fasted prior to probe implantation procedures to clear the stomach contents, as described above in Section 2.5. After the fasting period, the rats were pre-anesthetized by isoflurane inhalation. The rats were then given a subcutaneous injection of a ketamine (67.5 mg/kg), xylazine (3.4 mg/kg), acepromazine (0.67 mg/kg) mixture. The rat's body temperature was maintained throughout the surgery and experimentation at 37°C by placing the rat on a heating pad (CMA 150 Temperature Controller, North Chelmsford, MA, USA). Two milliliters of 2.5% dextrose in lactated Ringer's was given subcutaneously as a means to replenish fluid to the rat while under anesthesia. The hair on the abdomen and neck was shaved and excess hair was wiped away with 70% isopropyl alcohol. Anesthesia was monitored during the entire length of experimentation and intramuscular injections of 20-40 mg/kg ketamine were given as needed to maintain adequate anesthesia.

The stomach was exposed by a midline incision on the abdomen. This incision was held open with a Bowman retractor (2.5 cm spread) (Fine Science Tools, Foster City, CA, USA). To contain a constant volume of fluid in the stomach lumen,

the stomach was ligated closed at the cardiac and pyloric sphincters. Figure 2.5 shows the ligation of the pyloric sphincter. To ligate the pyloric sphincter, the stomach and duodenum junction was cleared of mesenteric tissue by gently rubbing the tissue away from the junction with a soaked cotton swab as shown in Figure 2.5a. Once the mesentery tissue was cleared, a 3-0 silk suture was threaded under the pyloric sphincter, as shown in Figure 2.5b. Figure 2.5c shows the suture tied off at the pyloric sphincter to keep the stomach contents from passing to the duodenum.

Artificial gastric solution was injected into the stomach of the anesthetized rat by a gavage tube. Figure 2.6 shows the insertion of the gavage tube and cardiac sphincter ligation. The gavage tube was a 12-14 inch piece of MRE-80 tubing (2.0 mm o.d., 1.0 mm i.d.) (Braintree Scientific, Braintree, MA, USA). As shown in Figure 2.6a, the gavage tube was passed through the mouth, down the esophagus, past the cardiac sphincter and into the stomach lumen. A 3-0 silk suture was used to ligate the cardiac sphincter to contain gastric contents in the stomach as well as hold the gavage tube in place during experimentation, as shown in Figures 2.6b and 2.6c. The exposed end of the gavage tube was connected to a blunt 18-gauge hypodermic needle that was connected to a 5 mL plastic syringe. The stomach was flushed several times with water and with artificial gastric solution until the solution in the stomach was clear. All stomach solution was removed and 3 mL of fresh gastric solution was injected into the stomach via the gavage tube. Figure 2.7 shows the fully ligated stomach with 3 mL of gastric solution injected into the stomach lumen. The procedures described up to this point were performed to prepare the stomach for

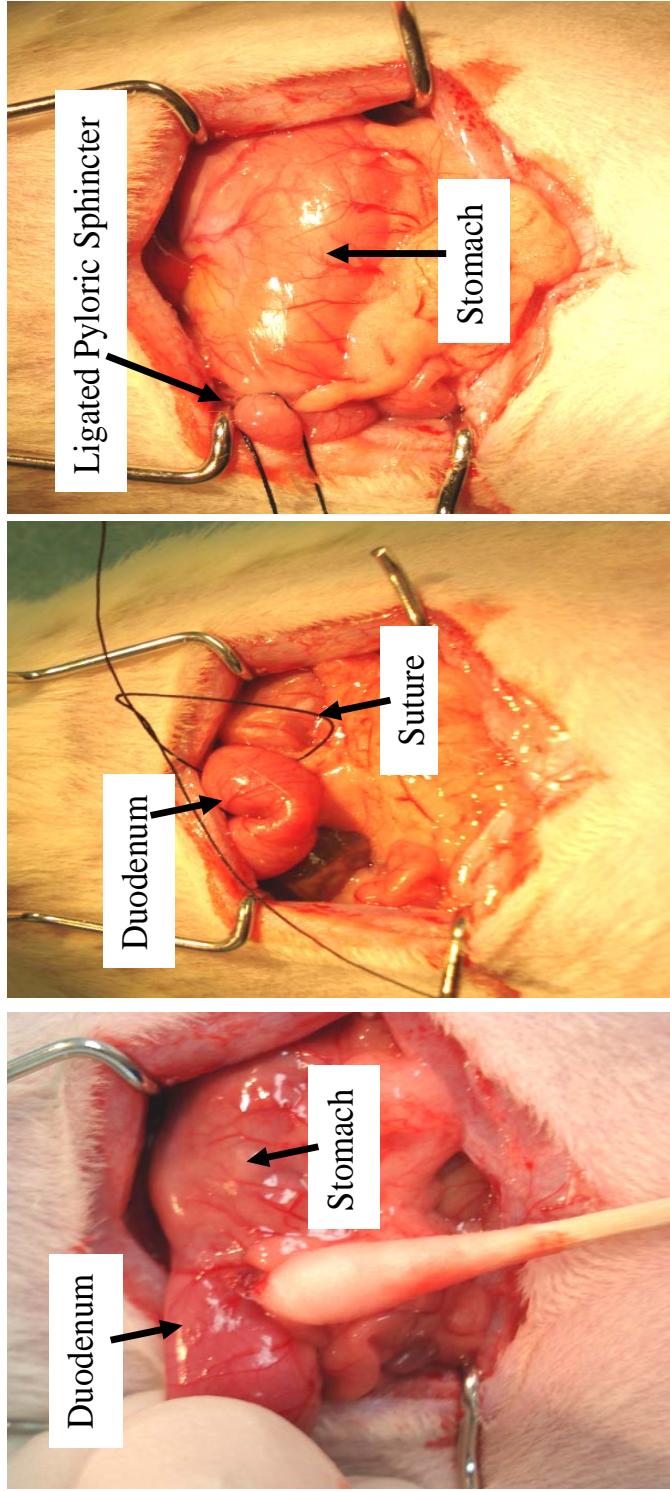


Figure 2.5. Pyloric sphincter ligation. (a) Clearing mesenteric tissue from the stomach/duodenum junction, (b) setting the suture in place for ligation and (c) a completed ligated pyloric sphincter.

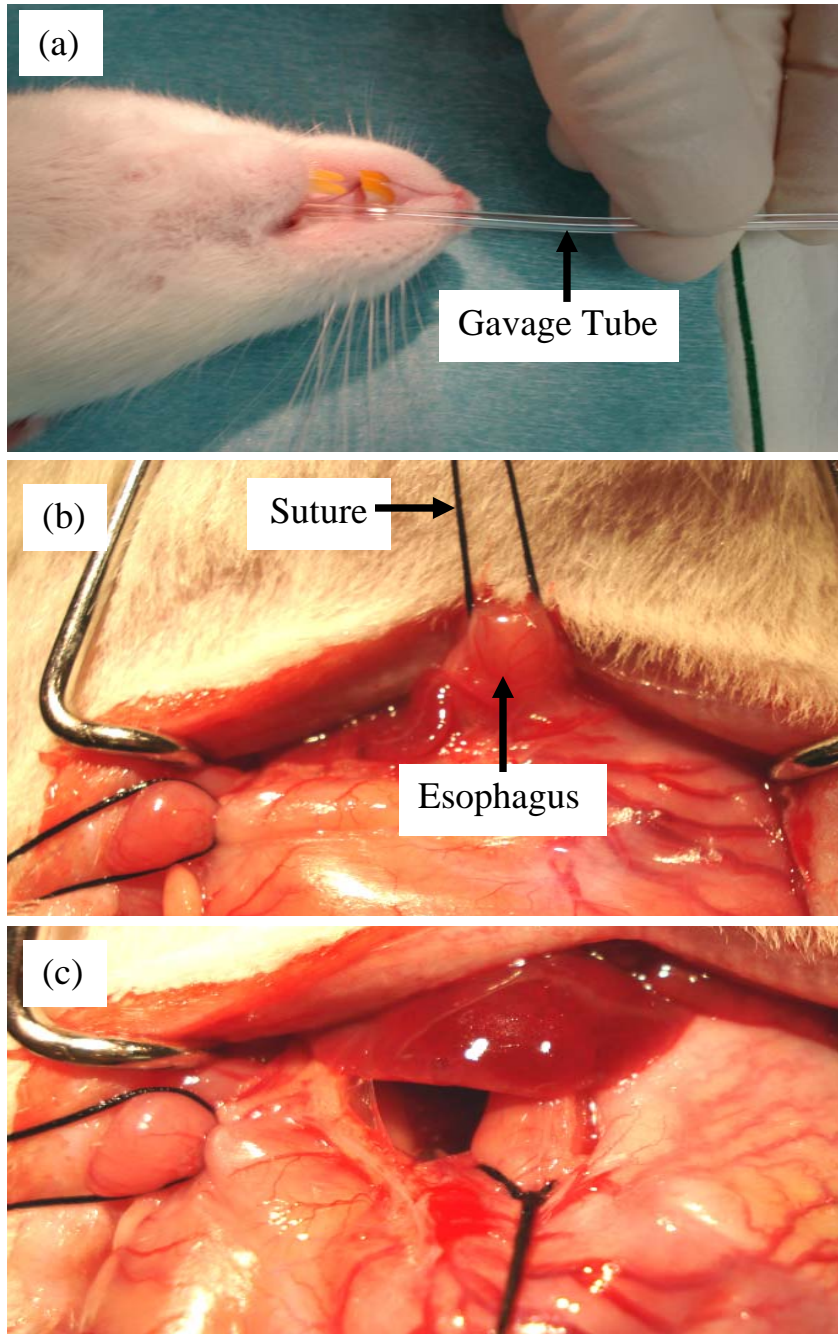


Figure 2.6. Gavage tube insertion and cardiac sphincter ligation. (a) Insertion of gavage tube through the mouth, (b) suture in place near the cardiac sphincter and (c) gavage tube ligated in place at the cardiac sphincter.

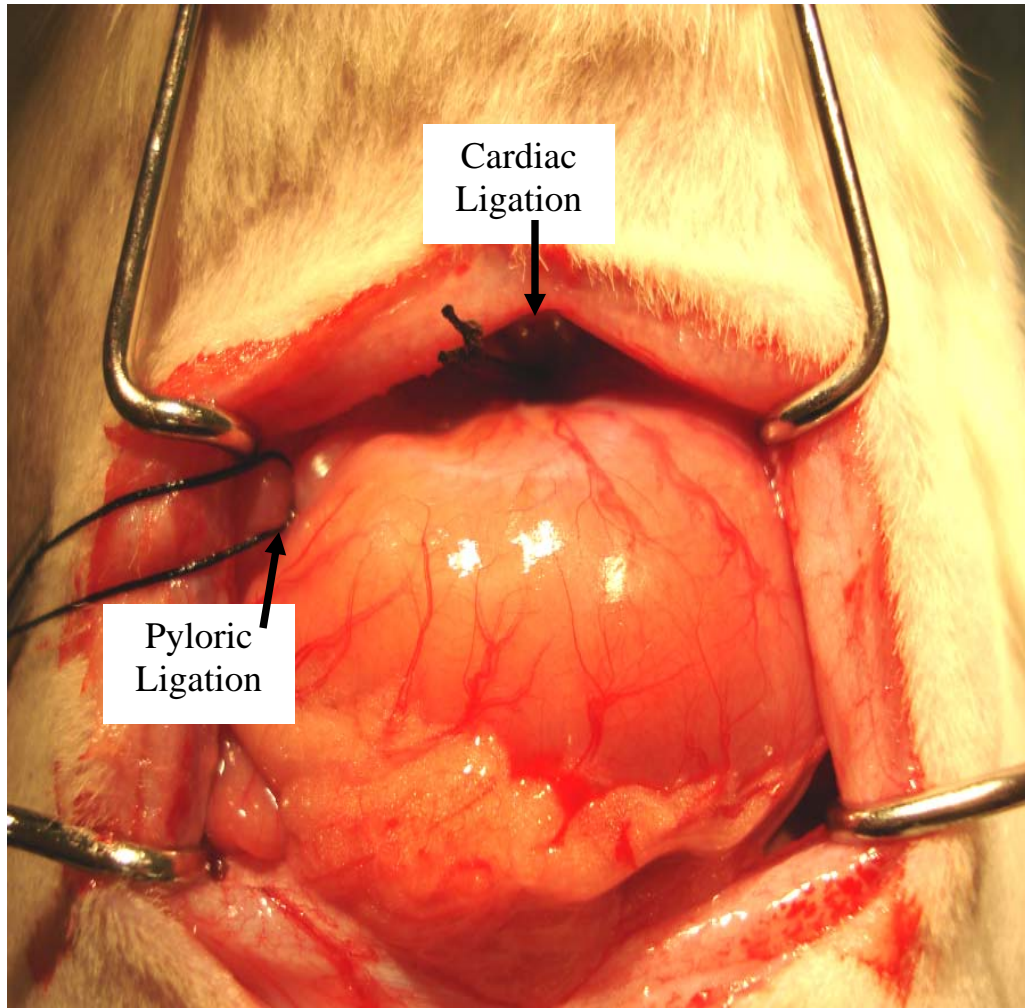


Figure 2.7. Stomach ligated at the cardiac and pyloric sphincters with 3 mL of artificial gastric solution injected into the stomach via gavage tube.

probe implantation. Probe implantation techniques in the submucosa, mucosa, lumen and blood are described in the following sections.

2.6.1.1.3 Submucosa Implantation

The submucosa and mucosa are of different tissue types, the submucosa is connective tissue and the mucosa, comprised mostly of lamina propria, is a more dense tissue relative to the submucosa [22]. The visual difference between a guide needle implanted in the submucosa and the mucosa was exploited to determine the correct layer of probe placement during the implantation procedure. The submucosa is transparent on the serosal surface of the stomach. Figure 2.8 shows the procedure of linear probe implantation in the submucosa. The stomach can be classified into four regions: the fundus, body, antrum and pylorus [22]. The body is the region of the stomach with the most surface area and also is the region where most absorption occurs in the stomach [22]. The body was therefore the target region of the stomach for probe implantation. As shown in Figure 2.8a, the guide needle (25-gauge; 1.5 inch length) punctured the stomach just below the serosal surface. The needle was clearly visible underneath the serosal surface, indicating the guide was in the submucosa. Care was taken to avoid tunneling the guide across major blood vessels that were visible on the serosal side. As shown in Figure 2.8b, the guide was tunneled through the tissue enough to ensure that the probe membrane was completely embedded in the tissue once implanted. The beveled end of the guide was used to exit the tissue. The outlet of the linear probe was then threaded through the lumen of the needle, shown in Figure 2.8c. The needle was removed from the tissue,

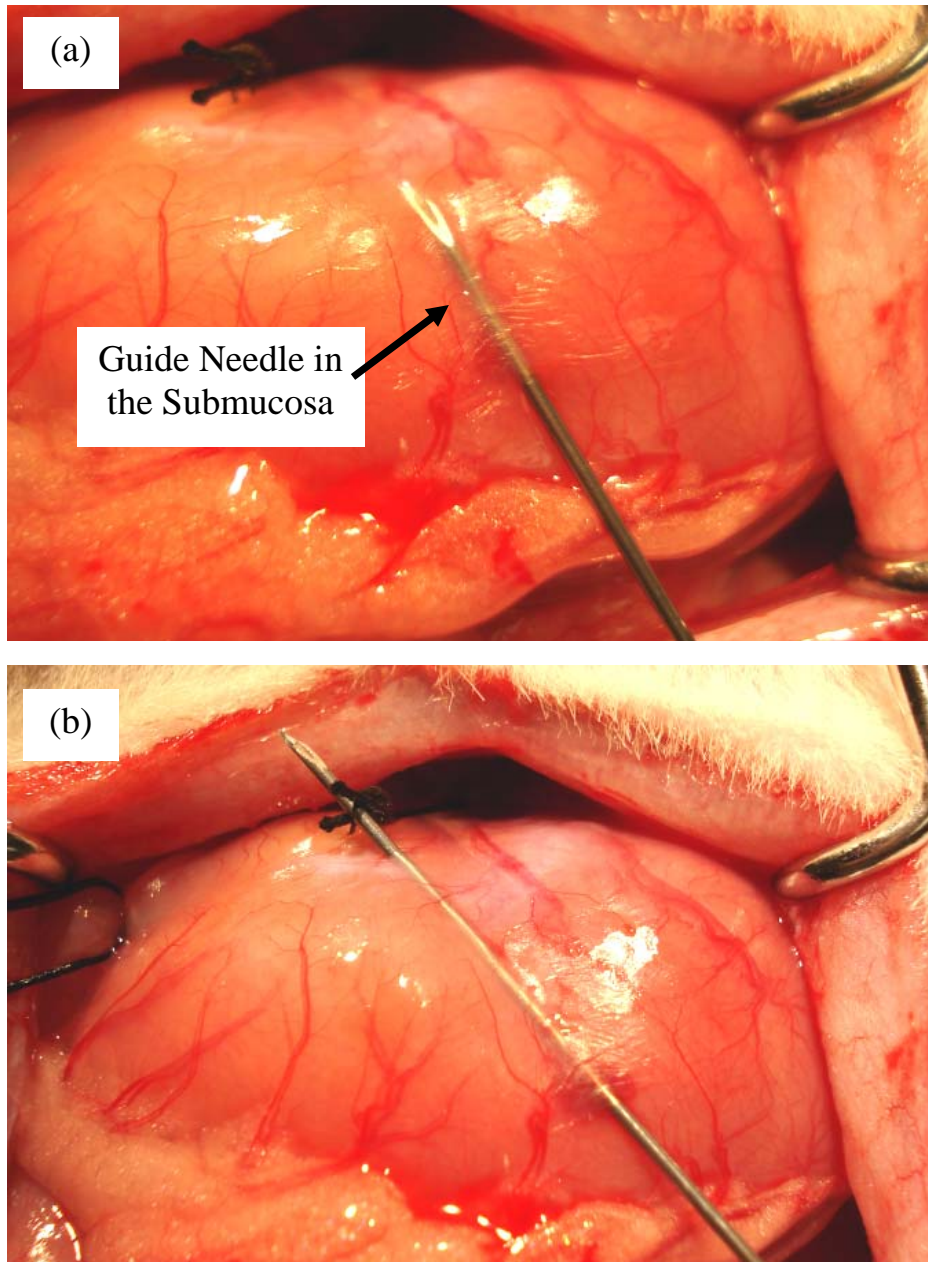


Figure 2.8. Microdialysis probe implantation in the stomach submucosa. (a) Guide needle inserted into the stomach submucosa and (b) guide needle tunneled through the submucosa and then exiting the tissue. Figures 2.7c-e on the following page.

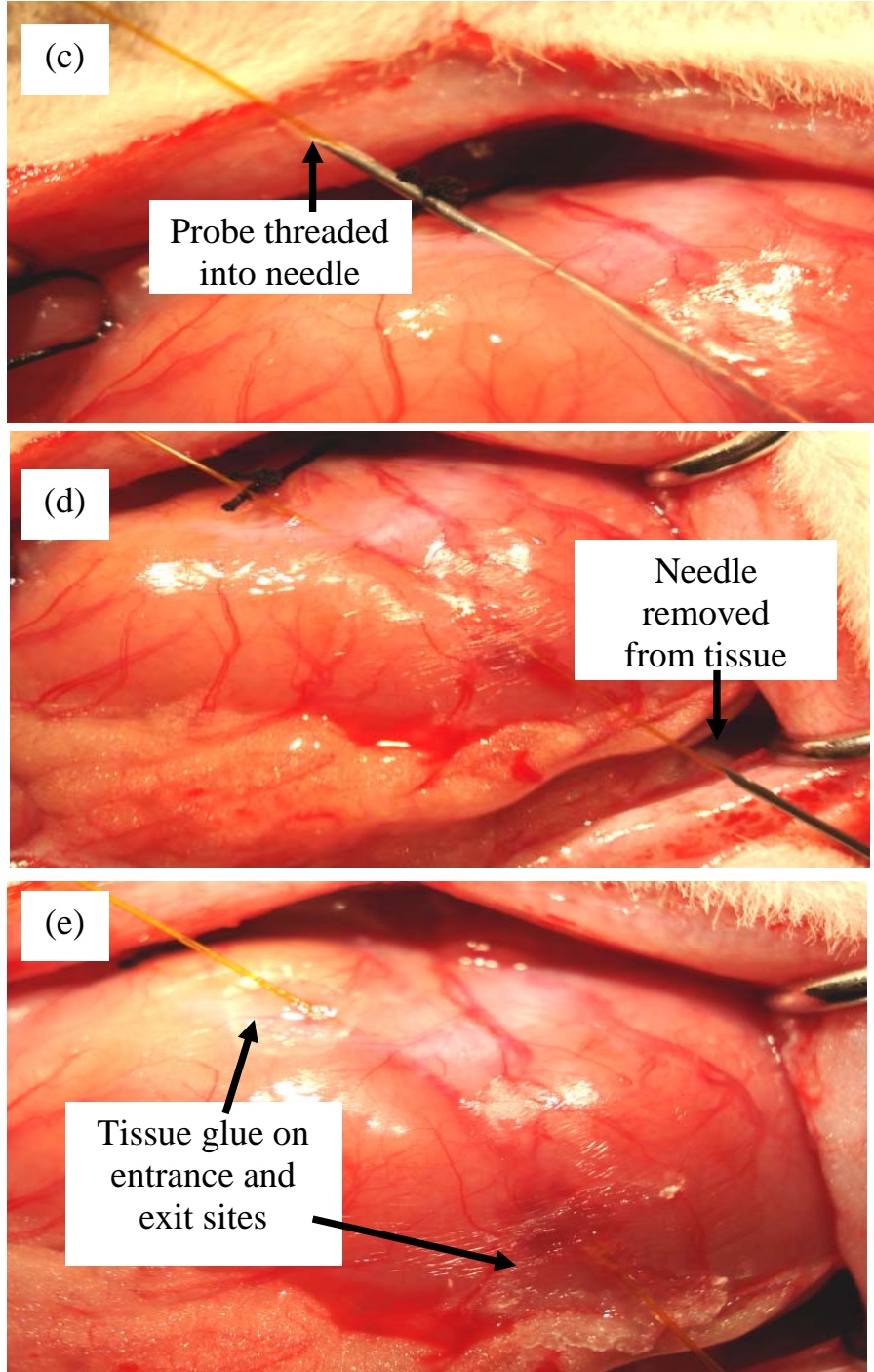


Figure 2.8 continued. Microdialysis probe implantation in the stomach submucosa. (c) Probe outlet threaded into the needle lumen, (d) Needle exiting tissue leaving probe in tissue and (e) probe implanted and secured in tissue. Figures 2.8a-b are on the previous page.

leaving only the probe embedded in the tissue, as shown in Figure 2.7d. The membrane of the probe was positioned until it was completely embedded in the tissue. Tissue glue was used to close the probe entrance and exit sites as well as hold the probe in place in the submucosa. Figure 2.8e shows the completed implantation of a linear probe in the stomach submucosa.

2.6.1.1.4 Mucosa Implantation

Linear probe implantation into the stomach mucosa was performed in the same manner as the implantation of a linear probe in the submucosa. Figure 2.9 shows the procedure of implanting a probe in the mucosa next to a probe that was previously implanted in the submucosa. As mentioned previously, the visual difference between a guide needle implanted in the mucosa relative to the submucosa was used to correctly implant probes in the appropriate layer. Because the probes were implanted by hand and because of the sub-millimeter thickness of the mucosa and submucosa layers, this visual difference between the guide implanted in each layer was imperative in determining the location for probe implantation. As illustrated in Figures 2.9a and 2.9b, when the guide needle (25-gauge, 1.5 inch length) entered and tunneled into the mucosa, the guide needle is not as visible on the serosal surface as previously seen when implanting in the submucosa (Figure 2.8a and 2.8b). After the guide needle was tunneled through the mucosa to an appropriate distance, the beveled end of the guide was used to exit the tissue. The outlet of the linear probe was then threaded into the lumen of the guide needle, as shown in Figure 2.9c. As

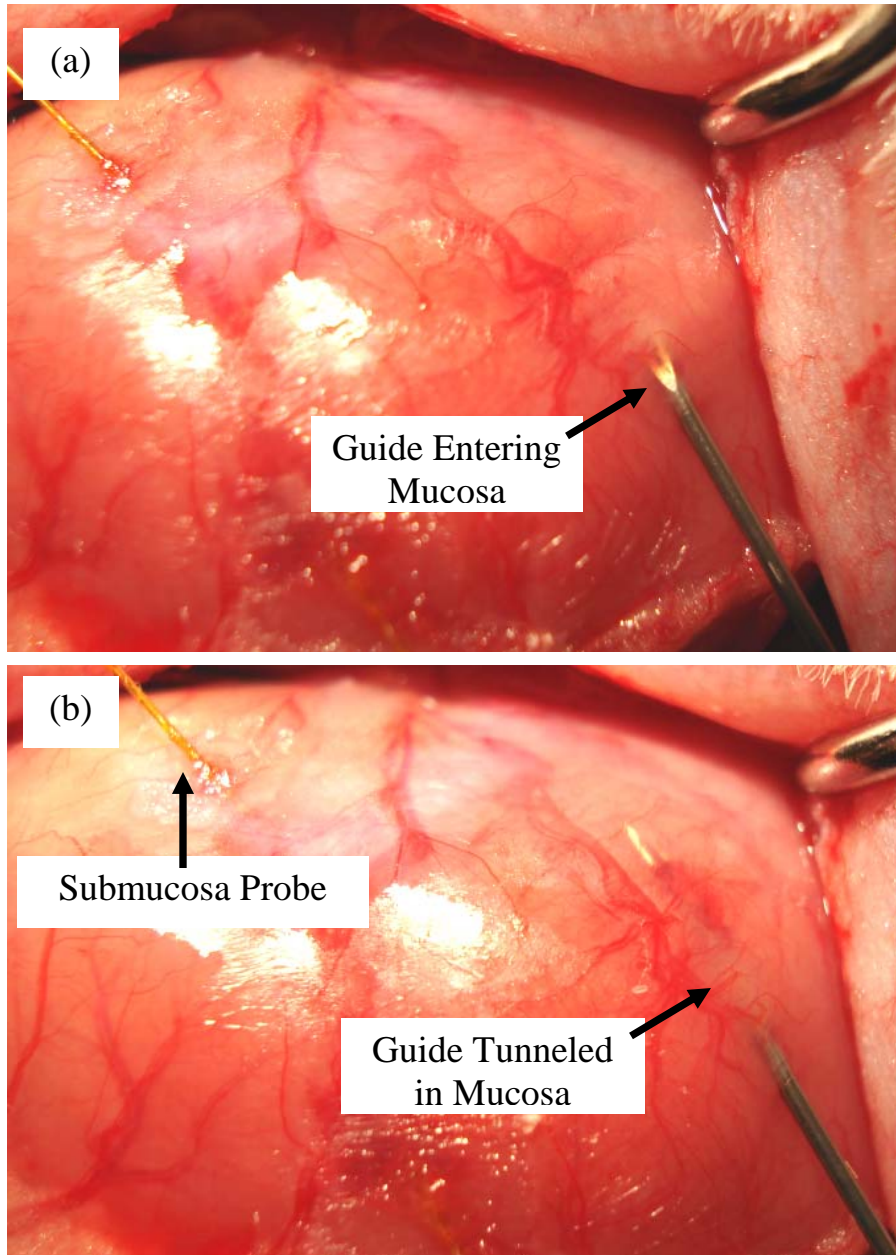


Figure 2.9. Microdialysis probe implantation in the stomach mucosa. (a) Guide needle penetrating the mucosa layer and (b) guide needle tunneled through the mucosa layer. Figures 2.9c-d are on the following page.

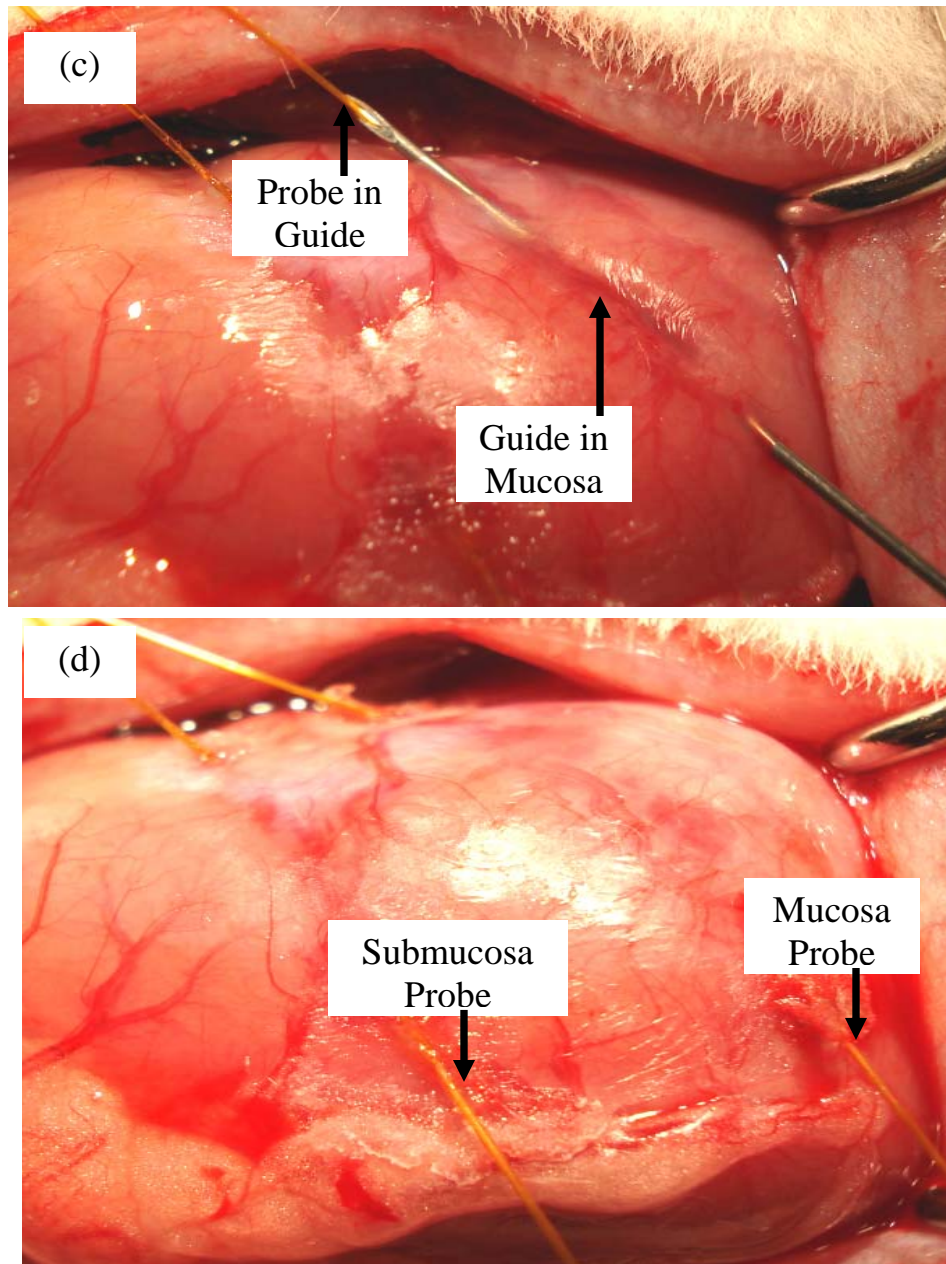


Figure 2.9 continued. Microdialysis probe implantation in the stomach mucosa. (c) Guide needed tunneled through and exited from the mucosa and probe threaded in the guide and (d) probes implanted and secured in the mucosa and submucosa. Figures 2.9a-b are on the previous page.

with the submucosal implantation, the guide needle was removed leaving the probe embedded in the mucosa. The probe was appropriately positioned so the entire probe membrane was embedded in the tissue and the entrance and exit wounds were closed with tissue glue. Figure 2.9d shows the successful implantation of linear probes implanted in both the mucosa and submucosa simultaneously in the rat stomach.

2.6.1.1.5 Lumen Implantation

A guide needle (25-gauge; 1.5 inch length) was used to implant a linear probe into the stomach lumen, similar to the previously described techniques for implantation in both the submucosa and mucosa. Figure 2.10 shows the guide needle in place in the lumen of a stomach with submucosa and mucosa probes previously implanted. With the submucosa and mucosa probes previously implanted, limited surface area on the ventral side of the stomach body remained for probe implantation in the stomach lumen. Therefore, the guide needle was inserted perpendicular to the direction of mucosa and submucosa probe implantation. As previously shown in Table 2.1, the entire stomach thickness is approximately 1.5 mm, therefore penetration of the guide needle in the lumen was not as intricate as implantation directly into the stomach tissue layers. Once the guide needle was positioned in the lumen, the probe was threaded in the needle and the needle was removed leaving only the probe in place in the lumen. As previously used for the submucosa and mucosa probe, tissue glue was used to close the entrance and exit wounds and hold the lumen probe in place.

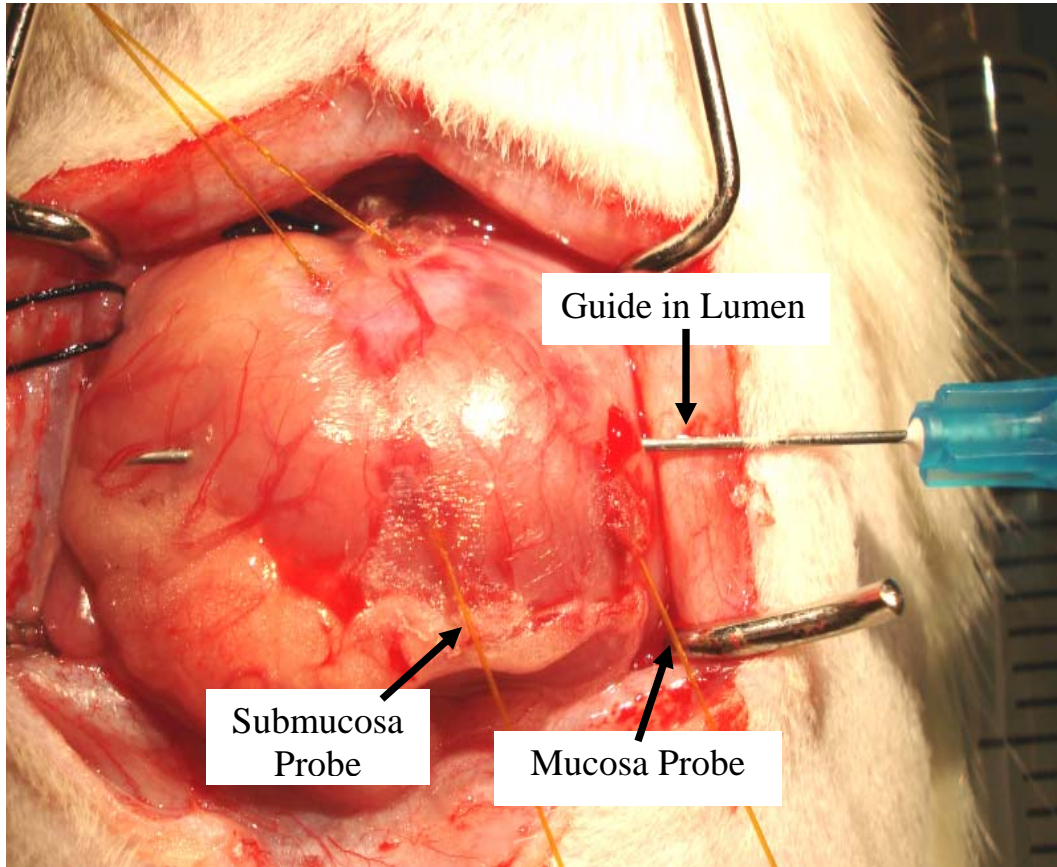


Figure 2.10. Microdialysis probe implantation in the stomach lumen.

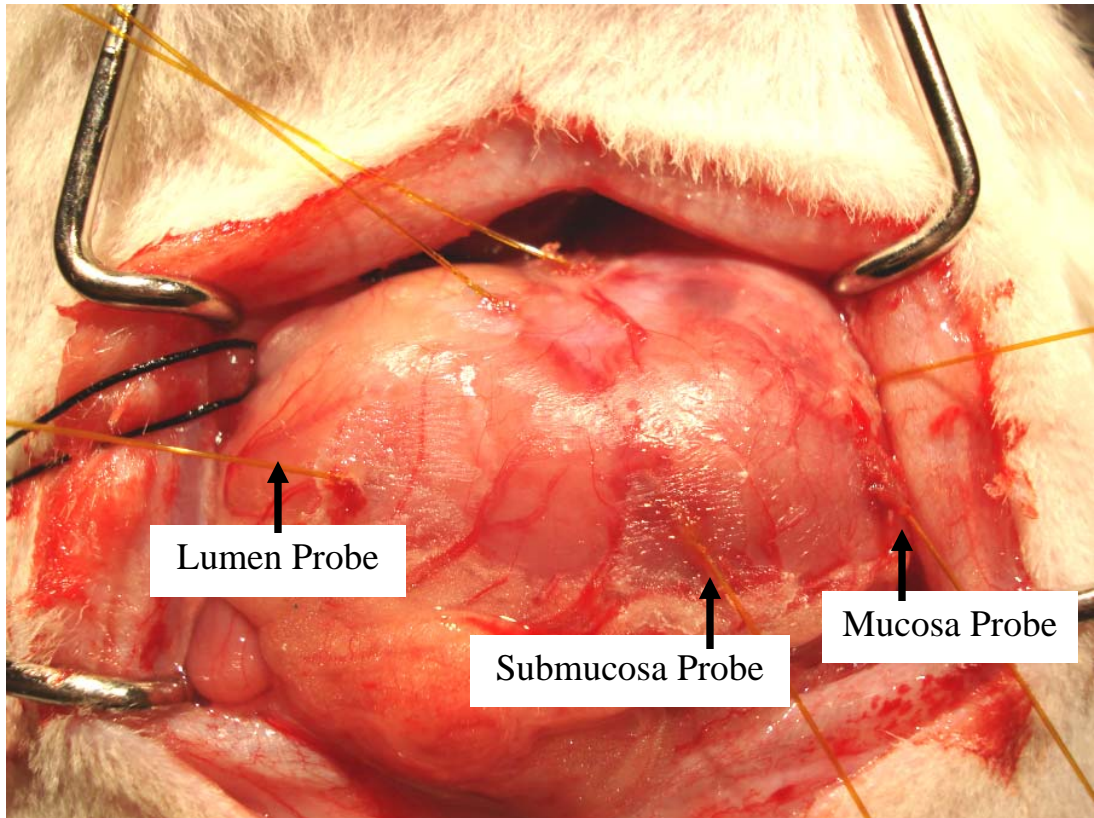


Figure 2.11. Linear microdialysis probes simultaneously implanted in the lumen, mucosa and submucosa of the rat stomach.

Figure 2.11 shows the simultaneous implantation of linear microdialysis probes simultaneously in the submucosa, mucosa and lumen of the normal rat stomach. The incision on the abdomen was covered with wetted gauze and plastic wrap to keep the abdomen hydrated during experimentation. In addition to the implantation of probes in the stomach, a vascular probe was implanted in the jugular vein of the same rat, resulting in four probe simultaneously implanted in one rat. The procedures for probe implantation in the jugular vein are described in the next section.

2.6.1.2 Vascular Probe Implantation

A flexible cannula-style probe was implanted for systemic blood sampling in rats that had linear microdialysis probes implanted in the stomach. The jugular vein was used for sampling because the vein was large enough to implant a probe into without tearing the vessel and also because the jugular vein is superficial and easily accessed. Figure 2.12 demonstrates the procedure for isolation of the jugular vein. An incision was made on the skin of the neck and adipose tissue superficial to the vein was separated to expose the right jugular vein as shown in Figure 2.12a. Extra tissue was cleaned from the vein and the vein was isolated onto a metal spatula, as shown in Figure 2.12b. Figure 2.13 shows the procedure of vascular probe implantation in the jugular vein. After isolation of the vein, a small cut was on the vein with spring scissors (Fine Science Tools, Foster City, CA, USA) as shown in Figure 2.13a. A dental pick, used as the probe guide, was inserted into the small cut made on the vessel, as shown in Figure 2.13b. The guide was gently removed while

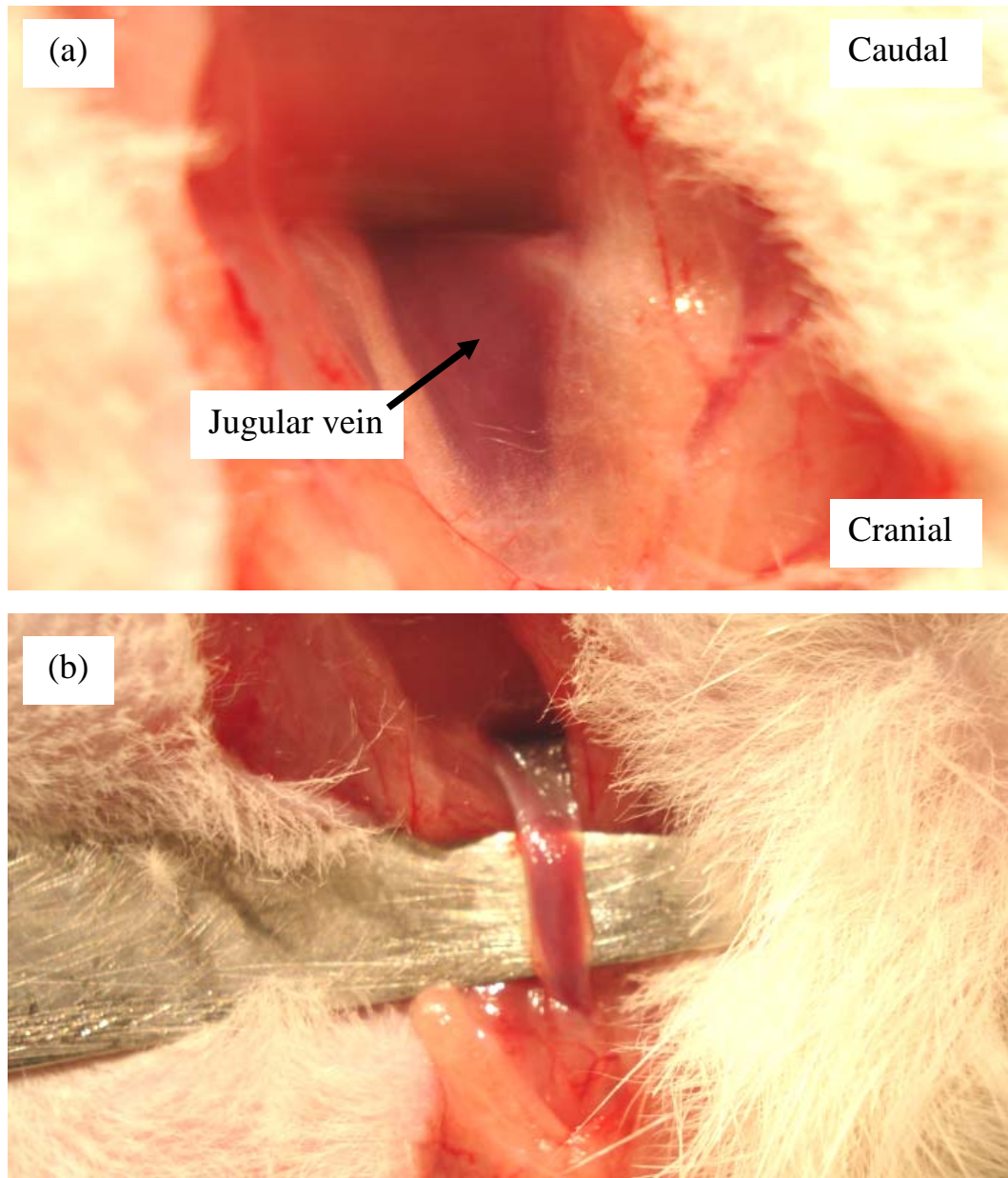


Figure 2.12. Isolation of the jugular vein. (a) Separated skin and adipose tissue to expose the jugular vein and (b) isolation of the jugular vein onto a metal spatula.

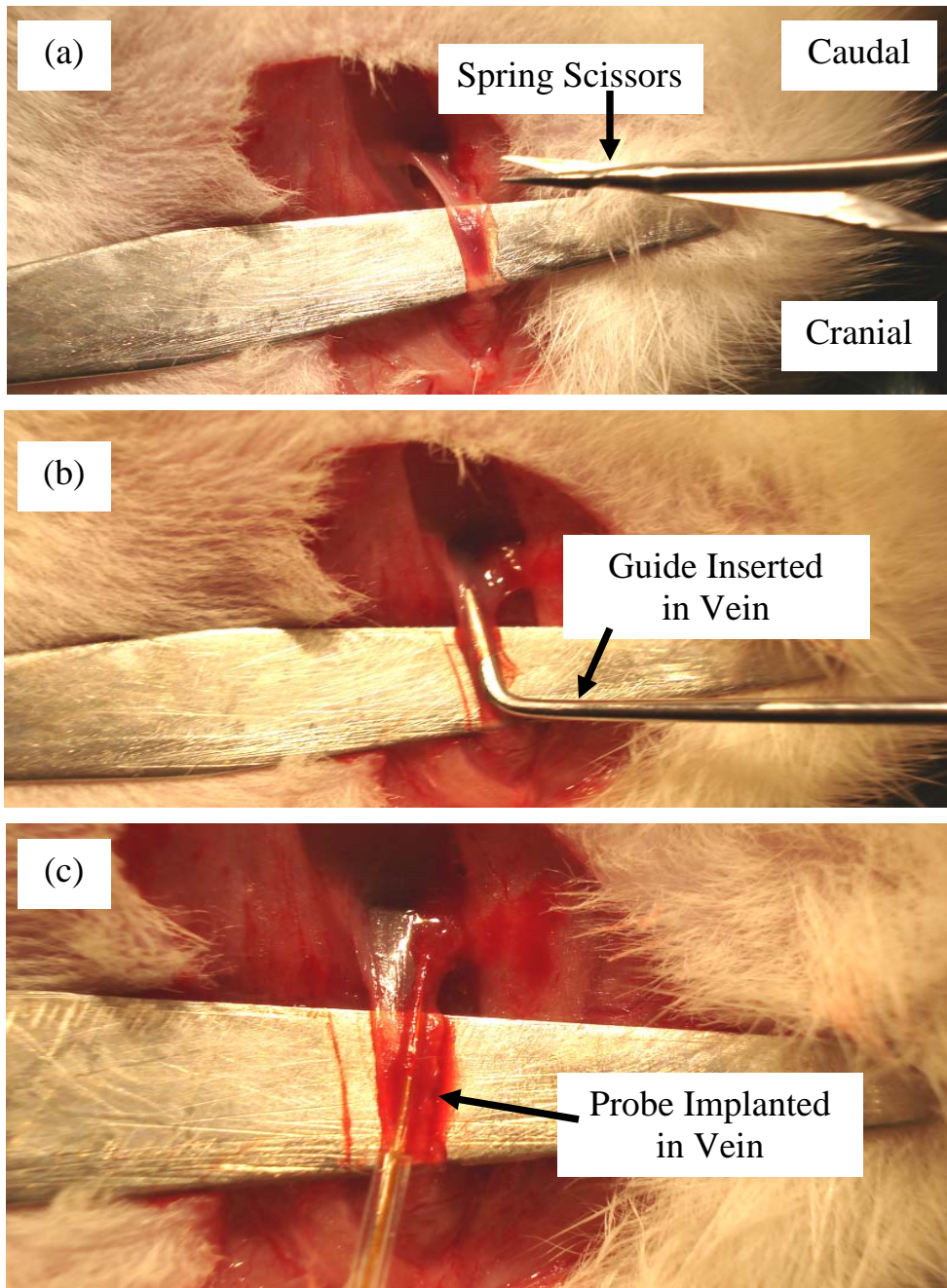


Figure 2.13. Microdialysis probe implantation in the jugular vein. (a) Making a small cut on vein, (b) insertion of a guide into the vein and (c) probe inserted into vessel. Figures 2.13d-f are on the following page.

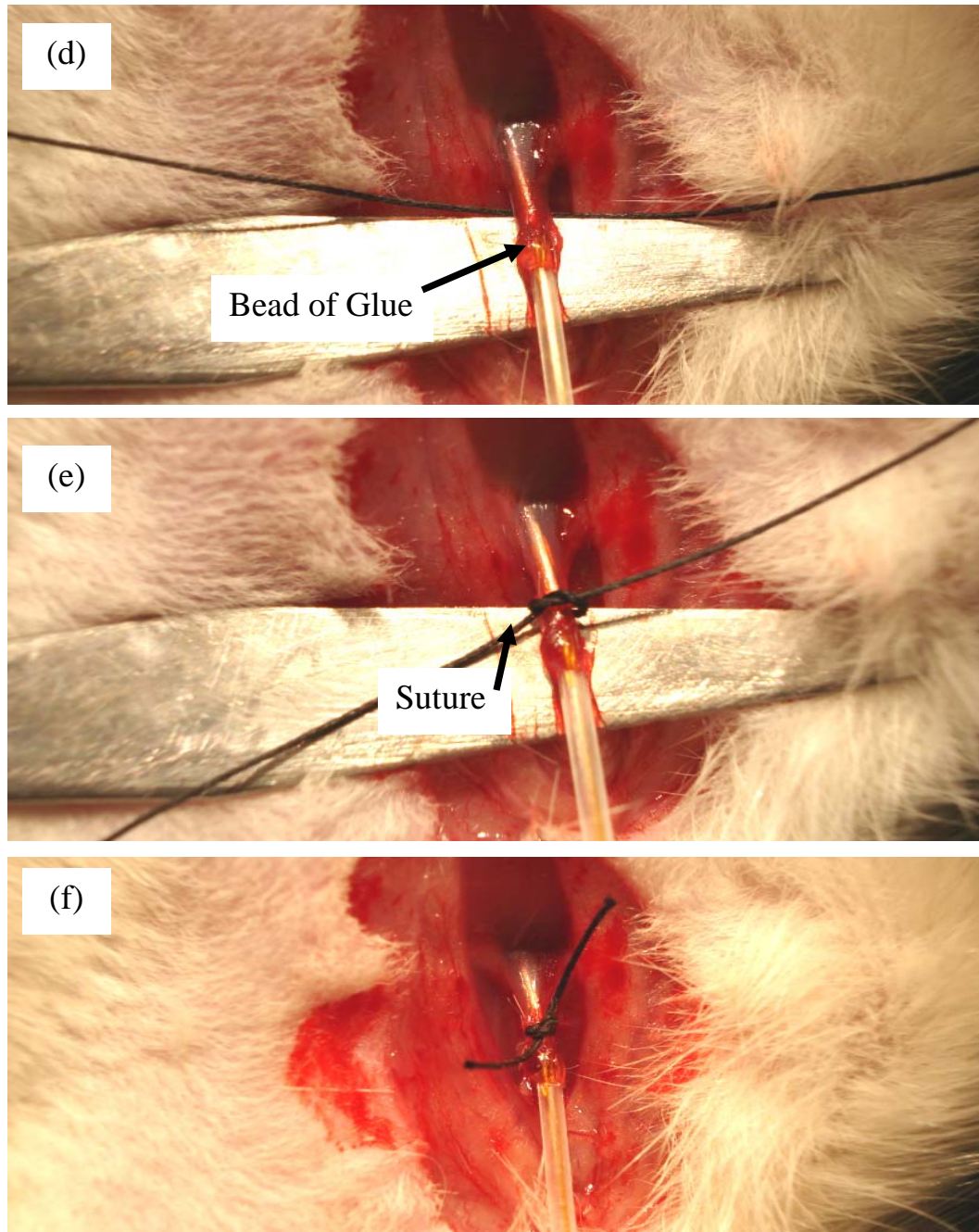


Figure 2.13 continued. Microdialysis probe implantation in the jugular vein. (d) Probe inserted in the vein until the glue stop, (e) suture tied to hold the probe in place and (f) completed probe implantation in the jugular vein. Figures 2.13a-c are on the previous page.

simultaneously sliding the tip of the probe through the cut. Once the guide was removed, the vascular probe remained in the vein with the probe membrane directed towards the heart as shown in Figure 2.13c. The probe was inserted until the bead of glue of the probe reached the cut on the vessel as shown in Figure 2.13d. This bead of glue was used as a stopper and also to prohibit sliding of the probe further in the vein. The jugular vein was ligated with a 3-0 silk suture to further hold the probe in place as shown in Figures 2.13e and 2.13f. The probe inlet and outlet were externalized through the incision and the incision was carefully closed with wound clips.

2.6.1.3 Tissue Response to Probe Implantation

Microdialysis probes have been shown to cause an inflammatory tissue response once implanted [14,16,23-25]. An inflammatory response has been shown to decrease microdialysis probe performance over time in long-term experiments (> 24 hours) [14,24,25]. Studies by Ericsson *et al.* showed that when linear microdialysis probes were implanted into the stomach submucosa, inflammatory cells peaked around the third day after probe implantation and that a subtle edema and fibrotic layer were present throughout the entire experiment [16]. Because of the consistent small amount of edema and fibrotic tissue, it was determined that the amount of inflammatory cells present was the major factor in determining the tissue response to probe implantation in the submucosa. Therefore, three days after probe implantation was sufficient for animal recovery from probe implantation for long-term sampling in the submucosa [16]. Studies have reported that in the first 24 hours,

little or no inflammatory response occurs and that probe performance, monitored by delivery, was stable for 24 hours [14,24,25]. A “tissue equilibration” time of approximately 1 hour was found to be sufficient to allow for vasodilation to return to normal in order to begin sampling for short-term (< 24 hour) sampling [23].

Because multiple microdialysis probes have not previously been implanted in the stomach, tissue response to probe implantation needed to be monitored for this research. Probe implantation effects in the mucosa and submucosa were determined by histological examination as previously performed in the study by Ericsson *et al.* [16]. In addition to studying tissue response to probe implantation, the tissue slice results were used to verify the location of probe implantation in the mucosa and submucosa.

At the completion of experimentation, stomachs were harvested after rat euthanasia and tissue slices were mounted onto microscope slides as described in Section 2.6.1.1.1. For tissue visualization, the slides were stained with H and E dyes. The results of several slides were discussed with a hospital pathologist.

Microdialysis sampling for this research was performed on anesthetized rats over a maximum of 12 hours. The tissue response over time was studied at different time points throughout an experiment length. Normal rat stomachs were harvested at certain time-points after microdialysis probes were implanted into the stomach tissue and were processed for histological examination. Figure 2.14 shows the histology from stomachs harvested directly after, 2 hours after and 12 hours after implantation. The lack of inflammatory cells around the probe was an indication that a significant

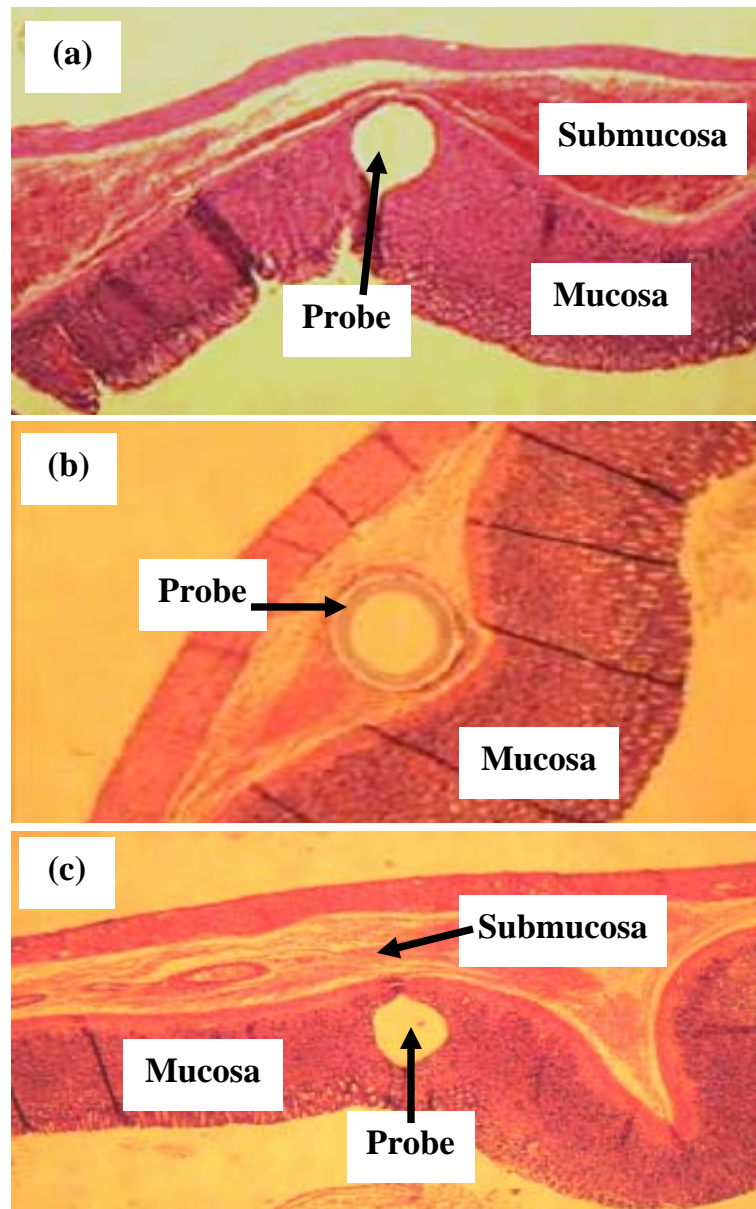


Figure 2.14. Histology images of linear probe implantation (a) in the mucosa right after implantation, (b) in the submucosa 2 hours post implantation; right before probe calibration and (c) in the mucosa 12 hours after implantation. Tissues stained with H and E dyes. Figures 2.14a and 2.14c at 20x magnification, 2.14b at 40x magnification.

immune response did not occur over the course of the entire 12-hour experiment. The results in Figure 2.14 illustrated that probes could be successfully implanted into the individual tissue layers in the stomach without penetration of the membrane into the other layers.

2.6.1.4 Optimization of Linear Probe Membrane Length

Several factors affect microdialysis probe recovery including perfusion fluid flow rate, membrane and analyte properties, diffusion rates from and across the probe and probe geometry [26]. In conjunction with development of probe implantation techniques, the length of probe membrane (*i.e.* probe surface area) was optimized to maximize recovery through the probe. Generally, microdialysis probe recovery increases with longer membrane lengths, whereas shorter membrane lengths have less surface area and, therefore, less recovery at the same flow rate [27]. Decreasing the flow rate can help increase recovery and can be used to optimize recovery when shorter membrane lengths are used, but decreasing the flow will also increase the sampling rate since analytical systems are volume limited [26,28]. Although different membrane lengths have been used, a 10 mm membrane length for linear probes is frequently used since this length is small enough and exhibits good recoveries [5,8,11,29,30]. However, the probability of maintaining a shorter membrane in 500-700 μm heterogeneous tissue layers is greater than with a longer membrane. Therefore, the effect on recovery due to decreased membrane lengths *in vivo* was studied. After probe implantation in the stomach lumen, mucosa and submucosa by both 10 mm and 5 mm probes, extraction efficiencies by delivery of 10 μM salicylic

acid at 1 $\mu\text{L}/\text{min}$ were determined. Probe calibration by delivery was previously discussed in Section 1.4.2.4. As illustrated in Table 2.2, with a 5 mm membrane length, recovery decreased by 24% relative to the 10 mm length. Even though there was a loss in recovery with the 5 mm membrane, concentrations in the dialysate samples were still above the limits of detection (LOD), as will be discussed in Chapter Three. Therefore, a 5 mm membrane length was used for this research to increase the probability of proper probe implantation within the separate stomach tissue layers.

Probe Location	Extraction Efficiencies	
	10 mm Membrane	5 mm Membrane
Lumen	77.5 \pm 12.9 (n = 9)	56.6 \pm 14.7 (n = 12)
Mucosa	59.7 \pm 3.8 (n = 2)	37.9 \pm 13.1 (n = 6)
Submucosa	64.1 \pm 19.3 (n = 9)	33.8 \pm 11.4 (n = 13)

Table 2.2. Comparison of *in vivo* extraction efficiencies in the stomach layers from 10 mm and 5 mm linear microdialysis probes determined from the delivery of 10 μM salicylic acid at a 1 $\mu\text{L}/\text{min}$.

2.6.2 Probe Implantation in the Ulcerated Rat Stomach

As a further application, the multiple probe approach was utilized to sample from different tissue types in the same stomach. To simultaneously monitor healthy and diseased tissue, methods of multiple probe microdialysis sampling in the ulcerated stomach were developed to directly compare ulcerated to healthy tissue.

After chemical induction of an ulcer in the rat stomach, multiple probes were implanted in the stomach lumen, submucosa of normal and ulcerated tissue and also in the blood.

The same type and weight range of female Sprague-Dawley rats used for implantation techniques in the normal stomach were used and housed the same for implantation in the ulcerated stomach. All experiments were in accordance with the *Principles of Laboratory Animal Care* (NIH Publication no. 85-23, revised 1985) and approved by the University of Kansas IACUC committee.

2.6.2.1 Chemical Ulcer Induction

Several models of chemically induced ulceration in the stomach have been reported [31-35]. Typically, administration of the ulcer-causing agent is via a gavage to the stomach lumen [31,34]. These methods have shown to be successful in creating multiple ulcerations within the stomach; however, the extent of ulceration was only visible from the stomach luminal side. Endoscopic techniques or tissue excision was needed to visualize the ulcerated tissue [31-35]. In order to implant microdialysis probes into intact ulcerated tissue, the ulcerated tissue must be visible on the serosal side of the stomach. A method originally developed by Takagi *et al.* of injecting 20% acetic acid (v/v) into the stomach submucosa reported ulcers visible on the serosal surface three days after acid injection [36]. This fit the necessary criterion for microdialysis probe implantation in a contained ulcer tissue on an intact stomach.

For ulcer induction, all tools used were autoclaved with a Harvey SterileMax benchtop autoclave prior to use. The rats were anesthetized using an isoflurane

vaporizer (VetEquip, Inc., Pleasanton, CA, USA). A 95:5% O₂:CO₂ medical oxygen mix (Linweld Inc., Topeka, KS, USA) was delivered at 50 psi from the cylinder and metered by a flowmeter to 1-1.5 liters per minute to the vaporizer. The oxygen was mixed with 2-3% isoflurane and delivered to a rodent nose cone which enabled the rat to inhale the anesthetic. The excess isoflurane was scavenged with an activated charcoal filter. A CMA/150 temperature controller and heating pad (North Chelmsford, MA, USA) was used to maintain the rat body temperature at 37°C. The hair on the left side of the rat just below the ribcage was shaved and cleaned with alternate scrubs of betadine and 70% isopropyl alcohol. This scrub procedure was repeated three times to sterilize the surgical area. An incision was made just below the ribcage and the stomach was exposed. A 27-gauge hypodermic needle was connected to a 1 mL syringe containing 20% acetic acid. The needle was inserted into the submucosa of the body of the ventral side of the stomach and 50 µL of acid was injected into the submucosal space. The muscle was sutured closed with 5-0 silk suture and the skin was closed with wound clips. The rat was removed from anesthesia and given a subcutaneous injection of 0.1 mg/kg buprenorphine HCl as post-operative care. The ulcer was allowed to form for the following three days.

After the ulcer formation period, the ulcerated tissue, from the serosal surface, was circular with characteristic white tissue and blood engorgement at the ulcer base. Figure 2.15a demonstrates an ulcer from the serosal side of the stomach induced by acetic acid injection. Histology slices from the ulcerated stomach were processed as

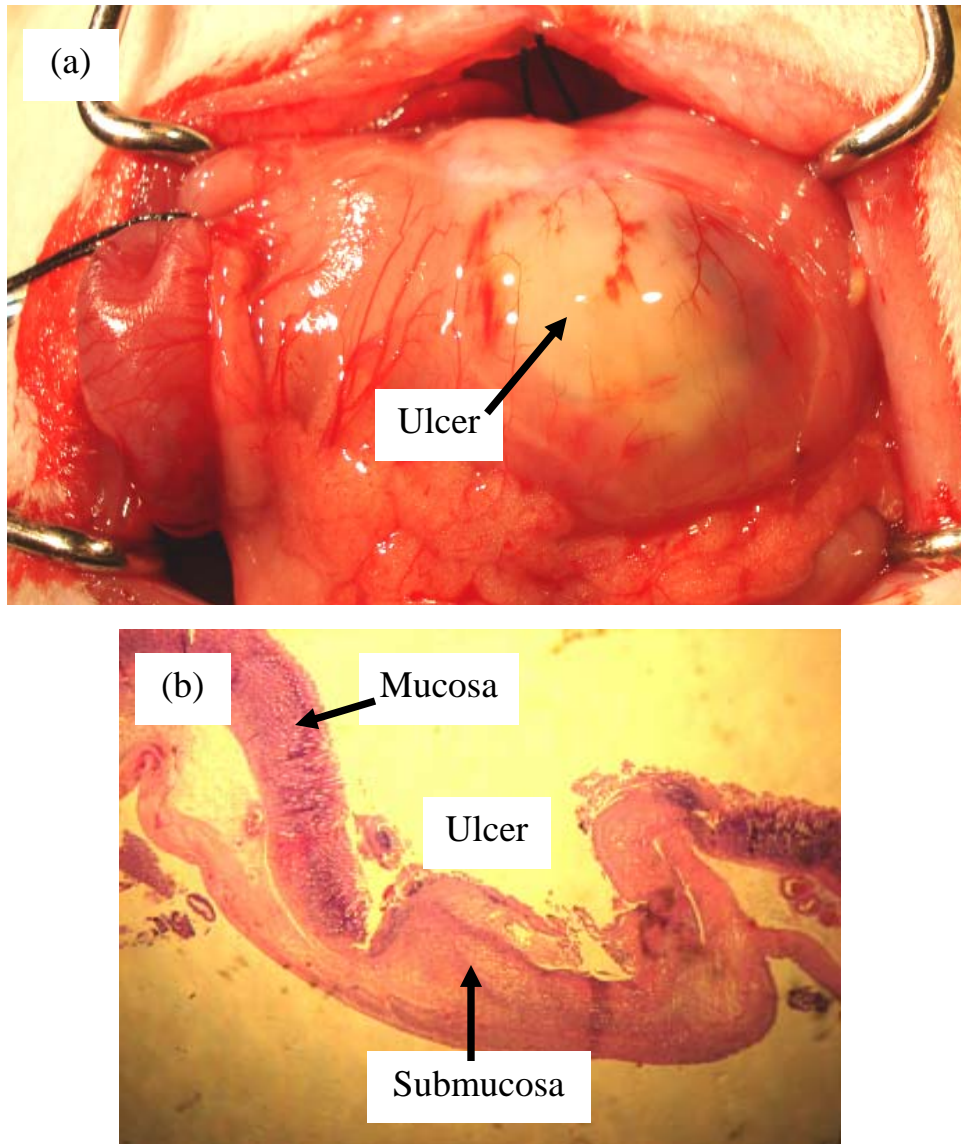


Figure 2.15. Gastric ulcer formed by injection of 20% acetic acid into the submucosa. (a) Ulcer visibility from the serosal surface and (b) histology of ulcer. Tissue stained with H and E dyes. Image at 20x magnification.

described previously in Section 2.6.1.1.1. Figure 2.15b illustrates the histology results from an ulcer induced by acetic acid injection. This figure shows that this method was successful in creating a gastric ulcer with the complete degradation of the mucosal layer. A subsequent increase in the submucosal layer thickness was also observed in the ulcerated tissue.

A disadvantage to the acetic acid injection method of ulcer induction was that neighboring tissues (*i.e.* liver and adipose) would frequently strongly adhere to the ulcerated tissue. Due to the fragile nature of the ulcerated tissue, the adhesion would cause the ulcerated tissue to perforate upon gentle manipulation. The success rate of ulcers that did not perforate from adhering tissues was 65%. Therefore, alternative methods of ulcer induction to decrease the frequency of perforation were explored. Initially, less severe ulcer causing agents were injected to determine if decreasing the severity of ulceration affected the amount of tissue adherence. Figure 2.16 shows the histology results from stomach tissues three days after the injection of 50 μ L of (a) 10% acetic acid, (b) absolute ethanol and (c) 7 mM indomethacin in ethanol. The histology results showed that all three chemicals injected resulted in only inflammation of the mucosa tissue. A true gastric ulcer results in the complete erosion of the mucosal layer. Therefore, these injected chemicals were not suitable as an ulcer model for this research.

Another explored procedure to reduce tissue adherence was to coat the ulcer with sterile lubricant (E. Fougera & Co, Melville, NY, USA) directly after acid injection. With a small amount of lubricant on the ulcer, the tissues easily separated

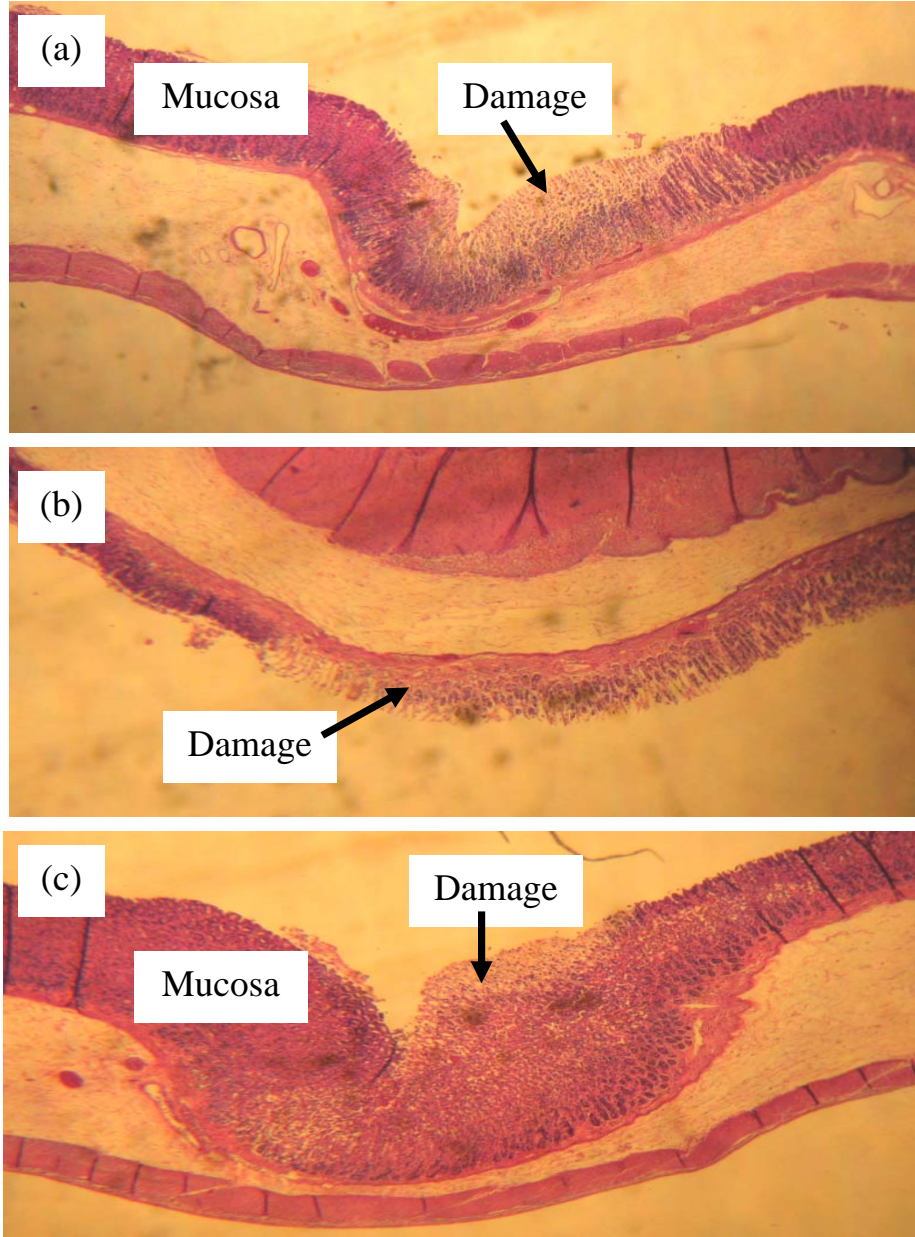


Figure 2.16. Histology from the injection of (a) 10% acetic acid, (b) absolute ethanol and (c) 7 mM indomethacin in ethanol.

without perforating the ulcer with a success rate of non-perforated ulcers increasing to 76%. However, the resulting ulcers appeared smaller when viewed on the serosal surface. This decrease in ulcer size was confirmed when comparing the ulcer index (UI) values, measured as the ulcer area (mm²) on the mucosal side, after the stomach tissue was harvested [37]. Table 2.3 shows the ulcer indices of both ulcers formed by the normal acetic acid injection method (no lubricant used) and the same method with lubricant application after injection. The traditional method resulted in ulcers that were twice the size of ulcers formed with lubricant used. During the ulcer formation period, the lubricant may have absorbed into the stomach tissue, partially protecting the mucosa during ulcer formation. Ultimately, the lubricant was used to control ulcer size (*i.e.* small ulcers (10-20 mm²) versus large ulcers (30-40 mm²)).

	UI (mm²)
Large Ulcer	37 ± 8
Small Ulcer	17 ± 4

Table 2.3. Ulcer index values for large ulcers (no lubricant used) and small ulcers (lubricant used) (n = 9).

2.6.2.2 Probe Implantation in Ulcerated Submucosa

As described in Section 2.6.2.1, an ulcer was formed in the stomach by acetic acid injection and allowed to form for the following three days. The rats were fasted 15-20 hours prior to probe implantation by the optimized fasting procedure described

in Section 2.5. The same procedures described in Section 2.6.1.1.2 to prepare the stomach for probe implantation in the normal stomach were used in the ulcerated stomach.

Any tissue adhered to the ulcer was gently separated from the ulcer by rubbing the tissues with a wetted cotton swab. As previously described for implantation of linear probes in the normal stomach, a guide needle (25-gauge; 1.5 inch length) was used to implant a linear probe in the ulcerated tissue. As shown in Figure 2.17, the guide needle penetrated the ulcerated tissue, was tunneled through the tissue and exited through the tissue using the beveled edge of the guide. The probe was threaded through the inside of the guide and the guide alone was removed leaving the probe in place in the tissue. The entrance and exit wounds were closed with tissue glue. For implantation in the ulcer, tunneling the guide needle across the entire ulcer area was found to be more successful because of the fragile nature of the tissue. Guide needles that exited through the middle of the ulcerated tissue caused the ulcer tissue to leak gastric solution through the serosal surface. In addition to implanting a probe in the ulcerated submucosa, linear probes were implanted in the stomach lumen and submucosa of normal tissue as described in Sections 2.6.1.1.3 and 2.6.1.1.5. The incision on the abdomen was covered with wetted gauze and plastic wrap to keep the abdomen hydrated during experimentation. A vascular probe was also implanted in the same rat as described in Section 2.6.1.2.

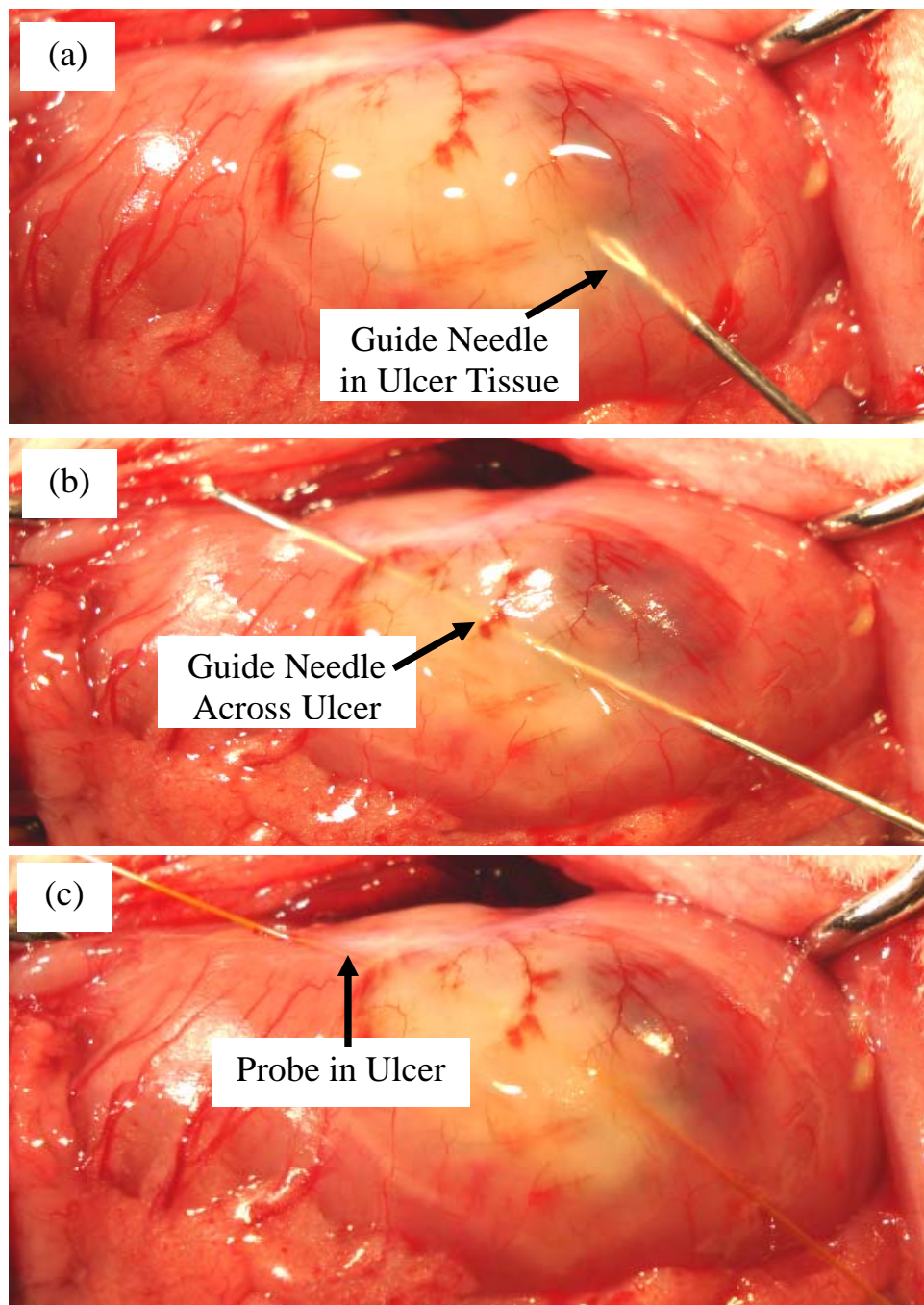


Figure 2.17. Microdialysis probe implantation in the submucosa of ulcerated tissue. (a) Guide needle penetrating the ulcer, (b) guide needle across the ulcerated tissue and (c) probe implanted in the ulcerated tissue.

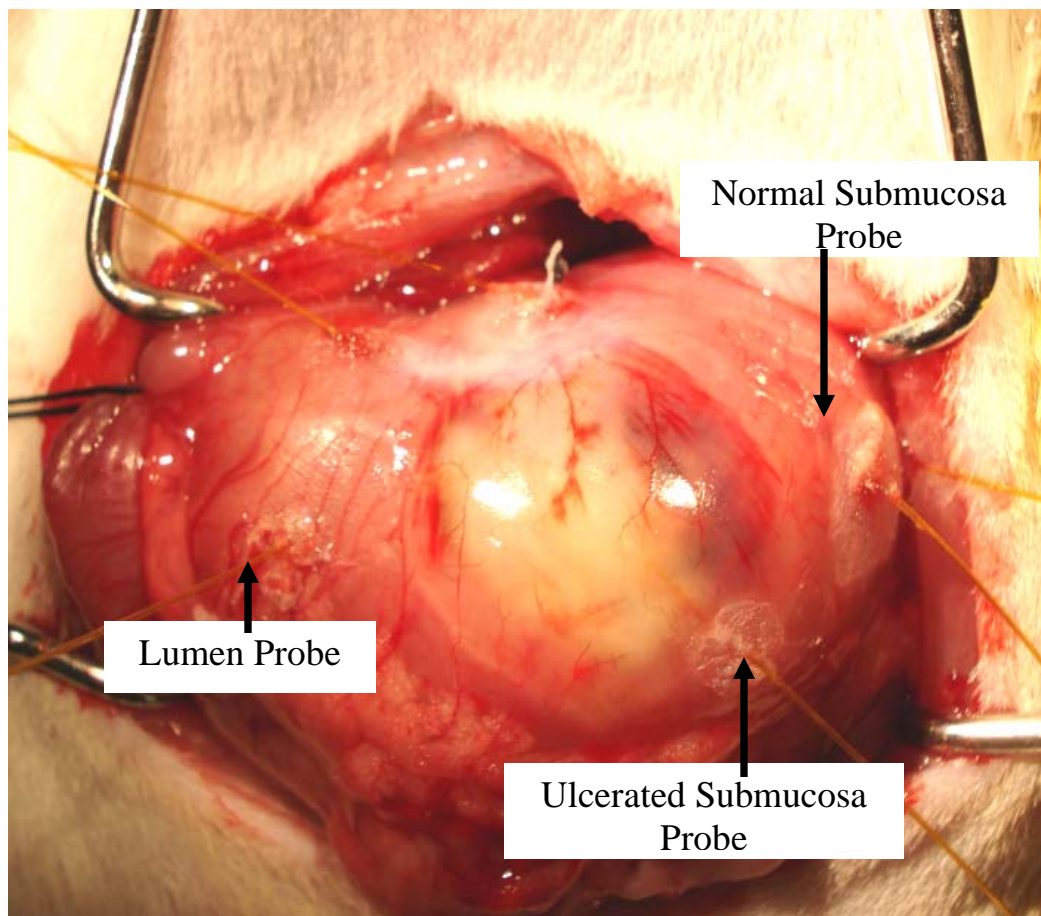


Figure 2.18. Linear microdialysis probes simultaneously implanted in the lumen and submucosa of both ulcerated and normal tissue.

Figure 2.18 shows the completed implantation of linear microdialysis probes simultaneously in the lumen and submucosa of normal and ulcerated tissue in the ulcerated rat stomach.

2.6.2.3 Verification of Probe Location

As describe previously, histology slides were processed from the tissue after experimentation to verify the location of the probe within the normal and ulcerated submucosa. Harvested stomach tissue was mounted onto microscope slides as described previously in Section 2.6.1.1.1. For tissue visualization, the slides were stained with H and E dyes. Results of several slides were discussed with a hospital pathologist. Figure 2.19 shows a representative result of a linear probe implanted in the submucosa of ulcerated tissue. From the slides, the complete erosion of the mucosa layer was observed as well as the successful probe implantation into the ulcerated submucosa.

2.7 Conclusions

The research presented in this chapter focused on the development of techniques for implanting multiple microdialysis probes in rat stomach. To compare different tissue layers, microdialysis probes were simultaneously implanted in the stomach lumen, mucosa, submucosa and in the blood. It was determined that linear probes could successfully be implanted in the different stomach tissues with the use of a 25-gauge guide hypodermic needle. Although a 24% decrease in the *in vivo*

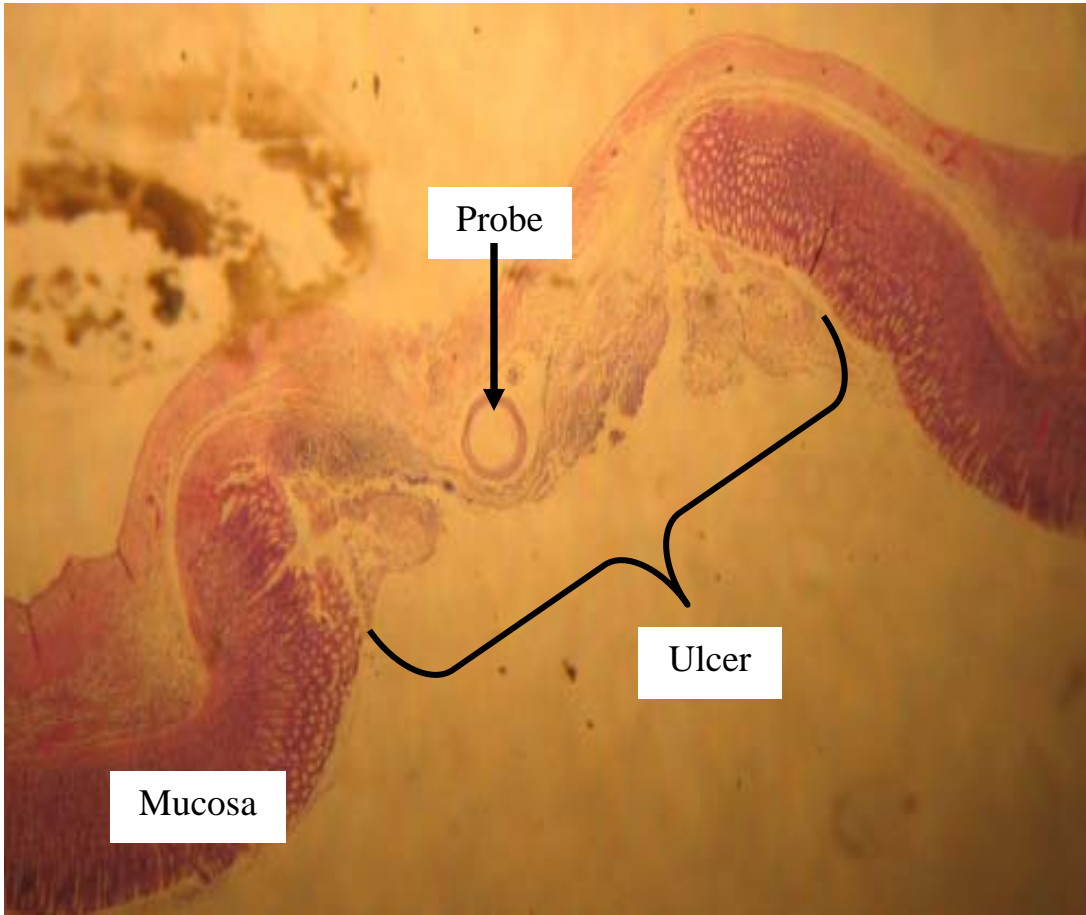


Figure 2.19. Histology of a linear microdialysis probe implanted in the stomach submucosa of ulcerated tissue. Tissue stained by H and E dyes. Image at 20x magnification.

extraction efficiency was observed with a linear probe of a 5 mm effective membrane length relative to a 10 mm membrane at 1 $\mu\text{L}/\text{min}$, a 5 mm membrane length was still found to be suitable for this research. This shorter membrane length increased the probability of correct probe implantation without significantly sacrificing probe recovery. Tissue response to probe implantation in the stomach mucosa and submucosa were studied. No significant immune response was observed for up to 12 hours post probe implantation in both the mucosa and submucosa.

As a further use for a multiple probe approach, a similar method was used to compare ulcerated and normal tissue in the same stomach. An ulcerated stomach model was developed based on a literature method of chemical induction by injection of 20% acetic acid into the stomach submucosa. A frequent problem with this method of ulcer induction was the adherence of neighboring tissues to the ulcer that could eventually perforate the ulcer. To circumvent this adherence problem, sterile lubricant was used to coat the ulcer. The lubricant effectively reduced tissue adherence, but also reduced the ulcer size. This resulted in the ability of controlling ulcer size (large versus small) for studies as a function of ulcer size. Multiple microdialysis probes were successfully implanted in the stomach lumen and submucosa of both ulcerated and normal tissue in the same rat. A vascular probe was also implanted in the jugular vein resulting in a four-probe design in the ulcerated stomach model.

Finally, procedures to fast the rat prior to experimentation were developed since the frequently used method of removal of food did not result in a truly fasted rat

and caused the appearance of large, unidentified peaks in lumen basal dialysate. Fasting procedures were optimized by placing the rat in a metabolism cage with an Elizabethan collar affixed around their neck for 15-20 hours prior to experimentation.

Overall, the research discussed in the present chapter presented successful methods of multiple probe implantation techniques in both normal and ulcerated rat stomach. To test the significance of sampling with this multiple probe approach, comparisons of drug concentrations determined at each study site from oral drug absorption studies were made. The results from monitoring drug absorption in the normal stomach model as well as the large and small ulcer model will be presented in the next chapter.

2.8 References

- [1] Bunnett, N. W.; Walsh, J. H.; Debas, H. T.; Kauffman, G. L., Jr.; Golanska, E. M., Measurement of prostaglandin E2 in interstitial fluid from the dog stomach after feeding and indomethacin. *Gastroenterology* **1983**, 85, (6), 1391-1398.
- [2] Meirieu, O.; Pairet, M.; Sutra, J. F.; Ruckebusch, M., Local release of monoamines in the gastrointestinal tract: an in vivo study in rabbits. *Life Sciences* **1986**, 38, (9), 827-834.
- [3] Yanagisawa, K.; Tache, Y., Intracisternal TRH analogue RX 77368 stimulates gastric histamine release in rats. *American Journal of Physiology* **1990**, 259, (4 Pt 1), G599-604.
- [4] Iversen, H. H.; Celsing, F.; Leone, A. M.; Gustafsson, L. E.; Wiklund, N. P., Nerve-induced release of nitric oxide in the rabbit gastrointestinal tract as measured by in vivo microdialysis. *British Journal of Pharmacology* **1997**, 120, (4), 702-706.
- [5] Kitano, M.; Norlen, P.; Hakanson, R., Gastric submucosal microdialysis: a method to study gastrin- and food-evoked mobilization of ECL-cell histamine in conscious rats. *Regulatory Peptides* **2000**, 86, (1-3), 113-123.
- [6] Bernsand, M.; Hakanson, R.; Norlen, P., Tachyphylaxis of the ECL-cell response to PACAP: receptor desensitization and/or depletion of secretory products. *British Journal of Pharmacology* **2007**, 152, (2), 240-248.
- [7] Cibicek, N.; Micuda, S.; Chladek, J.; Zivny, P.; Zadak, Z.; Cermakova, E.; Palicka, V., Lithium microdialysis and its use for monitoring of stomach and colon submucosal blood perfusion--a pilot study using ischemic preconditioning in rats. *Acta Medica (Hradec Kralove)* **2006**, 49, (4), 227-231.
- [8] Fykse, V.; Solligard, E.; Bendheim, M. O.; Chen, D.; Gronbech, J. E.; Sandvik, A. K.; Waldum, H. L., ECL cell histamine mobilization and parietal cell stimulation in the rat stomach studied by microdialysis and electron microscopy. *Acta Physiology* **2006**, 186, (1), 37-43.

- [9] Kitano, M.; Bernsand, M.; Kishimoto, Y.; Norlen, P.; Hakanson, R.; Haenuki, Y.; Kudo, M.; Hasegawa, J., Ischemia of rat stomach mobilizes ECL cell histamine. *American Journal of Physiology- Gastrointestinal and Liver Physiology* **2005**, 288, (5), G1084-1090.
- [10] Bostrom, E.; Simonsson, U. S.; Hammarlund-Udenaes, M., In vivo blood-brain barrier transport of oxycodone in the rat: indications for active influx and implications for pharmacokinetics/pharmacodynamics. *Drug Metabolism and Disposition* **2006**, 34, (9), 1624-1631.
- [11] Mathy, F. X.; Lombry, C.; Verbeeck, R. K.; Preat, V., Study of the percutaneous penetration of flurbiprofen by cutaneous and subcutaneous microdialysis after iontophoretic delivery in rat. *Journal of Pharmaceutical Sciences* **2005**, 94, (1), 144-152.
- [12] Tsai, P.; Tsai, T. H., Simultaneous determination of berberine in rat blood, liver and bile using microdialysis coupled to high-performance liquid chromatography. *Journal of Chromatography A* **2002**, 961, (1), 125-130.
- [13] Wu, Y. T.; Tsai, T. R.; Lin, L. C.; Tsai, T. H., Liquid chromatographic method with amperometric detection to determine acteoside in rat blood and brain microdialysates and its application to pharmacokinetic study. *Journal of Chromatography B Analytical Technologies in the Biomedical and Life Sciences* **2007**, 853, (1-2), 281-286.
- [14] Ault, J. M.; Riley, C. M.; Meltzer, N. M.; Lunte, C. E., Dermal microdialysis sampling in vivo. *Pharmaceutical Research* **1994**, 11, (11), 1631-1639.
- [15] Telting-Diaz, M.; Scott, D. O.; Lunte, C. E., Intravenous microdialysis sampling in awake, freely-moving rats. *Analytical Chemistry* **1992**, 64, (7), 806-810.
- [16] Ericsson, P.; Norlen, P.; Bernsand, M.; Alm, P.; Hoglund, P.; Hakanson, R., ECL cell histamine mobilization studied by gastric submucosal microdialysis in awake rats: methodological considerations. *Pharmacology & Toxicology* **2003**, 93, (2), 57-65.
- [17] Norlen, P.; Ericsson, P.; Kitano, M.; Ekelund, M.; Hakanson, R., The vagus regulates histamine mobilization from rat stomach ECL cells by controlling their sensitivity to gastrin. *Journal of Physiology* **2005**, 564, (Pt 3), 895-905.

- [18] Astroff, A. B.; Young, A. D.; Holzum, B.; Sangha, G. K.; Thyssen, J. H., Conduct and interpretation of a dermal developmental toxicity study with KBR 3023 (a prospective insect repellent) in the Sprague-Dawley rat and Himalayan rabbit. *Teratology* **2000**, 61, (3), 222-230.
- [19] Brown, C., Restraint collars. Part I: Elizabethan collars and other types of restraint collars. *Lab Animal (NY)* **2006**, 35, (2), 23-25.
- [20] Hernandez, A. D.; Sukhdeo, M. V., Host grooming and the transmission strategy of *Heligmosomoides polygyrus*. *Journal of Parasitology* **1995**, 81, (6), 865-869.
- [21] Sauvez, F.; Drouin, D. S.; Attia, M.; Bertheux, H.; Forster, R., Cutaneously applied 4-hydroxytamoxifen is not carcinogenic in female rats. *Carcinogenesis* **1999**, 20, (5), 843-850.
- [22] Magee, D. F.; Dalley II, A. F., *Digestion and the Structure and Function of the Gut*. Karger: Basel, 1986; Vol. 8.
- [23] Anderson, C.; Anderson, T.; Wardell, K., Changes in skin circulation after insertion of a microdialysis probe visualized by laser Doppler perfusion imaging. *Journal of Investigative Dermatology* **1994**, 102, 807-811.
- [24] Davies, M. I.; Lunte, C. E., Microdialysis sampling for hepatic metabolism studies. Impact of microdialysis probe design and implantation technique on liver tissue. *Drug Metabolism and Disposition* **1995**, 23, (10), 1072-1079.
- [25] Mathy, F. X.; Denet, A. R.; Vroman, B.; Clarys, P.; Barel, A.; Verbeeck, R. K.; Preat, V., In vivo tolerance assessment of skin after insertion of subcutaneous and cutaneous microdialysis probes in the rat. *Skin Pharmacology and Applied Skin Physiology* **2003**, 16, (1), 18-27.
- [26] Davies, M. I.; Cooper, J. D.; Desmond, S. S.; Lunte, C. E.; Lunte, S. M., Analytical considerations for microdialysis sampling. *Advanced Drug Delivery Reviews* **2000**, 45, (2-3), 169-188.
- [27] Zhao, Y.; Liang, X.; Lunte, C. E., Comparison of recovery and delivery in vitro for calibration of microdialysis probes. *Analytica Chimica Acta* **1995**, 316, 403-410.
- [28] Hansen, D. K.; Davies, M. I.; Lunte, S. M.; Lunte, C. E., Pharmacokinetic and metabolism studies using microdialysis sampling. *Journal of Pharmaceutical Sciences* **1999**, 88, (1), 14-27.

- [29] Bernsand, M.; Ericsson, P.; Bjorkqvist, M.; Zhao, C. M.; Hakanson, R.; Norlen, P., Submucosal microinfusion of endothelin and adrenaline mobilizes ECL-cell histamine in rat stomach, and causes mucosal damage: a microdialysis study. *British Journal of Pharmacology* **2003**, 140, (4), 707-717.
- [30] Sorg, B. S.; Peltz, C. D.; Klitzman, B.; Dewhirst, M. W., Method for improved accuracy in endogenous urea recovery marker calibrations for microdialysis in tumors. *Journal of Pharmacological and Toxicological Methods* **2005**, 52, (3), 341-349.
- [31] Chandranath, S. I.; Bastaki, S. M.; Singh, J., A comparative study on the activity of lansoprazole, omeprazole and PD-136450 on acidified ethanol- and indomethacin-induced gastric lesions in the rat. *Clinical and Experimental Pharmacology and Physiology* **2002**, 29, (3), 173-180.
- [32] Kamada, T.; Hata, J.; Kusunoki, H.; Sugiu, K.; Tanimoto, T.; Mihara, M.; Hamada, H.; Kido, S.; Dongmei, Q.; Haruma, K., Endoscopic characteristics and Helicobacter pylori infection in NSAID-associated gastric ulcer. *Journal of Gastroenterology and Hepatology* **2006**, 21, (1 Pt 1), 98-102.
- [33] Okabe, S.; Amagase, K., An overview of acetic acid ulcer models--the history and state of the art of peptic ulcer research. *Biological and Pharmaceutical Bulletin* **2005**, 28, (8), 1321-1341.
- [34] Singh, L. P.; Kundu, P.; Ganguly, K.; Mishra, A.; Swarnakar, S., Novel role of famotidine in downregulation of matrix metalloproteinase-9 during protection of ethanol-induced acute gastric ulcer. *Free Radical Biology & Medicine* **2007**, 43, 289-299.
- [35] Wang, L.; Hu, C. P.; Deng, P. Y.; Shen, S. S.; Zhu, H. Q.; Ding, J. S.; Tan, G. S.; Li, Y. J., The protective effects of rutaecarpine on gastric mucosa injury in rats. *Planta Medica* **2005**, 71, (5), 416-419.
- [36] Takagi, K.; Okabe, S.; Saziki, R., A new method for the production of chronic gastric ulcer in rats and the effect of several drugs on its healing. *Japanese Journal of Pharmacology* **1969**, 19, (3), 418-426.
- [37] Fukawa, K.; Kawano, O.; Misaki, N.; Uchida, M.; Irino, O., Experimental studies on gastric ulcer. (4). Sequential observation and evaluation of gastric ulcers by endoscope in the rat. *Japanese Journal of Pharmacology* **1983**, 33, (1), 175-179.

CHAPTER THREE

Monitoring Drug Absorption in the Stomach by Multiple Probe Microdialysis Sampling

3.1 Introduction

As described in Chapter Two, microdialysis probes were successfully implanted simultaneously into the different tissue layers of the stomach, namely the mucosa and submucosa layers. A multiple probe microdialysis sampling approach will improve upon current uses of gastric microdialysis sampling, which are performed with a single probe in the submucosa layer. In addition, multiple probes were implanted simultaneously in normal and diseased tissue of an ulcerated stomach model. By this approach, a direct comparison of normal and ulcerated tissue of the same stomach was achieved.

Although multiple probes were implanted in this design, the significance of sampling by a multiple probe approach needed to be determined. This was achieved by monitoring compounds with known absorption characteristics through the stomach after oral administration. Schanker *et al.* originally studied the absorption of different

classes of compounds through the rat stomach by *in situ* closed loop methods that were described in Section 1.3.2.2 [1]. Based on this previous study, test compounds of differing degrees of passive absorption in the rat stomach were used to compare the extent of absorption determined from microdialysis sampling to their predicted absorption rates. In addition, comparison of the test compound concentrations determined in each studied site by this microdialysis sampling design was used to assess the significance of this multiple probe approach.

3.2 Specific Aims of this Research

The specific goals of this research were to use the previously described multiple probe design of microdialysis sampling in both normal and ulcerated stomach to monitor drug absorption after an oral dose was given to anesthetized rats. Three previously characterized test compounds with different degrees of absorption in the rat stomach were dosed by oral gavage to the ligated stomach. The test compounds salicylic acid (SA), caffeine and metoprolol were chosen to represent high, moderate and low absorption in the rat stomach, respectively. A summary of the chosen test compounds showing the structures, pK_a values, $\log D$ (pH 2-3) values and the reported absorption rates of each compound in the rat stomach is presented in Table 3.1 [1-4]. Analysis of concentration-time curves and pharmacokinetics modeling for each test compound and each probe location will be presented in this chapter to assess the efficacy of this microdialysis sampling method in the stomach.

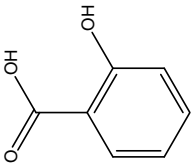
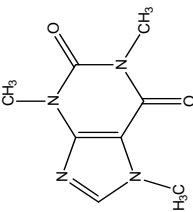
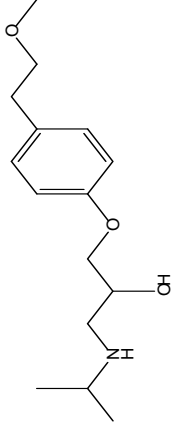
Analyte	Structure ^a	pK _a ^a (25°C)	log D ^c (pH 2-3)	Absorption in Stomach
SA		3.0	2.06	High ^b
Caffeine		14.0	-0.13	Moderate ^b
Metoprolol		9.7	-1.31	Low ^d
Reference ^a [3] ^b [1] ^c [2] ^d [4]				

Table 3.1. Properties of the chosen analytes representing various degrees of drug absorption in the rat stomach.

3.3 Materials and Methods

3.3.1 Chemicals and Reagents

Caffeine, metoprolol tartrate and salicylic acid; sodium salt (SA), were purchased from Sigma (St. Louis, MO, USA). Ammonium acetate, sodium acetate, glacial acetic acid, 85% *o*-phosphoric acid and HPLC grade acetonitrile were purchased from Fisher Scientific (Fair Lawn, NJ, USA). Ammonium phosphate was purchased from Mallinckrodt Chemical Works (St. Louis, MO, USA). Ringer's solution consisted of 145 mM NaCl, 2.8 mM KCl, 1.2 mM CaCl₂ and 1.2 mM MgCl₂. Artificial gastric solution (pH 2.5-3.0) consisted of 87.4 mM NaCl, 4.0 mM KCl, 0.8 mM MgSO₄, 2.1 mM Na₂SO₄ and 19.3 mM mannitol. All chemicals for Ringer's solution and artificial gastric solution were purchased from Sigma or Fisher Scientific. Water for buffer, mobile phase, Ringer's solution and artificial gastric solution was processed through a Labconco WaterPro Plus water purification system (18 MΩ/cm) (Kansas City, MO, USA). Buffer, Ringer's and artificial gastric solution were filtered through a 47 mm, 0.22 μm nylon filter prior to use. Isoflurane was purchased from Fort Dodge Animal Health (Fort Dodge, IA, USA). Xylazine was purchased from Lloyd Laboratories (Shenandoah, IA, USA). Acepromazine was purchased from Boehringer Ingelheim Vetmedica, Inc. (St. Joseph, MO, USA). Lactated Ringer's and 5% dextrose in lactated Ringer's were purchased from B Braun Medical Inc. (Irvine, CA, USA).

3.3.2 Microdialysis Probes

The linear microdialysis probes used for implantation into the stomach were fabricated as previously described in-depth in Section 2.4.1. All linear probes were constructed to a 5 mm effective membrane length. The construction of vascular microdialysis probes for sampling in the blood was previously described in Section 2.4.2.

3.3.3 Surgical Procedures

Female Sprague-Dawley rats (225-300 grams) (Charles River Laboratories, Inc., Wilmington, MA, USA) were initially housed with access to food and water in temperature and humidity controlled rooms on a 12-hour light/dark cycle. All experiments were in accordance with the *Principles of Laboratory Animal Care* (NIH Publication, no. 85-23, revised 1985) and approved by the University of Kansas IACUC committee. The procedures for ulcer induction, fasting, stomach ligation, oral gavage insertion and probe implantation for both normal and ulcerated stomach studies were described in-depth in Chapter Two. At the completion of each experiment, the stomach was harvested after animal euthanasia and histology slices were processed as described in Section 2.6.1.1.1.

For test compounds given intravenously, an incision was made on the skin of the inner hind leg to expose the femoral vein/artery/nerve bundle. Extra connective tissue was cleared from the bundle by rubbing the area with a cotton swab applicator soaked in saline. The femoral vein was isolated from the rest of the bundle and a

small cut was made on the vein with spring scissors, similar to techniques described in Section 2.6.1.2. MicroRenathane® (MRE-033) (838 μm o.d.; 356 μm i.d.; Braintree Scientific, Braintree, MA, USA) tubing was used as the dosing cannula and was inserted into the vein through the small cut. The tubing was tunneled and positioned near the heart. The femoral vein was ligated with 3-0 suture to hold the cannula in place. The cannula was externalized through the incision and the incision was closed with wound clips carefully around the cannula. The exposed end of the cannula was connected to a 23-gauge hypodermic needle on a 3 mL syringe of saline.

3.3.4 Microdialysis System

Four Hamilton gastight syringes (1 mL) (Reno, NV, USA) were placed in a CMA model 400 syringe pump (North Chelmsford, MA, USA). The inlets of the microdialysis probes were connected to the syringes and perfused at 1 $\mu\text{L}/\text{min}$. The outlets of the microdialysis probes were placed into BASi Honey Comb fraction collectors (West Lafayette, IN, USA) set to collect samples every 15 minutes. The microdialysis samples were collected into 250 μL polypropylene microcentrifuge tubes (Fisher Scientific, Fair Lawn, NJ, USA). A schematic of the microdialysis setup is shown in Figure 3.1.

3.3.5 Experimental Design

Initially, a “tissue equilibration” period of 1-2 hours was performed where the probes were flushed with perfusion fluid. In the normal stomach studies,

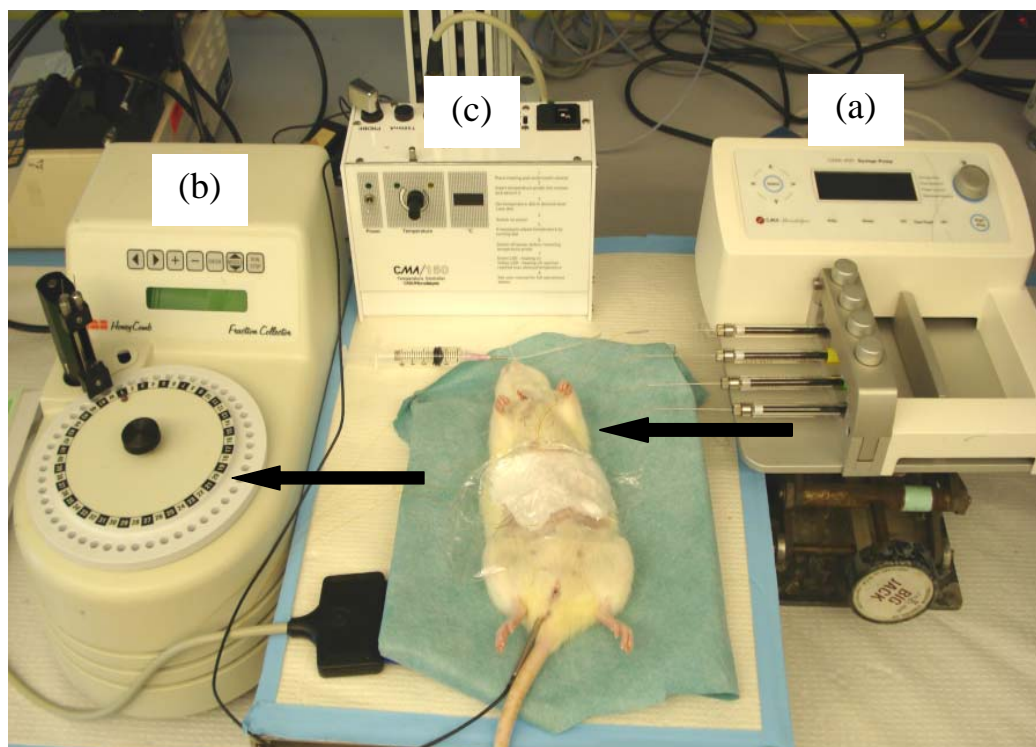


Figure 3.1. Microdialysis sampling setup. (a) Syringe pump to deliver perfusate, (b) fraction collector to sample dialysate and (c) temperature controller to maintain a 37°C body temperature. Arrows indicate the direction of perfusate flow.

Ringer's solution was perfused through the mucosa, submucosa and vascular probes and artificial gastric solution was perfused through the lumen probe. In the ulcerated stomach studies, Ringer's solution was perfused through the normal submucosa, ulcerated submucosa and vascular probes and artificial gastric solution was perfused through the lumen probe. During the equilibration time, dialysate samples were collected.

Calibration of the microdialysis probes was performed *in vivo* by delivery of the analyte. Calibration by this method was described previously in Section 1.4.2.4. The perfusate contained either 10 or 25 μM of the analyte to deliver through the probe. The probes were perfused until a steady-state dialysate concentration was achieved (~45 minutes). After the achieved steady-state, five samples were collected to determine the delivery extraction efficiency (EE_d). The EE_d was calculated using Equation 8, as described in Section 1.4.2.4. The determined EE_d values for both the normal and ulcerated stomach studies will be discussed in Section 3.4.

To prepare the system for dosing, the calibration solution needed to be flushed from the microdialysis probes. This was achieved by perfusion with Ringer's or artificial gastric solution through the probes. The probes were flushed for approximately 1.5 hours and dialysate samples were collected and chromatographically analyzed to determine if any analyte remained in the dialysate.

When no analyte was detectable in the dialysate, the solution in the stomach was removed by pulling on the syringe connected to the gavage tube. Test compound was given by gavage as a bolus dose by replacing the 5 mL syringe containing the

removed stomach solution with another 5 mL syringe containing 5 mM analyte dissolved in artificial gastric solution. Three milliliters of the dose was injected into the ligated stomach through the gavage tube. Sampling from the microdialysis probes started after correcting for probe dead volume and then microdialysis samples were collected for 6 hours post dose from each probe.

3.3.6 Sample Analysis by HPLC-UV

All microdialysis samples were analyzed by high performance liquid chromatography with ultraviolet detection (HPLC-UV). Because of the number of samples generated for each probe, two analytical systems were used to increase sample throughput. Each system consisted of a Shimadzu LC10-AD pump, a Shimadzu SPD-10AV UV-Vis spectrophotometric detector and a Shimadzu SCL-10Avp system controller (Columbia, MD, USA). Sample injections were made into a Rheodyne model 7125i injector. The injection was an underfill of 10 μ L into a 25 μ L PEEK sample loop. Data was acquired using Shimadzu EZ Start version 7.3 software for the mucosa and both ulcerated and normal submucosa samples. Chrom & Spec version 1.5 software (Ampersand International Inc., Beachwood, OH, USA) was used to acquire data for the lumen and blood samples.

The Food and Drug Administration (FDA) Guidance of Bioanalytical Method Development and a report by Peters *et al.* were consulted for the acceptance criterion for the selectivity, intra-assay precision, linearity and limits of detection (LOD) for the HPLC-UV systems [5,6]. The calibration curves were constructed by spiking

analyte into Ringer's or artificial gastric solution in the concentration range of 1-200 μM , analyzed in triplicate. Each calibration curve was constructed using Microsoft Excel and the method of least squares was applied to determine linearity. The lumen dialysate samples were diluted 1:5 or 1:10 to maintain the samples in the tested concentration range. The results of method validation will be discussed in Section 3.4.1.

3.3.6.1 Analysis of Salicylic Acid (SA)

Separation of SA was achieved on a Phenomenex Gemini C₁₈ RP column (150 x 2.00 mm, 5 μm particle). The mobile phase consisted of 25 mM ammonium phosphate, adjusted to pH 2.5 with *o*-phosphoric acid, with 25% acetonitrile (v/v) [7]. The flow rate used for this system was 0.35 mL/min. Detection of SA was performed at 300 nm.

3.3.6.2 Analysis of Caffeine

Separation of caffeine was achieved on a Phenomenex Gemini C₁₈ RP column (150 x 2.00 mm, 5 μm particles). The mobile phase for this system was 30 mM sodium acetate, adjusted to pH 4.0 with glacial acetic acid, with 10% acetonitrile (v/v). The flow rate used was 0.35 mL/min. Detection of caffeine was performed at 280 nm.

3.3.6.3 Analysis of Metoprolol

Separation of metoprolol was achieved on an Agilent Zorbax Bonus-RP column (100 x 2.1 mm, 3.5 μm particles). The mobile phase consisted of 25 mM ammonium acetate, adjusted to pH 4.0 with glacial acetic acid, with 10% acetonitrile

(v/v). The flow rate for this system was 0.30 mL/min. Detection of metoprolol was performed at 275 nm.

3.3.7 Data Analysis

3.3.7.1 Determination of Tissue Concentrations from Dialysate Samples

The extracellular concentration (C_{sample}) in each of the studied areas was determined by correcting for the extraction efficiency (EE) of the probe from the concentration analyzed in the dialysate sample ($C_{\text{dialysate}}$) as described in Equation 9 from Section 1.4.2.4.

3.3.7.2 Concentration-Time Curves

Plots of concentration versus time were generated with Microsoft Excel (Redmond, WA, USA) and Microcal OriginLab software version 6.0 (Northampton, MA, USA). To display all probe locations onto a single plot, a semilog plot was generated for each study.

3.3.7.3 Pharmacokinetics Modeling

Pharmacokinetics (PK) parameters for each of the compounds in each of the studied sites were calculated for further affirmation and interpretation of the concentration-time curves. The pharmacokinetics parameters were calculated using WinNonlin version 4.1 software (Pharsight Corporation, Mountain View, CA, USA) with confirmation of some results with Microsoft Excel.

A catenary compartmental model was used to describe the transport of drug from the lumen across the mucosa and submucosa to the blood as described in Figure

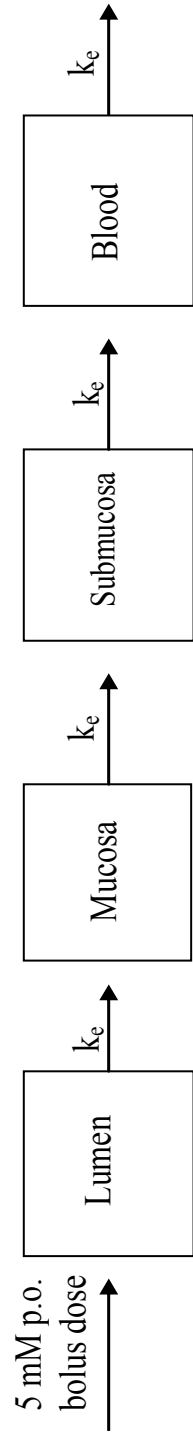


Figure 3.2. Catenary compartmental modeling to describe the transport of drug from the lumen, across the stomach tissue and into the blood after an oral dose. k_e represents the elimination rate constant from each compartment.

3.2 [8-10]. Each box represents a compartment (*i.e.* probe location) and k_e represents the elimination from each compartment (*i.e.* transfer to the next compartment).

To describe the absorption from the lumen, a one-compartment model with bolus input and first order elimination was used. The equation to describe this model is described by Equation 1, which is commonly used to assess disappearance of drug from the lumen:

$$C_{(t)} = \frac{D}{V} e^{-k_e t} \quad (1)$$

where $C_{(t)}$ is the concentration at time t , D is the original dose given, V is the volume of distribution and k_e is the first order transfer rate constant from the lumen [9].

The modeling for the mucosa, submucosa and blood can be described by a one compartment, first-order process shown in Equation 2:

$$C_{(t)} = \frac{Dk_e}{V(k_a - k_e)} \left(e^{-k_e t} - e^{-k_a t} \right) \quad (2)$$

where $C_{(t)}$ is the concentration in the studied area, D is the dose given, V is the volume of distribution and k_a and k_e are the input and output transfer rate constants, respectively [9]. The area under the curve (AUC) was determined by the trapezoidal rule in all modeled areas. Statistical analysis of the PK parameters were performed with Microcal OriginLab software by the one-way analysis of variance (ANOVA)

followed by a Tukey test to determine differences between the studied sites as well as between SA, caffeine and metoprolol in each probe location. A level of $p < 0.05$ was considered statistically different.

3.4 Microdialysis Sampling to Monitor Drug Absorption in the Stomach

3.4.1 HPLC-UV Method Validation

Overall, the HPLC-UV systems exhibited acceptable selectivity, linearity and repeatability for analysis of dialysate samples in both the normal and ulcerated stomach studies. Figure 3.3 is an example chromatogram from mucosal dialysate taken prior to and 15 minutes after a 5 mM oral dose was SA was given by gavage. This figure illustrates acceptable system selectivity for SA in the dialysate sample. The same selectivity was observed with all test compounds in all probe locations for both normal and ulcerated stomach studies. The calibration curves were linear over the range of 1-200 μM with a goodness of fit of 0.99-1. The intra-assay precision was 97% or greater for all calibration curves. The limits of detection (LOD) for SA, caffeine and metoprolol were approximately 200, 100 and 200 nM, respectively, for the HPLC-UV system used for mucosa and submucosa of both ulcerated and normal tissue. The LOD for SA, caffeine and metoprolol were approximately 300, 200 and 600 nM, respectively, for the system used for the lumen and blood samples.

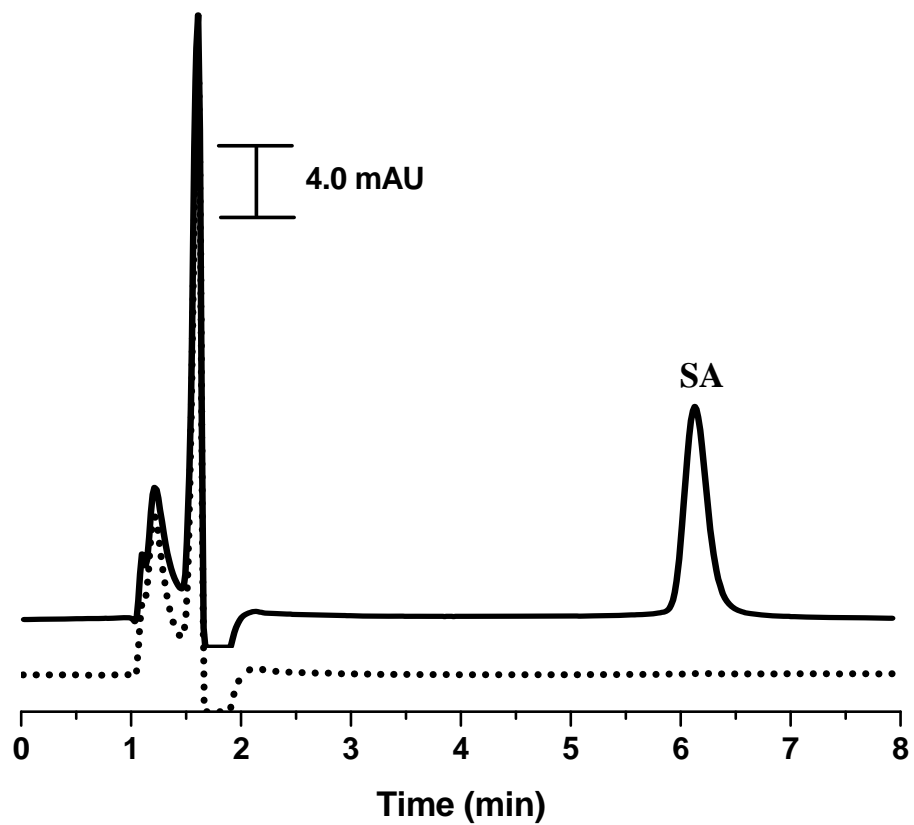


Figure 3.3. Representative chromatogram of SA in mucosa dialysate prior to (dotted) and 15 minutes after (solid) a 5 mM oral dose of SA. The concentration of the SA peak is 31 μM .

3.4.2 Normal Stomach Absorption Studies

Monitoring drug absorption in the normal stomach was performed in order to assess the significance of using microdialysis sampling simultaneously in the stomach lumen, mucosa, submucosa and in the blood. The results of microdialysis sampling by this multiple probe approach from orally dosed SA, caffeine and metoprolol to the ligated stomach are presented in the following section.

3.4.2.1 *In Vivo* Probe Extraction Efficiency

The microdialysis probe EE_d values for the compounds investigated in each probe location are shown in Table 3.2.

Location of Probe	Extraction Efficiency (%)		
	Salicylic Acid	Caffeine	Metoprolol
Lumen	61.8 ± 6.6 (8)	63.0 ± 11.5 (11)	44.2 ± 19.2 (7)
Mucosa	37.9 ± 13.1 (6)	36.3 ± 6.0 (5)	29.7 ± 8.5 (7)
Submucosa	32.7 ± 12.4 (9)	39.4 ± 13.6 (14)	30.8 ± 6.5 (7)
Blood	52.8 ± 12.6 (19)	54.6 ± 13.0 (15)	32.7 ± 7.1 (6)

Table 3.2. EE_d values for multiple probes in the normal rat stomach. Values are average ± standard deviation (n value).

In general, EE_d values between test compounds within each studied region were similar. Higher extraction efficiencies were generally seen in the lumen and blood.

This was expected based on a more hydrodynamic environment around the probes implanted in these areas relative to the stomach tissue, where approximately 30% delivery was determined for both the mucosa and submucosa.

3.4.2.2 Salicylic Acid

SA has been reported to exhibit rapid absorption in the rat stomach [1]. From Table 3.1, the reported pK_a and $\log D$ (pH 2-3) values are 3.0 and 2.06, respectively [2,3]. This indicates that SA is mostly unionized at low pH values (*e.g.* the stomach lumen) and has good lipophilic properties ($\log P > 0$), which are both favorable for passive absorption to occur in the stomach [11,12].

Figure 3.4 shows the semilog plot of the SA concentration determined in the extracellular space as a function of time observed in the lumen, mucosa, submucosa and blood. SA was detected in all of the studied areas in the first 15 minute sample taken. In the lumen, initial high concentrations (mM) were observed that decreased over the course of the experiment. Initially in the first 15 minutes, approximately 100 μM and 40 μM SA was observed in the mucosa and submucosa, respectively. Consistently higher concentrations of SA were observed in the mucosa relative to the submucosa in the first hour of sampling. For both the mucosa and submucosa, the peak concentration was reached by the first 15 minute sample. This indicates that during this sampling experiment, the sampling rate would need to be decreased to describe the absorption phase into the mucosa and submucosa. An absorption phase was seen in the blood that was most likely due to the time needed for diffusion to occur across the stomach tissue and into the systemic circulation.

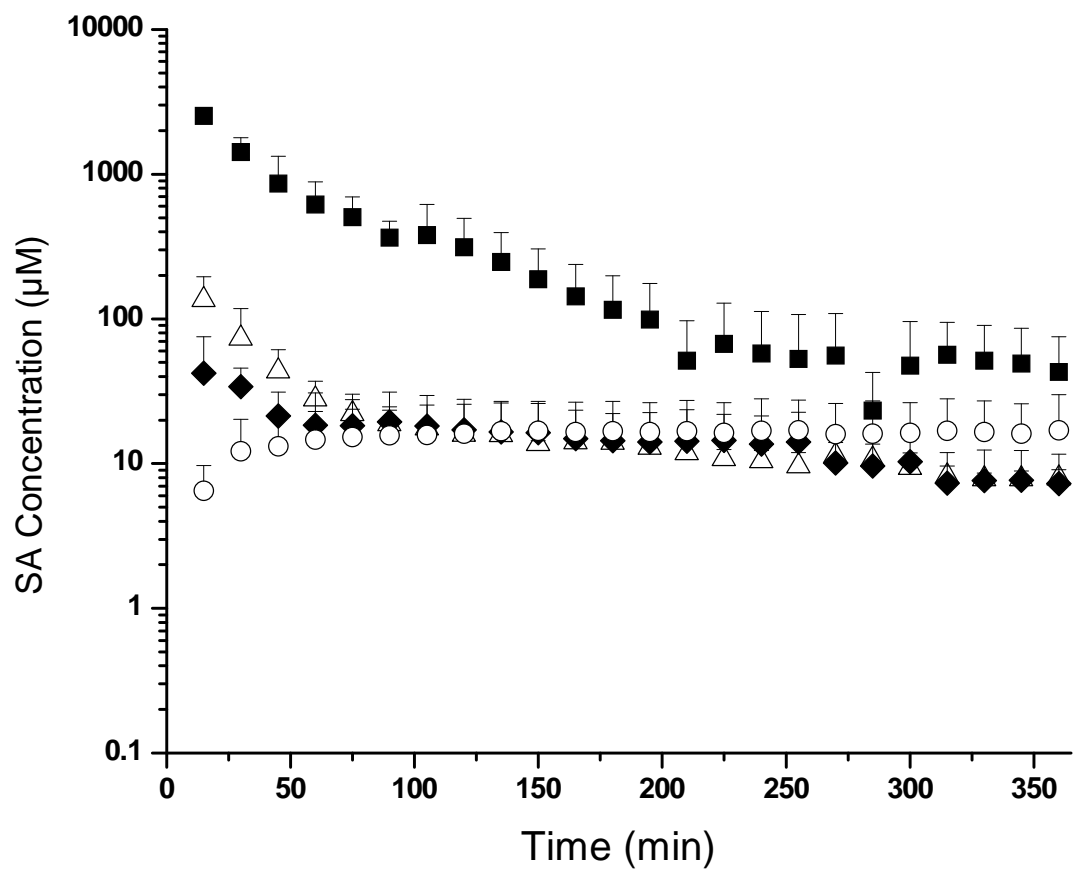


Figure 3.4. Salicylic acid determined from microdialysis sampling in the stomach lumen (■), mucosa (Δ), submucosa (◆) and in blood (○) after a 5 mM SA oral dose (n = 4).

Overall, the profile of rapid decrease in the lumen, the detection of SA in all of the studied areas in the first 15 minutes and the completion of the absorption phase in the stomach tissue prior to the first 15 minute sample indicate that orally dosed SA exhibited rapid absorption in the rat stomach. This was consistent with the predicted extent of absorption for SA in the stomach. Although the profiles were quite similar, higher concentrations in the mucosa relative to the submucosa were observed for the first 1.5 hours of sampling.

3.4.2.3 Caffeine

Caffeine has been reported to exhibit moderate absorption in the stomach and was used as a predicted intermediate absorbing test compound [1]. Based on the pK_a , and log D values of caffeine shown in Table 3.1, caffeine is mostly found in an ionized state in the stomach; however, exhibits an equal distribution between both the lipophilic and aqueous phases ($\log D \sim 0$) [2,3].

Figure 3.5 shows the semilog plot of the caffeine concentration as a function of time after 5 mM caffeine was orally dosed. As previously seen with SA, caffeine was detected in all of the studied areas immediately after administration. Concentrations of caffeine in the lumen steadily decreased over the course of the experiment, but this decrease was slower than that observed with SA (Figure 3.4). In contrast to SA, an absorption phase was observed in the mucosa and submucosa for caffeine. The profiles in the mucosa and submucosa were identical with peak concentrations of approximately 100 μM around 30-45 minutes, whereas small differences were detected between the mucosa and submucosa for the first hour of

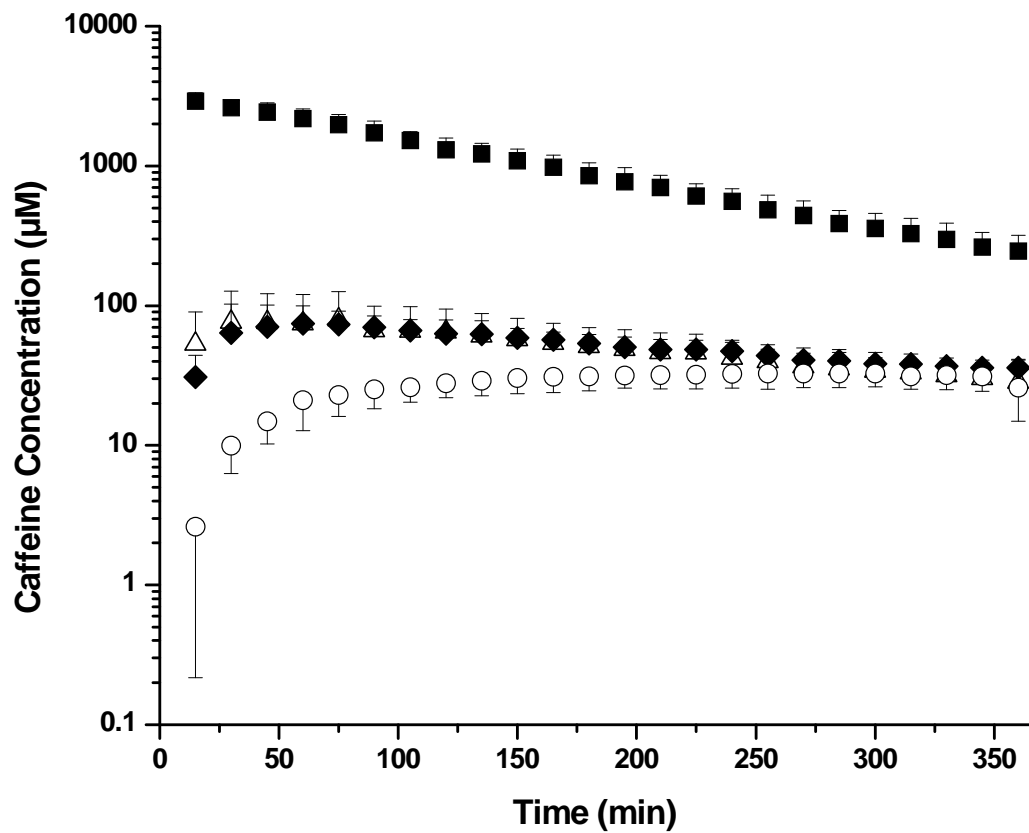


Figure 3.5. Caffeine determined from microdialysis sampling in the normal stomach lumen (■), mucosa (Δ), submucosa (◆) and in blood (○) after a 5 mM SA oral dose (n = 4).

sampling when SA was dosed. Overall, the comparison of the profiles for both SA and caffeine indicate moderate absorption is observed with caffeine.

3.4.2.4 Metoprolol

Metoprolol is reported to have low absorption in the stomach [4]. Based on the physicochemical properties of metoprolol, the drug would mostly be in an ionized state in the stomach. Furthermore, the log D (pH 2-3) value indicates that metoprolol is more aqueous soluble in the low pH stomach lumen and therefore, would not be absorbed to any great extent in the stomach.

The semilog plot of the metoprolol concentration as a function of time after 5 mM metoprolol was orally dosed is shown in Figure 3.6. A steady concentration of metoprolol was observed in the lumen indicating very low absorption of metoprolol through the mucosal barrier in the stomach. Low concentrations of metoprolol (10-15 μM) were observed in the mucosa while metoprolol was not detectable in the dialysate from either the submucosa or the blood. Overall, these observations are again consistent with expectations based on absorption rates relative to SA and caffeine. Differences in the mucosa and submucosa layers are particularly present in this study with metoprolol observed in the mucosa and submucosal concentrations below the LOD.

3.4.2.5 Pharmacokinetics Analysis

Table 3.3 shows the results from modeling each drug for the lumen, mucosa, submucosa and blood. The transfer rate from the lumen (k_e) was faster for SA, then caffeine, and the slowest rate for metoprolol. Additionally, the elimination half-life

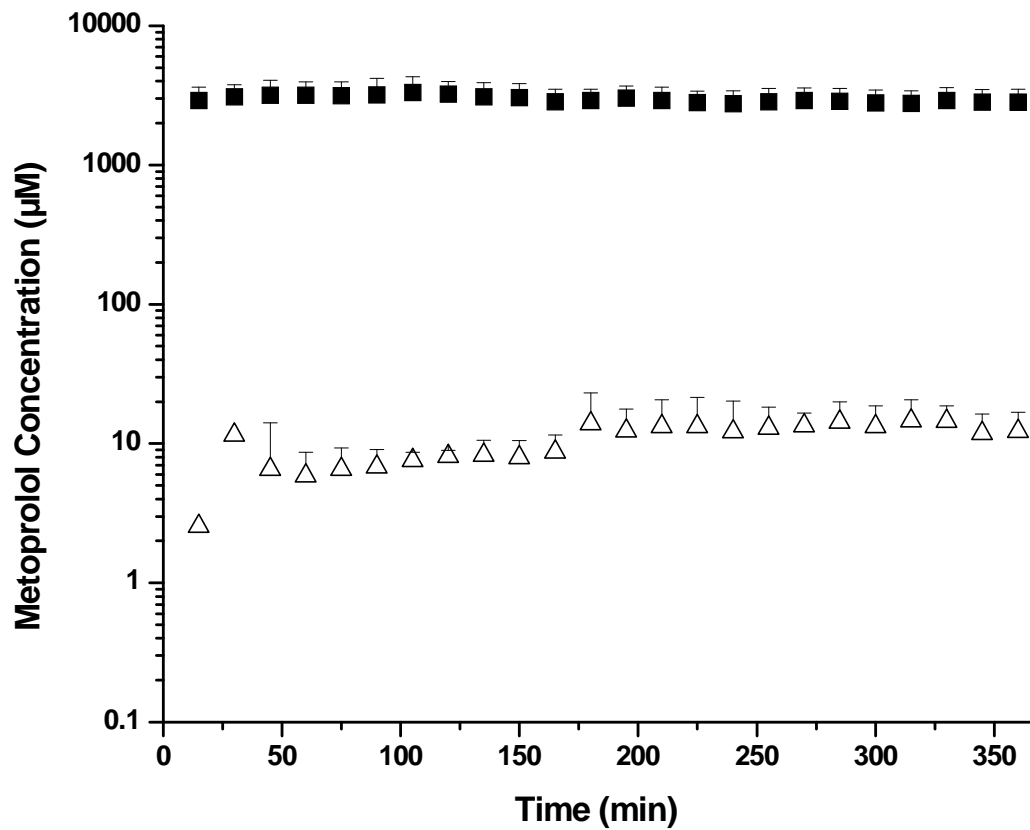


Figure 3.6. Metoprolol determined from microdialysis sampling in the stomach lumen (■) and mucosa (Δ) after a 5 mM SA oral dose (n = 4). No detectable metoprolol was observed in the submucosa or the blood.

		k_e (hr ⁻¹)	$t_{1/2}$ (hr)	C_{max} (μM)	AUC _{0-6 hr} (μM*hr)
Lumen	SA	0.95 ± 0.38	0.42 ± 0.15	3853 ± 670	2227 ± 460
	Caffeine	0.45 ± 0.054	1.57 ± 0.24	3335 ± 518	7499 ± 1400
	Metoprolol	0.024 ± 0.018	51 ± 46	3196 ± 832	93043 ± 859
Mucosa	SA	0.19 ± 0.09	4.40 ± 2.23	142 ± 57	125 ± 24
	Caffeine	0.20 ± 0.17	3.40 ± 1.91	83 ± 43	656 ± 301
	Metoprolol	0.033 ± 0.018	26 ± 17	14 ± 7	497 ± 110
Submucosa	SA	0.114 ± 0.054	8.63 ± 6.26	48 ± 30	88 ± 25
	Caffeine	0.156 ± 0.042	4.50 ± 1.12	78 ± 30	460 ± 117
	Metoprolol ^a	-	-	-	-
Blood	SA	0.0024 ± 0.0018	435 ± 383	20 ± 12	6637 ± 4864
	Caffeine	0.042 ± 0.003	199 ± 15	33 ± 7	1102 ± 851
	Metoprolol ^a	-	-	-	-

^a (-) Indicates no analysis was done; concentrations not detected in these sites

Table 3.3. Pharmacokinetics parameters from the results of microdialysis sampling in the lumen, mucosa, submucosa and blood (n = 4). Values are the average ± standard deviation. Statistical analysis by one-way ANOVA followed by a Tukey test (p <0.05).

($t_{1/2}$) increased from 0.42 hours for SA to 51 hours for metoprolol. Also the area under the curve (AUC) values were SA < caffeine < metoprolol, which further confirmed a faster absorption of salicylic from the lumen than seen with caffeine and metoprolol. The luminal C_{\max} values were very similar for all three compounds as the same dose was given in these studies.

The parameters generated for the mucosa and the submucosa were similar not only from layer to layer but also statistically similar between SA and caffeine. This similarity is evident in the results from SA and caffeine in the mucosa with k_e values around 0.20 hr^{-1} and $t_{1/2}$ values around 4 hours for both compounds. These k_e and $t_{1/2}$ values were also observed in the submucosa when caffeine was dosed. However, in the submucosa after dosing SA, one of the four rats exhibited slower elimination from the submucosa ($k_e = 0.42 \text{ hr}^{-1}$ and $t_{1/2} = 16 \text{ hr}$) resulting in the reported averaged data to be different with larger deviations. No modeling was performed with the metoprolol in the submucosa since the concentrations in that tissue were below the detection limits of the analytical system.

Also, since metoprolol concentrations in the blood were below the LOD for this study, only SA and caffeine were modeled in the blood. The rate of elimination was slow for both compounds but significantly slower with SA ($t_{1/2} = 435 \text{ hrs}$) than with caffeine ($t_{1/2} = 199$) ($p < 0.05$). Similar C_{\max} concentrations were observed with both compounds with this model, but the AUC for SA was higher than caffeine.

In conclusion, the predicted absorption trend of SA > caffeine > metoprolol was observed by microdialysis sampling in the normal stomach, indicating the current

sampling method is successful in monitoring the extent of drug absorption. For SA and caffeine, small differences between drug concentrations in the mucosa and submucosa were observed. With dosed metoprolol, this difference was significant since 10-15 μM was observed in the mucosa while metoprolol was below the detection limits (200 nM) in the submucosa. Differences from microdialysis sampling in the tissue layers were observed relative to blood, which supports the benefits of site-specific monitoring in the stomach tissue. Overall, the results indicate that microdialysis sampling in the stomach by a multiple probe design is a more representative sampling method for monitoring drug absorption in the normal stomach.

3.4.3 Ulcerated Stomach Absorption Studies

As described in Section 2.6.2, a multiple probe microdialysis sampling approach was developed to directly compare healthy and diseased tissue in the same stomach. Site-specific ulceration was chemically induced by injection of 20% acetic acid (v/v) directly into the submucosa. Subsequently, microdialysis probes were simultaneously implanted in the stomach lumen and submucosa of both ulcerated and normal tissue and also in the blood. As previously described in Section 2.6.2.1, the ulcers were measured to be 30-40 mm^2 on average, as determined by measuring the ulcer index (length x width) [13]. However, due to ulcer perforation, a modification to the induction method was performed. Coating the ulcer with lubricant during the ulcer induction period decreased perforation, but resulted in smaller ulcers of

approximately 15-20 mm². This resulted in the ability to control ulcer size for monitoring absorption as a function of ulcer size.

To assess the significance of this microdialysis sampling approach, drug absorption of the three previously tested compounds, SA, caffeine and metoprolol, was monitored in both the large and small ulcerated stomach using multiple probe microdialysis sampling. The results are presented in the following sections.

3.4.3.1 *In Vivo* Extraction Efficiency

The microdialysis probe EE_d values for each compound studied in each probe location for both large and small ulcer stomachs are displayed in Table 3.4. Even though the environment at the ulcerated tissue is affected by the lack of mucosa to

		Extraction Efficiency (%)		
Probe Location		Salicylic Acid	Caffeine	Metoprolol
Large Ulcers	Lumen	67.5 ± 4.7	42.0 ± 1.6	37.2 ± 5.9
	Submucosa of Ulcer	23.9 ± 11.1	31.7 ± 3.4	19.4 ± 2.7
	Normal Submucosa	23.8 ± 3.2	36.7 ± 8.7	20.7 ± 0.45
	Blood	40.9 ± 11.3	43.6 ± 2.6	34.8 ± 4.9
Small Ulcers	Lumen	61.3 ± 4.8	39.2 ± 9.2	44.1 ± 15.0
	Submucosa of Ulcer	23.7 ± 11.6	31.7 ± 3.3	33.3 ± 10.4
	Normal Submucosa	14.2 ± 2.4	33.4 ± 8.1	24.3 ± 5.8
	Blood	40.9 ± 13.2	36.8 ± 12.1	30.1 ± 15.6

Table 3.4. EE_d values for multiple probes in the ulcerated rat stomach. Values are average ± standard deviation (n = 3 for each value for large ulcers and n = 4 for small ulcers).

protect it from the luminal environment, the EE_d values between the normal and the ulcerated submucosal tissue are not significantly different indicating the submucosa is still intact in the ulcer. In addition, the EE_d values were comparable to what was previously determined in the normal stomach studies (Table 3.2).

3.4.3.2 Salicylic Acid

Large Ulcer - Figure 3.7 demonstrates the SA concentration in the stomach lumen, in the submucosa of the ulcer and normal tissue and in the blood after a 5 mM SA oral bolus dose was administered to a ligated rat stomach with a large gastric ulcer. High concentrations of SA were initially observed in the lumen and the concentration decreased over the course of the experiment. This profile was similar to lumen concentrations previously observed in the normal stomach studies (Figure 3.4). In addition, an identical profile and the same concentrations were determined in the submucosa of the ulcerated tissue relative to the lumen, suggesting that without the mucosal barrier present, luminal SA surges non-selectively into the ulcerated tissue. Rapid absorption was also seen in the normal, healthy submucosa and in the blood with profiles similar to what was previously observed in the normal stomach studies. By comparison of the submucosal probes, the concentration of drug in the ulcerated tissue was significantly higher than that in the normal submucosa, initially 50-fold higher in the ulcerated tissue which decreased over time to a 2-fold difference towards the end of the experiment.

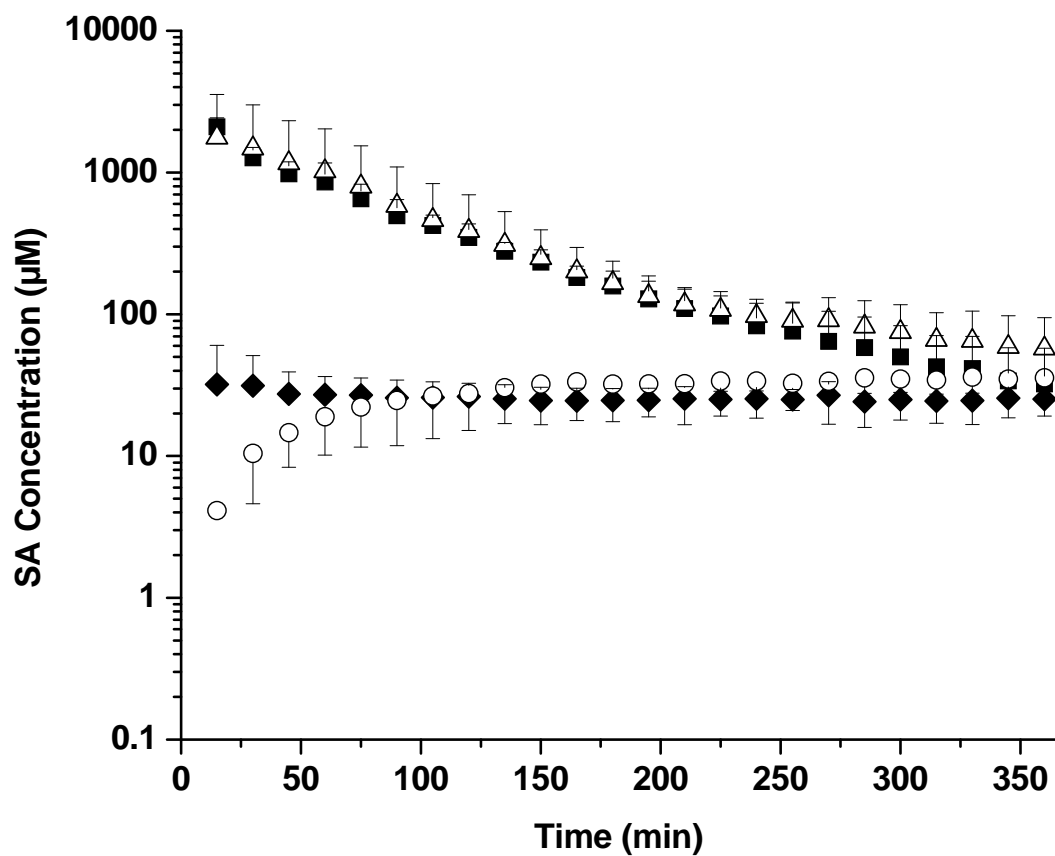


Figure 3.7. Salicylic acid determined from microdialysis sampling in the large ulcerated stomach lumen (■), submucosa of the ulcer (Δ), normal submucosa (◆) and in blood (○) after a 5 mM SA oral dose (n = 3).

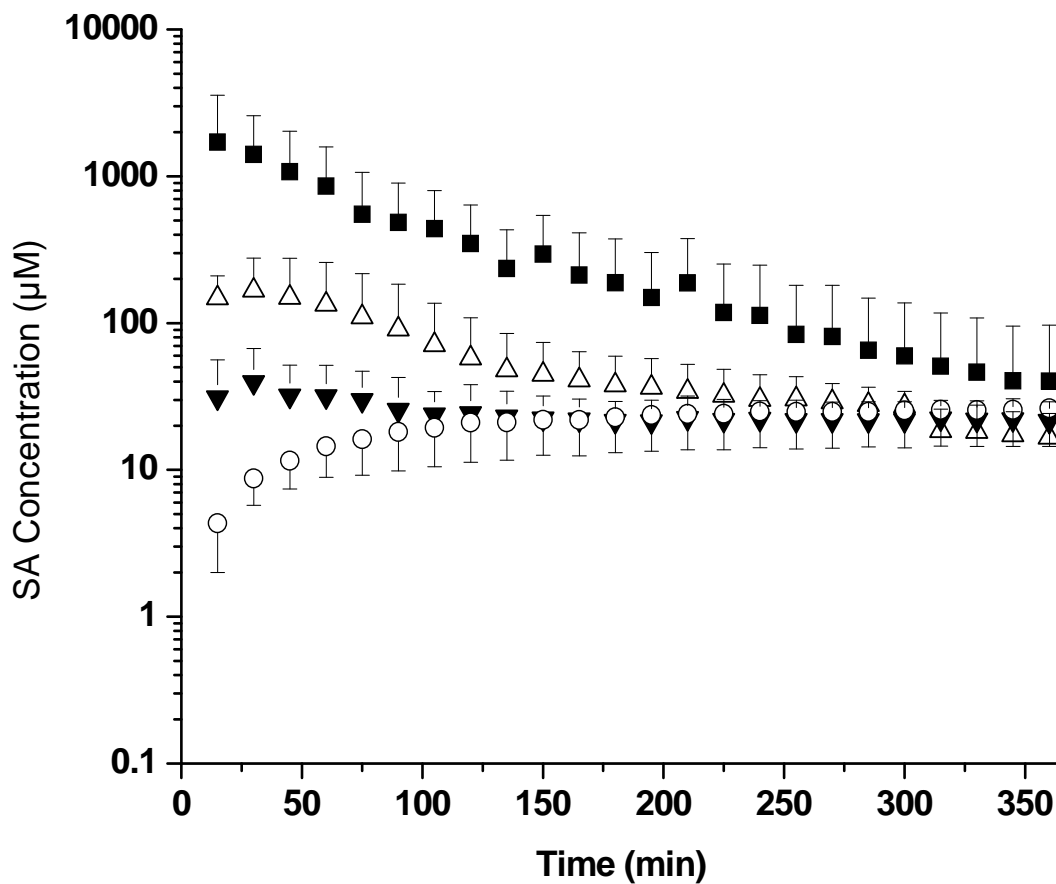


Figure 3.8. Salicylic acid determined from microdialysis sampling in the small ulcerated stomach lumen (■), submucosa of the ulcer (Δ), normal submucosa (▼) and in blood (○) after a 5 mM SA oral dose (n = 3).

Small Ulcer - Figure 3.8 shows the SA concentration as a function of time in the stomach lumen, submucosa of ulcerated and normal tissue and in blood after a 5 mM SA oral bolus dose was administered to rats with a small gastric ulcer. In comparison to Figure 3.7, the profiles for the lumen, normal submucosa and blood were the same. The concentrations in the ulcerated tissue were consistently greater in this tissue relative to the normal submucosa; however, the difference between these two tissue types was significantly greater in the large ulcer than in the small ulcer. This suggests that absorption in the ulcerated tissue is a function of ulcer size with increased absorption in larger relative to smaller ulcers.

3.4.3.3 Caffeine

Large Ulcer - Figure 3.9 shows the caffeine concentration as a function of time after 5 mM caffeine was orally dosed in stomachs with a large ulcer. Caffeine was detected in all of the studied areas in the first 15 minute sample. The concentration of caffeine in the lumen, normal submucosa and blood were similar to what was observed previously in the normal stomach studies (Figure 3.5). Higher concentrations of caffeine were observed in the ulcerated tissue relative to normal; however, in comparison to SA (Figure 3.7), less absorption was observed in the ulcerated tissue relative to normal tissue when caffeine was administered.

Small Ulcer - Figure 3.10 shows the PK curves for caffeine in the lumen, ulcerated and normal submucosa and in blood after a 5 mM caffeine oral bolus dose was administered in rat stomachs with a small ulcer induced. The profiles in the lumen, normal submucosa and blood are similar to what was observed in the large

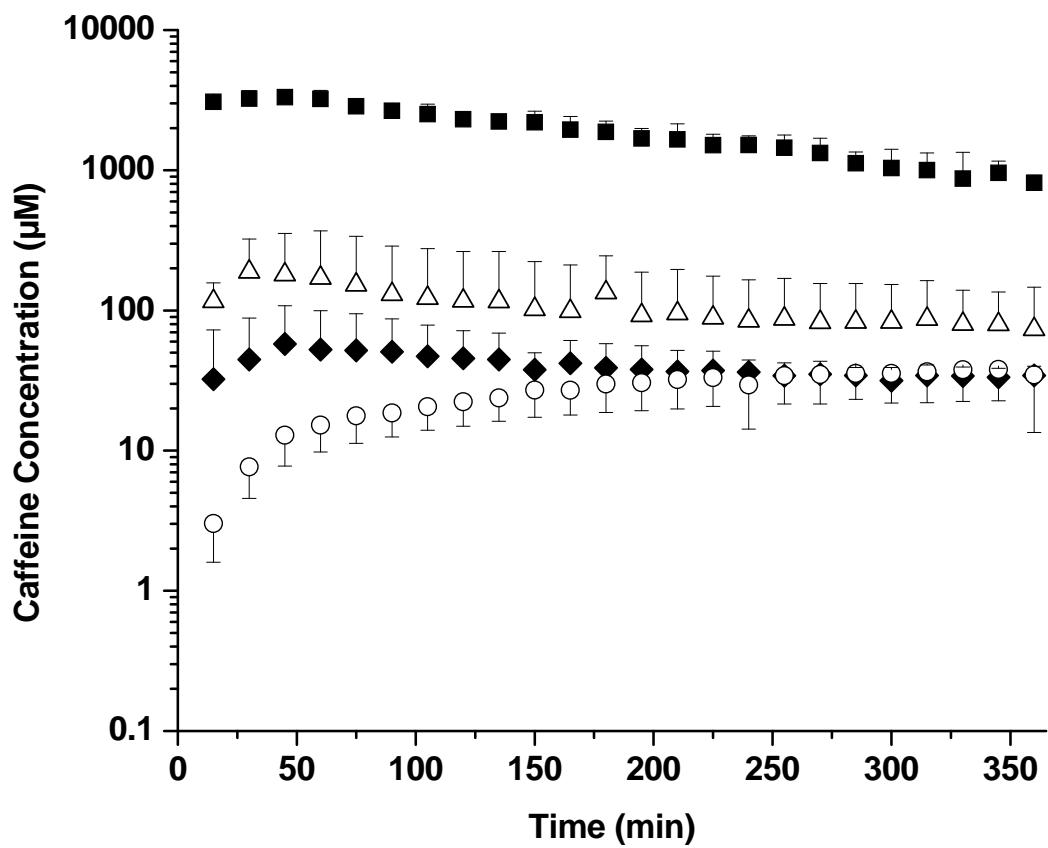


Figure 3.9. Caffeine determined from microdialysis sampling in the large ulcerated stomach lumen (■), submucosa of the ulcer (Δ), normal submucosa (◆) and in blood (○) after a 5 mM SA oral dose (n = 3).

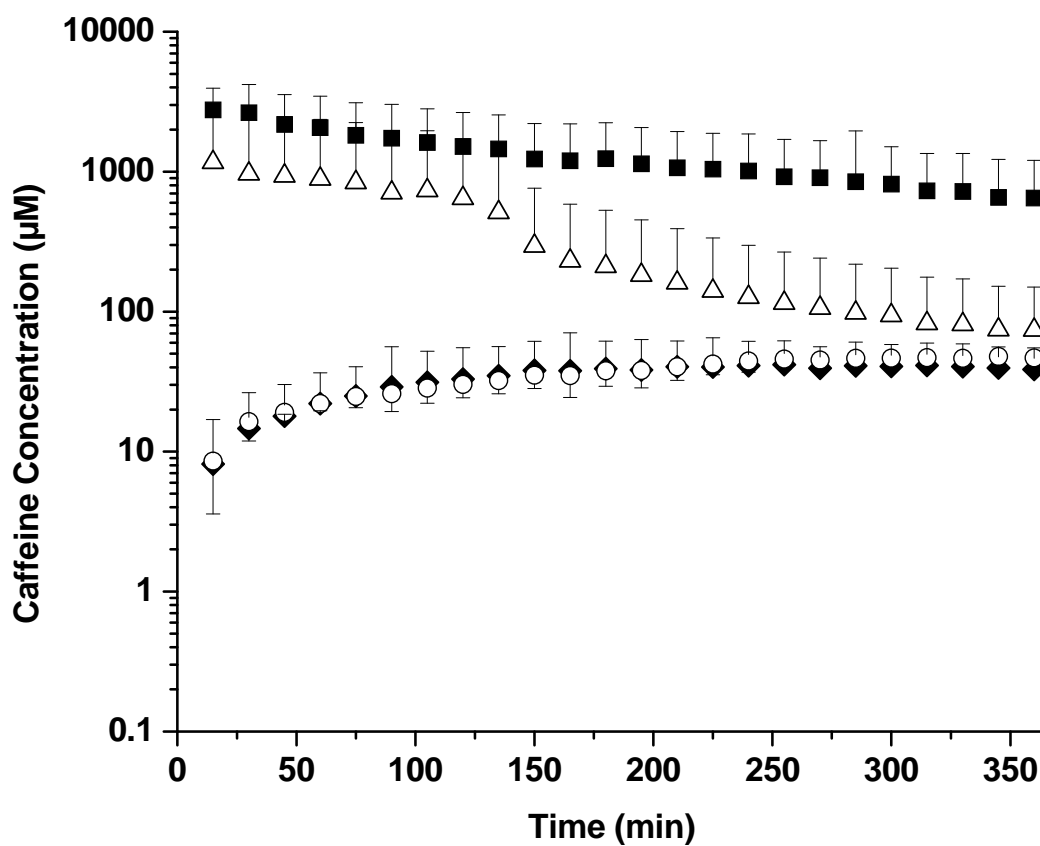


Figure 3.10. Caffeine determined from microdialysis sampling in the small ulcerated stomach lumen (■), submucosa of the ulcer (Δ), normal submucosa (◆) and in blood (○) after a 5 mM SA oral dose (n = 3).

ulcer study (Figure 3.9). Surprisingly, the average concentration in the ulcerated submucosa of the small ulcer was greater than the average concentration in the large ulcer. The probable cause of this is the extremely high concentrations obtained in one of the three rats used for this set of experiments in contrast to the remaining two rats, which were similar to normal submucosa concentrations were observed. Figure 3.11 describes the results of caffeine determined in the ulcerated submucosa from each individual rat that contributed to the average data represented in Figure 3.10. As illustrated, one rat had initial concentrations of approximately 3 mM in comparison to the other two rats where concentrations of caffeine were observed to be 500 and 10 μ M. The contribution of the one rat with millimolar concentrations resulted in the average biased towards this rat.

Further investigation of this unexpected increased concentration for this one rat was performed by examination of the histology slices of the three rats. Figure 3.12 shows the histology results from two of the rats used to generate Figure 3.11. Figure 3.12a corresponds to the results depicted as \blacktriangle in Figure 3.11, with high concentrations of caffeine observed in the ulcerated tissue. Figure 3.12b corresponds to the results depicted as \circ in Figure 3.11. As illustrated, when the probe was implanted in the ulcerated tissue at a depth closer to the lumen, high concentrations were observed in the ulcerated tissue. However, when the probe was implanted in ulcerated tissue closer to the serosal surface (*i.e.* more superficial), lower concentrations were observed. Also noted was the difference in ulcer thickness. The ulcer in Figure 3.12a is 500 μ m in comparison to Figure 3.12b, which is 1100 μ m.

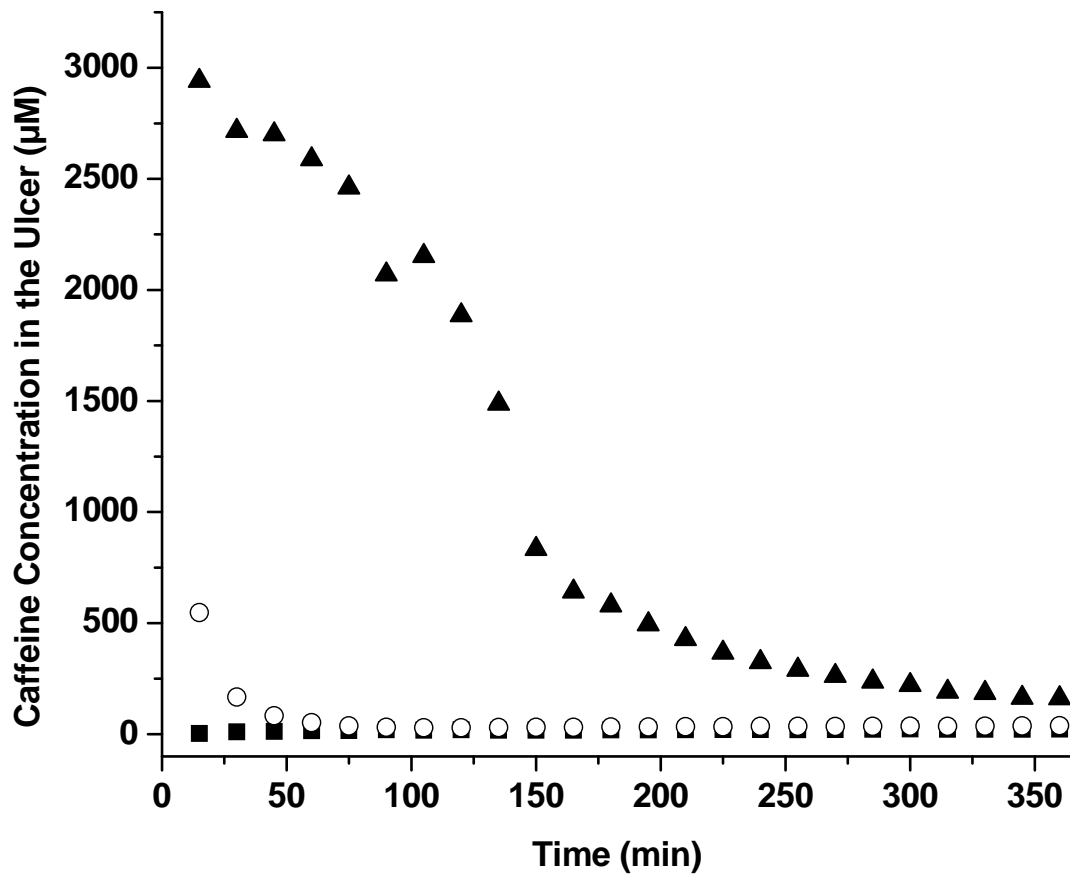


Figure 3.11. Individual curves of caffeine concentrations determined in the ulcerated submucosa in the small ulcer stomach. These three curves were averaged to give the resulting ulcerated submucosa curve in Figure 3.10.

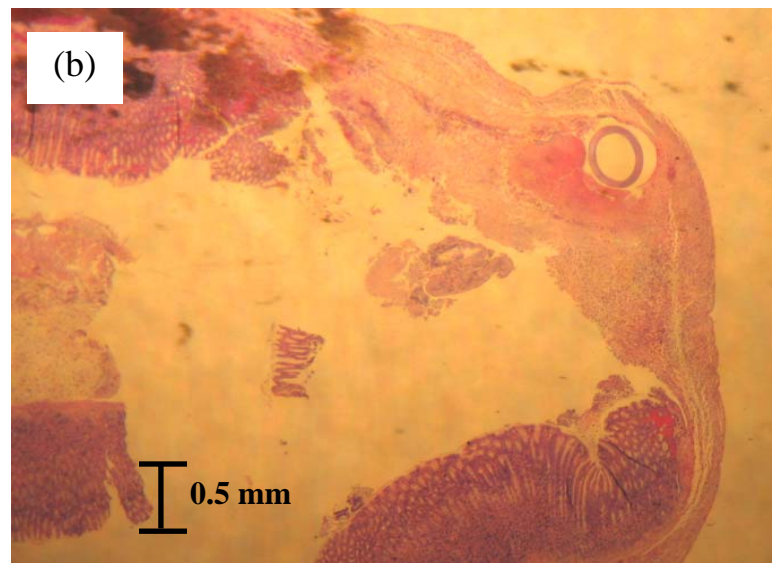
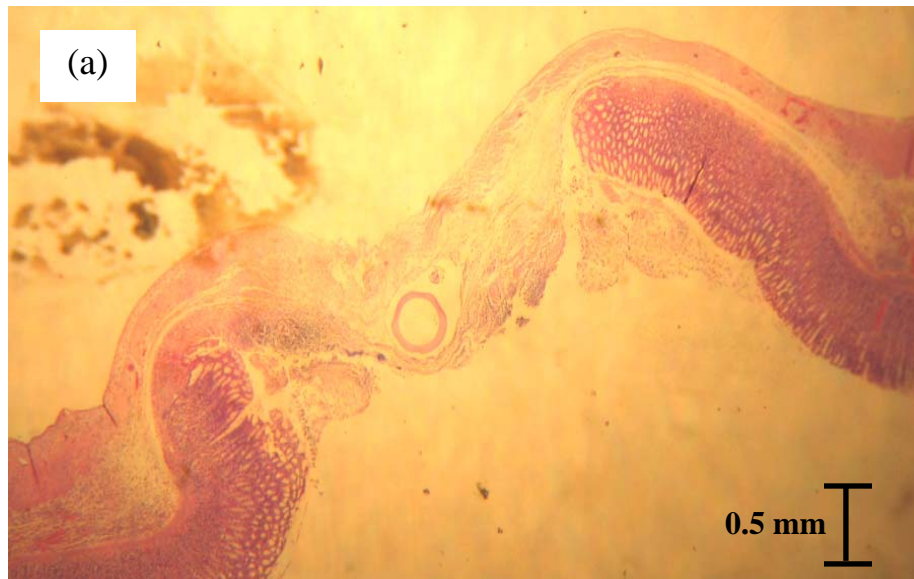


Figure 3.12. Histology slides of two difference ulcers. (a) Thinner ulcer with the probe implanted in the ulcer but closer to the lumen and (b) Thicker ulcer with the probe implanted in the ulcer but closer to the serosa. Images at 20x magnification.

Therefore, the results obtained suggest that increased concentrations in ulcerated submucosa tissue relative to normal tissue were as a result of decreased ulcer layer thickness and probe location within the submucosa, but closer to the luminal side.

3.4.3.4 Metoprolol

Large Ulcer - Figure 3.13 shows the plot of metoprolol concentration as a function of time after 5 mM metoprolol was dosed orally in a large ulcer study. A steady concentration of drug was observed in the lumen indicating minimal absorption from the stomach, as previously characterized in the normal stomach studies (Figure 3.6). The concentration in the submucosa of the ulcerated tissue showed concentrations similar to the luminal concentration, and also remained steady throughout the course of the experiment. In contrast to the normal stomach studies where metoprolol was not detected in the submucosa or blood, one of the three rats used in this study had detectable concentrations of metoprolol in the normal submucosa and in the blood. The other two rats had no detectable metoprolol in either the normal submucosa or the blood, similar to the normal stomach studies (Figure 3.6). The histology results gave no indication of differences in this experiment relative to other submucosal implantations. Since metoprolol was only detected in these locations in one rat, it was suggested that the appearance of metoprolol in these site were not due to natural absorption events, but rather experimental errors such as unintentional penetration of the guide needle into the mucosal tissue during submucosa probe implantation, which may not be visible histologically.

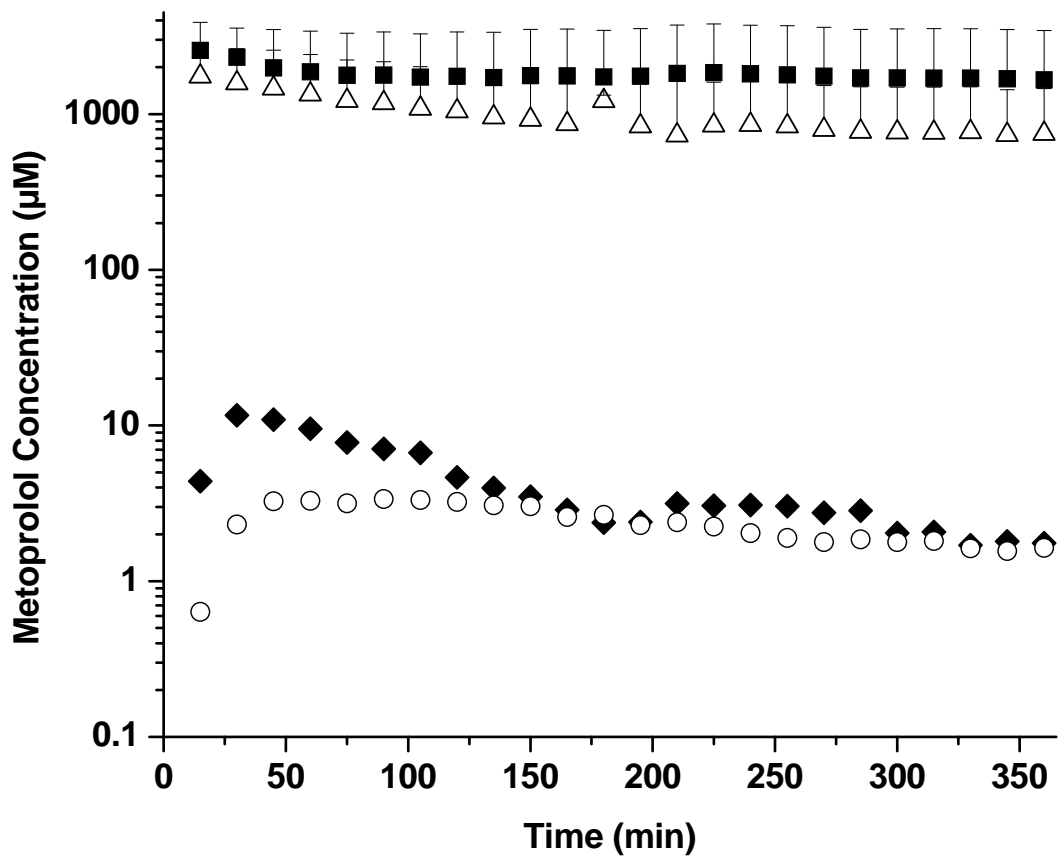


Figure 3.13. Metoprolol determined from microdialysis sampling in the large ulcerated stomach lumen (■), submucosa of the ulcer (Δ), normal submucosa (◆) and in blood (○) after a 5 mM SA oral dose (n = 3). Only one of the three rats had detectable metoprolol in both the normal submucosa and the blood.

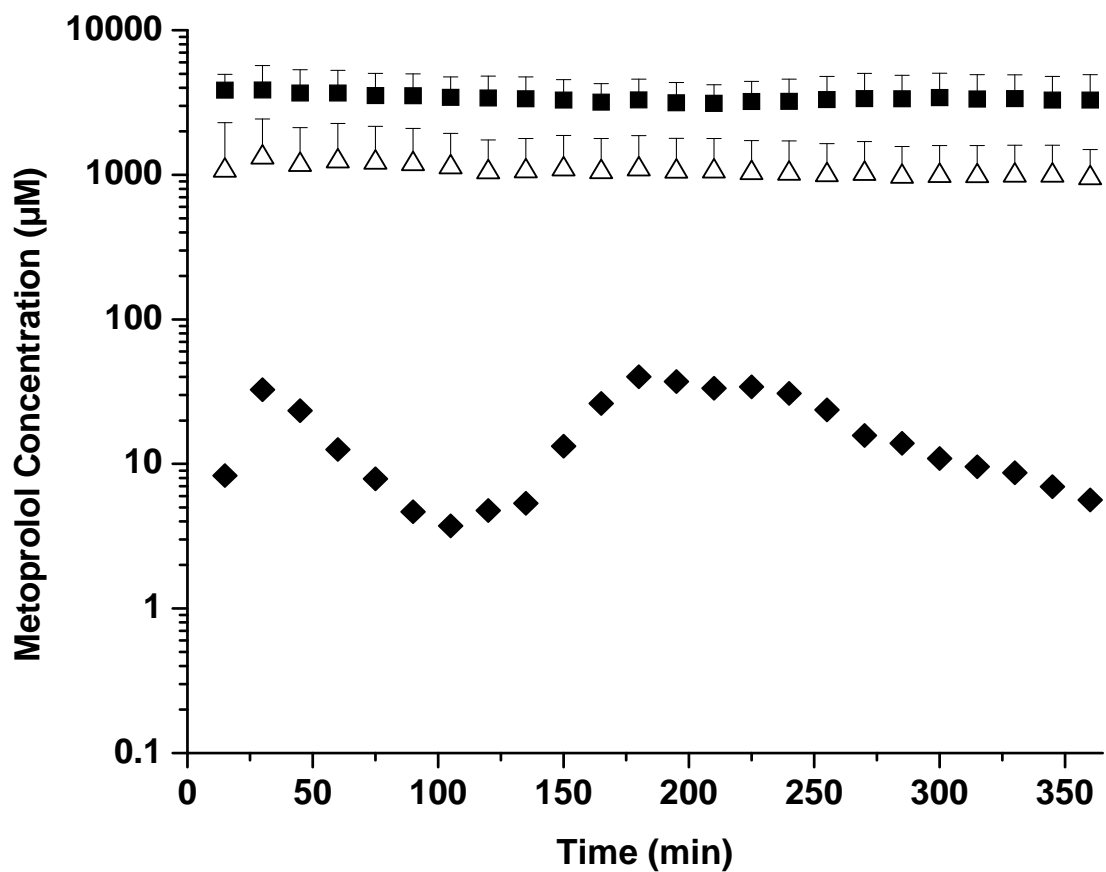


Figure 3.14. Metoprolol determined from microdialysis sampling in the small ulcer stomach lumen (■), submucosa of the ulcer (Δ), normal submucosa (◆) after a 5 mM SA oral dose (n = 3). Only one of the three rats had detectable metoprolol in the normal submucosa. All rats had no detectable metoprolol in the blood.

Small Ulcer – Figure 3.14 shows the plot of the metoprolol concentration in the stomach lumen, ulcerated and normal submucosa and in the blood after a 5 mM metoprolol oral bolus dose administered in rat stomachs with small ulcers induced. Higher concentrations closer to luminal concentrations were again observed in the ulcerated tissue. As with the large ulcer study, the unpredicted detection of metoprolol was observed in the normal submucosa of one of the three rats of this study. In contrast to the previous study, no metoprolol was detected in the blood for all experiments. The histology slides were further investigated to understand the source of metoprolol in the normal submucosa. For the small ulcer study, it is suggested that the appearance of metoprolol in the normal submucosa may be the result of the proximity of the probe implanted in the normal tissue to the ulcerated tissue. As presented in Figure 3.15, damage to the submucosa extended farther than was visible from the serosal side. In this case, although the probe was implanted in normal, healthy submucosal tissue, concentrations detected in the dialysate may be influenced by the adjacent ulcerated tissue. Because the body region of the stomach is limited by surface area, it may be challenging to avoid this problem with a multiple probe approach within the same tissue layer of the same region of the stomach. Although this may explain the appearance of metoprolol in the normal submucosa of this study, this does not appear to be the cause of the appearance of metoprolol in the large ulcer study. Further studies to determine the cause of the apparent non-native absorption of metoprolol to the normal submucosa would need to be performed.

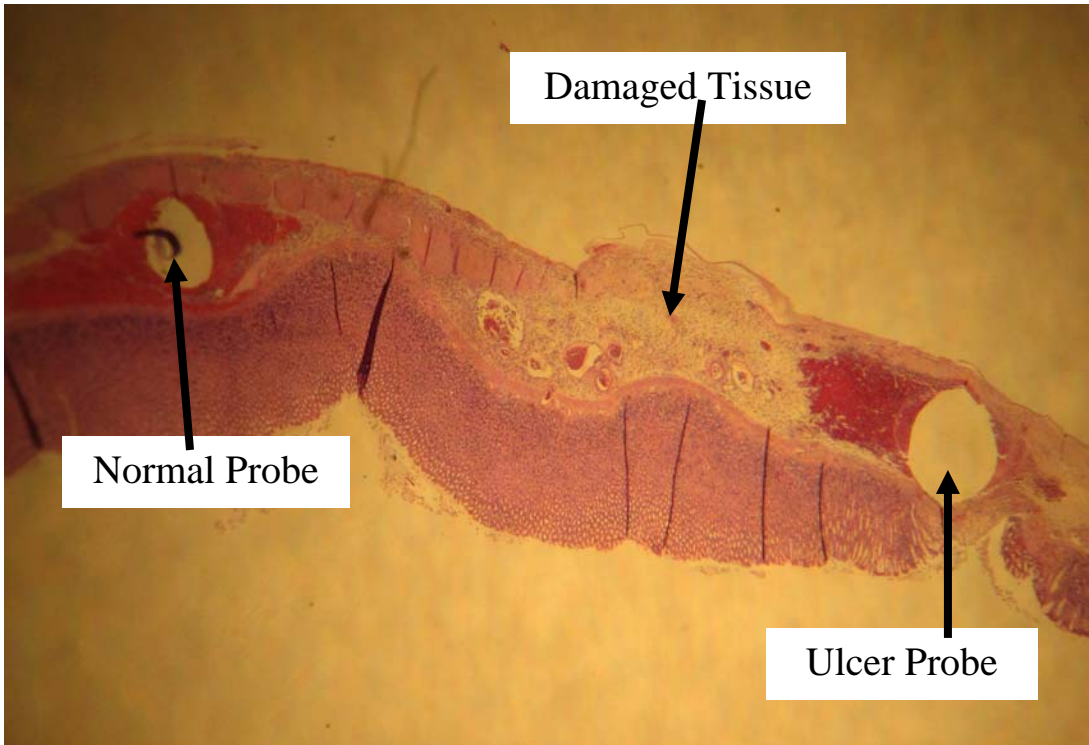


Figure 3.15. Histology image showing the proximity of a normal submucosal probe to ulcerated tissue. Image at 20x magnification.

3.4.3.5 Pharmacokinetics Analysis

Table 3.5 shows the PK parameters calculated for absorption through large ulcers and Table 3.6 shows the PK parameters calculated for the absorption through small ulcers. The transfer rate constants observed in the lumen for both large and small gastric ulcers were in the order SA > caffeine > metoprolol (for large ulcers; $k_{SA} = 0.75$; $k_{\text{caffeine}} = 0.25$; $k_{\text{metoprolol}} = 0.15 \text{ hr}^{-1}$ and for small ulcers $k_{SA} = 0.75$; $k_{\text{caffeine}} = 0.32$; $k_{\text{metoprolol}} = 0.021 \text{ hr}^{-1}$). A similar trend was observed in the k_e values for the ulcerated submucosa for both sizes of ulcers. Smaller k_e values were observed in the normal submucosal tissue and very slow elimination was observed in the blood. In most cases, high C_{max} values were determined in the lumen and ulcerated submucosa (1-3 mM) and lower values were observed in the normal submucosa and in the blood (7-45 μM) suggesting differences are seen in the ulcerated submucosa and normal submucosa. However, this is not confirmed statistically because no statistically significant differences were observed between the large and small ulcers when comparing each studied site for each compound ($p < 0.05$).

In conclusion, microdialysis sampling by a multiple probe approach can successfully be used to directly compare normal and ulcerated tissue in the same animal. It was expected that without the protective mucosal barrier present in ulcerated tissue, enhanced absorption in the ulcerated tissue would occur. The results of this study were in agreement with enhanced absorption observed in the ulcerated tissue relative to normal tissue. The concentrations in the lumen, normal submucosa and blood were comparable with what was determined in the previous study in

		k_e (hr ⁻¹)	$t_{1/2}$ (hr)	C_{max} (μM)	AUC _{0-6 hr} (μM*hr)
Lumen	SA	0.75 ± 0.32	0.78 ± 0.11	2123 ± 718	2310 ± 503
	Caffeine	0.25 ± 0.06	3.02 ± 0.85	3745 ± 85	16318 ± 4483
	Metoprolol	0.15 ± 0.16	9.85 ± 8.3	2575 ± 1330	16395 ± 12945
Ulcerated Submucosa	SA	0.57 ± 0.39	1.00 ± 0.39	2241 ± 2457	2682 ± 2303
	Caffeine	0.19 ± 0.02	3.80 ± 0.71	273 ± 132	2063 ± 291
	Metoprolol	0.18 ± 0.11	4.33 ± 1.97	1830 ± 519	11210 ± 10125
Normal Submucosa	SA	0.023 ± 0.016	65 ± 74	38 ± 23	2659 ± 1656
	Caffeine	0.10 ± 0.12	29 ± 36	57 ± 36	1328 ± 1614
	Metoprolol ^a	0.35	1.30	11.60	26.25
Blood	SA	0.031 ± 0.023	16.04 ± 2.89	36 ± 17	3069 ± 3045
	Caffeine	0.0049 ± 0.0034	311 ± 300	40 ± 17	23123 ± 23315
	Metoprolol ^a	0.186	3.12	3.29	20.5

^a Concentrations only detectable in one of three rats.

Table 3.5. Pharmacokinetics parameters from the results of microdialysis sampling from the lumen, submucosa of normal and ulcerated tissue and blood in large ulcer studies (n = 3). Values are the average ± standard deviation. Statistical analysis by one-way ANOVA followed by a Tukey test (p < 0.05).

		k_e (hr ⁻¹)	$t_{1/2}$ (hr)	C_{max} (μM)	$AUC_{0-6\text{ hr}}$ (μM*hr)
Lumen	SA	0.75 ± 0.26	0.64 ± 0.48	2121 ± 1776	2452 ± 1919
	Caffeine	0.32 ± 0.17	2.21 ± 1.55	2968 ± 1189	10909 ± 8908
	Metoprolol	0.021 ± 0.028	213 ± 304	3606 ± 1441	380022 ± 335039
Ulcerated Submucosa	SA	0.35 ± 0.23	1.61 ± 0.78	204 ± 132	394 ± 260
	Caffeine	0.34 ± 0.28	11.41 ± 11.62	2000 ± 1689	3822 ± 4239
	Metoprolol	0.034 ± 0.044	16.15 ± 21.70	1774 ± 871	10942 ± 13714
Normal Submucosa	SA	0.030 ± 0.019	14.27 ± 8.51	36 ± 14	1067 ± 1388
	Caffeine	0.051 ± 0.082	102 ± 91	44 ± 18	3300 ± 2281
	Metoprolol ^a	0.47	1.93	20	155
Blood	SA	0.0074 ± 0.0093	409 ± 543	22 ± 14	1420 ± 172
	Caffeine	0.025 ± 0.021	99 ± 84	45 ± 2	4341 ± 120
	Metoprolol ^b	-	-	-	-

^aConcentrations only detectable in one of three rats.

^b (-) indicates no modeling done since no concentrations were detected.

Table 3.6. Pharmacokinetics parameters from the results of microdialysis sampling from the lumen, submucosa of normal and ulcerated tissue and blood in small ulcer studies (n = 3). Values are the average ± standard deviation. Statistical analysis by one-way ANOVA followed by a Tukey test (p <0.05).

normal stomachs. Additionally, from these studies, it was concluded that absorption is a function of ulcer size in that larger ulcers resulted in more drug concentration determined in the tissue. However, larger variations were observed with this study relative to the normal stomach studies, which may be a function of probe location within the ulcer, the ulcer layer thickness and proximity of probes implanted in different tissue types.

3.4.4 Submucosal Probe Implantation Effects on Absorption

The submucosa houses the major blood vessels responsible for systemic uptake of drugs dosed to the GI tract. During the microdialysis probe implantation procedure, there is some damage to small blood vessels adjacent to the probe. Although precautions are taken to avoid probe implantation through blood vessels that are visible from the serosal side of the stomach, small blood vessels can be torn during implantation and small amounts of blood pooling in the submucosal layer can occur. Histologically, this is shown as dark red areas in the submucosa. Since probe implantation causes local damage to the blood vessels, studies were performed to see if probe implantation results in changes to overall systemic drug absorption. This was assessed by comparing drug concentration in the blood of rats with and without linear probes implanted into the submucosa. In one set of animals, a linear probe was implanted into the stomach lumen and a vascular probe was implanted in the blood. The mucosa and submucosa remained intact without any probes implanted to perturb the tissue. Caffeine was dosed orally (5 mM bolus dose via gavage tube) to the

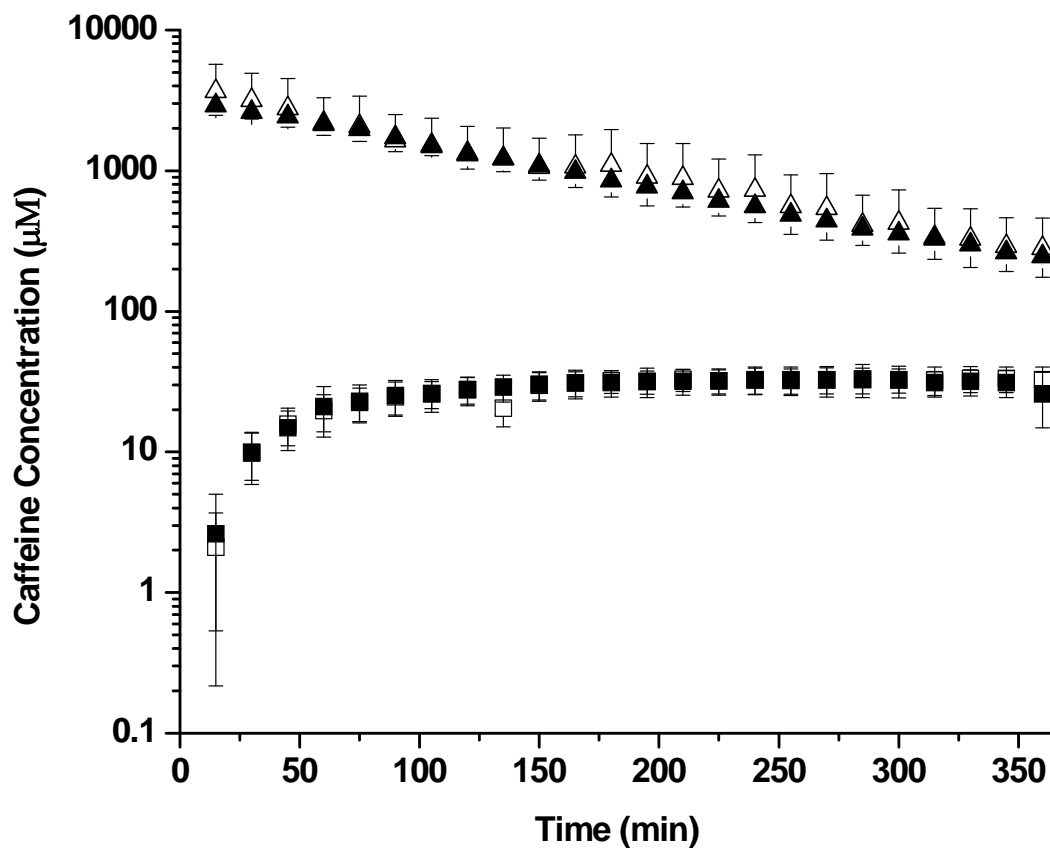


Figure 3.16. Submucosal probe implantation effects on drug absorption. Triangles and squares are lumen and blood caffeine concentrations, respectively. Open symbols are experiments from the two probe design ($n = 2$) and closed symbols are from the four probe design ($n = 4$).

anesthetized rat with stomachs ligated at the cardiac and pyloric sphincters to contain the dose in the stomach. The results from this study were compared with experiments where linear microdialysis probes were implanted in the stomach lumen, mucosa and submucosa and a vascular probe implanted in the blood with the same 5 mM caffeine oral dose to the ligated stomach (Figure 3.5). The results of the two groups of animals were compared and are shown in Figure 3.16. Even though there is local blood vessel damage in the submucosa during probe implantation, the results of these experiments indicate that implanting probes in the mucosa and submucosa do not affect the overall systemic drug absorption of caffeine into the systemic circulation. This was shown in the similarities of the blood concentrations. The concentrations in the lumen were used as a marker to indicate that the same dose was given for both sets of experiments.

3.4.5 Bi-directional Flow of Analyte Through the Tissue

As previously mentioned, it is widely accepted that drug transport occurs from the lumen, across the mucosa and into the submucosa for systemic uptake. Preliminary studies using microdialysis sampling in the stomach were performed to test the bi-directionality of the stomach tissue. For this research, high concentrations (5 mM) were dosed to the lumen. Therefore, the observed luminal concentrations would mask small changes in concentration due to the return of analyte to the lumen. The bi-directional transport of analyte across the stomach tissue was studied by Doluisio *et al.* [14]. It was reported that an intravenous (i.v.) dose of 1.5-5 times the

amount placed in the lumen resulted in no more than 5 % of the i.v. dose detected in the lumen by the *in situ* closed loop method.

To test the significance of bi-directional flow of analyte in the stomach, linear microdialysis probes were positioned in the stomach lumen and submucosa and a vascular probe was implanted in the jugular vein. A cannula was inserted into the femoral vein and a 20 mg/kg i.v. bolus dose of SA in saline was administered through the cannula. This dose was 2 times the oral dose of SA given in the orally dosed experiments, as will be discussed further in the next section. Table 3.7 shows the tabulated results of drug concentration calculated in the lumen, submucosa and blood post dose.

Time (min)	Concentration of SA (μM)			Ratio (%)	
	Lumen	Submucosa	Blood	Lumen:Dose	Submucosa:Dose
15	1.03	68.60	238.27	0.016	10.98
30	BLQ	69.73	208.65	ND	11.16
45	BLQ	77.87	205.41	ND	12.47
60	BLQ	78.14	189.54	ND	12.51
75	BLQ	75.71	179.37	ND	12.12
90	BLQ	72.61	184.00	ND	11.63
			Average	ND	11.81

BLQ = below the limits of quantitation

ND = not determined

Table 3.7. Microdialysis sampling study of bi-directional flow of SA across the stomach tissue after a 20 mg/kg i.v. bolus SA dose.

As demonstrated, this study was in support of less than 5% of the i.v. dose detected in the lumen, but also demonstrated 12% of the dose was present in the submucosa. The

results indicate that SA will diffuse from the blood into the stomach tissue. It is suggested that SA would penetrate into the lumen, but would be diluted to undetectable concentrations by the gastric solution. Linear probes were not successfully implanted in the mucosa for this study. However, based on the results from this study, it is predicted that a similar appearance of SA would be observed in the mucosa as was demonstrated in the submucosa since no significant transport barrier is present between the mucosa and submucosa. Further studies to determine the significance of bi-directional drug transport across the mucosa would be to include linear probes in the mucosa to further assess this importance.

3.4.6 Advantages and Disadvantages to this Approach

Overall, microdialysis sampling by a multiple probe approach to monitor drug absorption was successful for monitoring concentrations in the stomach lumen, mucosa, submucosa and blood in the normal, healthy stomach and in the lumen, submucosa of both ulcerated and healthy tissue and finally in the blood of an ulcerated stomach model. The advantages and disadvantages of this approach will be discussed in the following sections.

3.4.6.1 Advantages

Since the stomach is a heterogeneous tissue, the ability to site-specifically monitor the mucosa and submucosa simultaneously with this microdialysis sampling was achieved. This four-probe approach of microdialysis sampling simultaneously in the stomach lumen, mucosa, submucosa and in blood has not previously been

reported in literature and provides more accurate sampling in the stomach. The microdialysis probes are sufficiently small (350 μm o.d.) to be implanted in the mucosa and submucosa separately. This is an improvement over the current use of microdialysis sampling in the stomach, which is only performed in the submucosa. Typically, blood sampling is used to monitor drug absorption in the GI tract. The results of this research indicate differences in tissue concentration relative to blood were observed, which strengthens the need for this sampling technique to evaluate the drug concentrations in the stomach tissue.

In addition, differences in normal and diseased tissue can be observed with microdialysis sampling. A four-probe microdialysis sampling approach in the stomach lumen and submucosa of normal and ulcerated tissue and in the blood has not been previously reported in literature. Traditionally, excised ulcerated stomach tissues would be compared to control normal excised stomach tissue from a different animal. By monitoring diseased and healthy tissue of the same stomach, inherent biological variation is decreased by using one animal for the entire sampling period, whereas excised tissue studies require multiple animals and therefore results in increased study variability.

3.4.6.2 Disadvantages

This multiple probe approach to monitoring drug concentrations in the stomach also has limitations. The stomach tissue layers are approximately 500-700 μm thick. Therefore, a “skilled” surgeon is required to implant microdialysis probes into each tissue layer. Also, because of the limited surface area of the stomach,

proper probe spacing to limit cross-communication of tissue types may be challenging. Additionally, although the this approach to microdialysis sampling was demonstrated to be successful for in-depth drug absorption studies for SA, caffeine and metoprolol, this technique is not suitable for quick drug screening.

In the current ulcerated model, the ulcer must be visible on serosal surface to successfully implant a microdialysis probe into the intact tissue. The current ulcer induction model results in the increased probability of ulcer perforation because the muscularis externa can also become damaged during ulcer induction. This ulcer induction method resulted in ulcers that vary in tissue thickness and size, which along with probe location in the tissue caused increased variability within the study; however, this variability did not affect the ability to compare ulcerated and normal tissue in the same stomach. Even though there are some limitations with this technique, overall, this multiple probe approach is successful in providing more detailed information relative to traditional techniques of sampling from the stomach.

3.5 Conclusions

Overall, microdialysis by a multiple probe approach can be used to successfully monitor drug concentrations simultaneously in the stomach lumen, mucosa, and submucosa and in blood. By dosing test compounds with known degrees of absorption in the rat stomach, the method followed the expected trend of SA exhibiting rapid absorption, caffeine resulting in moderate and metoprolol

demonstrating low absorption in the stomach. Small differences were observed between the mucosa and submucosa for dosed SA and caffeine, but a greater difference was observed in metoprolol with concentrations of 10-15 μM in the mucosa and no detectable metoprolol in the submucosa (LOD 200 nM). In addition to monitoring different tissue layers, this multiple probe approach could successfully be utilized to directly compare normal and ulcerated tissue. In general, drug absorption was increased in the ulcerated tissue relative to normal tissue. This increase was determined to be a function of ulcer size and thickness and probe location within the ulcer.

3.6 References

- [1] Schanker, L. S.; Shore, P. A.; Brodie, B. B.; Hogben, C. A. M., Absorption of drugs from the stomach I. The rat. *Journal of Pharmacology and Experimental Therapeutics* **1957**, 120, (4), 528-539.
- [2] SciFinder Scholar™ 2006.
- [3] Clarke's Isolation and Identification of Drugs. In Moffat, A. C.; Jackson, J. V.; Moss, M. S.; Widdop, B., Eds. The Pharmaceutical Press: London, 1986.
- [4] Domenech, J.; Alba, M.; Morera, J. M.; Obach, R.; Pla Delfina, J. M., Gastric, intestinal and colonic absorption of metoprolol in the rat. *British Journal of Clinical Pharmacology* **1985**, 19 Suppl 2, 85S-89S.
- [5] CDER *Guidance for Industry: Bioanalytical Method Validation*; U.S. Food and Drug Administration: Rockville, MD, 2001.
- [6] Peters, F. T.; Drummer, O. H.; Musshoff, F., Validation of new methods. *Forensic Science International* **2007**, 165, (2-3), 216-224.
- [7] Steele, K. L.; Scott, D. O.; Lunte, C. E., Pharmacokinetic studies of aspirin in rats using in vivo microdialysis sampling. *Analytica Chimica Acta* **1991**, 246, 181-186.
- [8] Choi, Y. M.; Chung, S. M.; Chiou, W. L., First-pass accumulation of salicylic acid in gut tissue after absorption in anesthetized rat. *Pharmaceutical Research* **1995**, 12, (9), 1323-1327.
- [9] Shargel, L.; Yu, A. B. C., *Applied Biopharmaceutics & Pharmacokinetics*. New York, 1999.
- [10] Gallo, J. M., Pharmacokinetics: model structure and transport systems. *Clinical Research & Regulatory Affairs* **2001**, 18, (3), 235-266.
- [11] Lee, V. H. L.; Yang, J. J., Oral drug delivery. In *Drug Delivery and Targeting for Pharmacists and Pharmaceutical Scientists*, Hillery, A. M.; Lloyd, A. W.; Swarbrick, J., Eds. Taylor & Francis: New York, 2001; pp 145-183.
- [12] Waterbeemd, H. v. d., Intestinal permeability: prediction from theory. In *Oral Drug Absorption Prediction and Assessment*, Dressman, J. B.; Lennernäs, H., Eds. Marcel Dekker, Inc.: New York, 2000; Vol. 106, pp 31-49.

- [13] Fukawa, K.; Kawano, O.; Misaki, N.; Uchida, M.; Irino, O., Experimental studies on gastric ulcer. (4). Sequential observation and evaluation of gastric ulcers by endoscope in the rat. *Japanese Journal of Pharmacology* **1983**, 33, (1), 175-179.
- [14] Doluisio, J. T.; Billups, N. F.; Dittert, L. W.; Sugita, E. T.; Swintosky, J. V., Drug absorption. I. An in situ rat gut technique yielding realistic absorption rates. *Journal of Pharmaceutical Sciences* **1969**, 58, (10), 1196-200.

CHAPTER FOUR

Summary and Future Directions of Multiple Probe Microdialysis

Sampling in the Stomach

4.1 Summary of the Presented Research

Due to the heterogeneity of the stomach tissue, microdialysis sampling by implantation of a single probe into a tissue cannot accurately reflect sampling from the stomach. Observable differences between the tissue layers would be expected. Current uses of microdialysis sampling in the stomach include implanting a probe in the submucosa and monitoring analytes such as histamine release from the ECL cells in the mucosa [1-4]. Multiple probe microdialysis sampling in the mucosa and submucosa simultaneously would serve as an improvement to current methods of microdialysis sampling in the stomach. In addition, the use of a multiple probe approach with microdialysis sampling would enhance studies by allowing for the direct comparison of different tissue types in the same animal. This would effectively

reduce biological variability so small differences between these tissue types may be observed.

4.1.1 Implantation of Multiple Microdialysis Probes in the Rat Stomach

Implantation in the Normal Stomach. Chapter Two presented a multiple probe approach of microdialysis sampling in the normal stomach to sample different tissue layers. This was achieved by implanting probes simultaneously in the stomach lumen, mucosa and submucosa and in the blood. Initially, it was determined that the average tissue layer thickness of the mucosa and submucosa in the female Sprague-Dawley rat stomach were 700 and 500 μm , respectively. Therefore, it was established that the small outer diameter microdialysis probe (350 μm) would be sufficient to achieve sampling from separate layers once implanted into each layer. Successful methods of implanting linear microdialysis probes in the stomach lumen, mucosa and submucosa were achieved by the use of a 25-gauge hypodermic needle that served as a guide. Due to the sub-millimeter thickness of each tissue layer, the needle was implanted into the intact tissue using the visual difference of the implanted guide into each layer. Since probe implantation in the mucosa has not previously been reported in literature, tissue response to probe implantation was studied by harvesting stomach tissue at different time points and histologically examining tissue slices stained by hematoxylin and eosin. Over a 12-hour period, no significant tissue response to probe implantation was observed in both the mucosa and submucosa. More importantly, the histology results confirmed that methods of

simultaneously implanting microdialysis probes in the normal stomach lumen, mucosa, and submucosa and in blood were successful by this implantation method.

Implantation into the Ulcerated Stomach. In addition to multiple probe implantation procedures in the normal stomach, Chapter Two presented methods of multiple probe microdialysis sampling in the ulcerated stomach to sample different tissue types. This was achieved by implanting probes into the stomach lumen, submucosa of both ulcerated and normal tissue and in the blood of rats with a gastric ulcer induced. Induction was achieved by injection of 20% acetic acid (v/v) into the stomach submucosa [5]. The resulting ulcers were visible on the serosal side and had an ulcer index of approximately 30-40 mm². However, due to the fragile nature of the tissue, perforation of the ulcer upon probe implantation occurred with this method. To circumvent perforation, the ulcer was coated with lubricant during the induction and formation period. With the lubricant, less perforation of the ulcer was observed, but the ulcer index values decreased to 15-20 mm². The procedure for probe implantation into the ulcerated tissue was similar to described methods in the normal stomach. Examination of the tissue slices indicated that overall, microdialysis probes were successfully implanted simultaneously into the stomach lumen and submucosa of both ulcerated and normal tissue and in the blood.

4.1.2 Multiple Probe Microdialysis Sampling to Monitor Drug Absorption in the Stomach

Absorption in the Normal Stomach. Chapter Three presented studies to test the significance of a multiple probe microdialysis sampling in different tissue layers by monitoring drug absorption *in vivo* in the rat stomach. Salicylic acid (SA), caffeine and metoprolol were chosen as test compounds whose extent of absorption in the rat stomach have previously been studied [6,7]. The results of microdialysis sampling in the stomach were compared with the predicted absorption rates to determine the utility of this sampling technique. A 5 mM dose of test compound dissolved in artificial gastric solution was given to the anesthetized rat by oral gavage to fasted, ligated rat stomachs with microdialysis probes implanted in the stomach lumen, mucosa and submucosa and in blood. Concentrations-time curves and pharmacokinetics (PK) modeling from each probe location indicated that the expected trend of absorption, SA > caffeine > metoprolol, was observed by this multiple probe approach. Analytes were observed in all of the studied areas in the first 15 minute sample taken from all probe locations when SA and caffeine were dosed. Metoprolol in the submucosa and blood were below the limits of detection (LOD) for the 6 hour sampling period. Consistently higher concentrations were observed in the mucosa relative to the submucosa. This was particularly evident in the metoprolol studies where detectable concentrations were observed in the mucosa but concentrations were below detection limits in the submucosa. In all studies, the determined concentrations in both the mucosa and submucosa were significantly different than concentrations observed in the blood, which strengthens the application of this site-specific technique over traditional methods to study drug absorption such as blood sampling.

Based on the results, it was concluded that this multiple probe approach was successful to monitor drug concentrations in the different stomach tissue layers in the normal stomach.

Ulcerated Stomach Absorption. In addition to drug absorption studies in the normal stomach, Chapter Three presented research to study the significance of a multiple probe approach to directly compare drug absorption in both ulcerated and normal tissue of the same rat when both large and small gastric ulcers were induced. The previously dosed compounds SA, caffeine and metoprolol, were used for the ulcerated stomach studies to compare the results to the normal stomach studies. The same trend in the extent of absorption was observed in these studies showing rapid absorption of SA, moderate absorption of caffeine, and low absorption of metoprolol for both large and small ulcerated stomach studies. Overall, more absorption was observed in the ulcerated tissue relative to the normal submucosal tissue. Concentrations observed in the lumen, normal submucosa and blood were identical to what was observed in the normal stomach studies. Differences were also observed when comparing large and small ulcerated tissue. Higher drug concentrations were generally observed in the large ulcerated tissue relative to the small ulcer suggesting absorption is a function of ulcer size with increased absorption in larger ulcers. In general, more variation was observed with the ulcerated stomach studies relative to normal stomach studies, which was concluded to be a factor of ulcer size, tissue thickness and probe location within the ulcer. Even with this increased variation, overall, the results indicate that this multiple probe microdialysis approach was both

successful and significant to directly monitor drug absorption in ulcerated and normal tissue.

4.2 Future Directions of This Research

4.2.1 Continuation of Drug Absorption Studies in the Stomach

Future work of this research includes the continuation of the current studies by extending the range of analytes tested. Currently, three test compounds with different degrees of passive absorption in the stomach have been studied with this technique. To illustrate the use of microdialysis sampling in stomach drug absorption studies, the range and classes of compounds would need to be extended. This may aid in the determination of why caffeine absorption in the ulcerated tissue did not exhibit the expected trend of significantly increased absorption in the ulcerated tissue. By advancing this technique to several other analytes, it may be determined if the majority of moderate absorbing compounds exhibit the same absorption characteristics as caffeine.

Along with dosing compounds individually in drug development studies, this sampling technique can be further used to monitor drug concentrations in the stomach tissue in the presence of another drug or study the effects of excipients on drug absorption for formulation studies.

4.2.2 Extension of a Multiple Probe Approach in the Intestines

It is well known that absorption primarily occurs in the small intestines, therefore, extension of microdialysis sampling as a site-specific technique in the intestines would be valuable in drug absorption studies. Based on the anatomy of the small intestines, possible challenges with the implantation of microdialysis probes in the intestines relative to the stomach are the increased number and amplitude of the folds and microvilli present in the mucosa of the intestines and also the decreased surface area available for probe implantation. Initial optimization of a microdialysis sampling in the stomach indicates that transition of a similar approach would be successful. Ultimately, microdialysis probes can then be implanted in several locations throughout the GI tract to assess the extent and location of drug absorption. This offers a more complete understanding of drug absorption during development studies relative to the traditional sampling methods described in Chapter One.

4.2.3 Utilization of Multiple Probe Microdialysis Sampling in Awake Animals

The drug absorption studies presented in this research were performed on anesthetized rats. This is not representative of circumstances under which drugs are administered. Future use of this multiple probe microdialysis sampling technique into awake, conscious animals would augment the utility of the technique. In awake animal studies, the added dimension of physiological factors affecting drug absorption (*e.g.* presence of food and transit times) would be challenging in the assessment of drug absorption, but would be more representative of drug absorption

in the GI tract. Awake animal studies increases the chance of tissue tearing at the probe implantation site due to animal movement and peristalsis of the GI tract; however, studies of microdialysis sampling in stomach submucosa of awake rats has previously been achieved [2].

4.2.4 Enhancement of the Current Uses of Microdialysis Sampling in the Stomach

As previously mentioned in Section 4.1, microdialysis sampling has been performed in the stomach to monitor ECL cell histamine release in the mucosa by a probe implanted into the submucosa. To more accurately quantify histamine concentrations in the stomach tissue and circumvent the issue of degradation of histamine during diffusion to the sampling site, the methods of multiple probe microdialysis sampling presented in this research can be used. The results from this method can be compared to previous histamine studies with the addition of information from sampling in the mucosa layer.

4.2.5 Examination of Endogenous Compounds in Relation to GI Disease

Microdialysis sampling in the GI tract may be used to study analytes involved in ulcer formation in both gastric and duodenal ulcers. With microdialysis probes implanted in the mucosa and submucosa, an enhanced understanding of the chemistry involved during ulcer formation may be possible. Due to the potential of sampling for extended time periods, microdialysis sampling may be used to monitor analytes in

ulcerated tissue over the course of weeks from the same animal to improve the understanding of the mechanisms involved during ulceration and healing. In addition, microdialysis sampling is useful for sampling several analytes simultaneously within the tissue for a comparison of several markers of disease. Finally, this sampling technique may be extended to study the underlying mechanisms involved in other diseases of the GI tract.

4.3 References

- [1] Bernsand, M.; Hakanson, R.; Norlen, P., Tachyphylaxis of the ECL-cell response to PACAP: receptor desensitization and/or depletion of secretory products. *British Journal of Pharmacology* **2007**, 152, (2), 240-248.
- [2] Ericsson, P.; Norlen, P.; Bernsand, M.; Alm, P.; Hoglund, P.; Hakanson, R., ECL cell histamine mobilization studied by gastric submucosal microdialysis in awake rats: methodological considerations. *Pharmacology & Toxicology* **2003**, 93, (2), 57-65.
- [3] Norlen, P.; Ericsson, P.; Kitano, M.; Ekelund, M.; Hakanson, R., The vagus regulates histamine mobilization from rat stomach ECL cells by controlling their sensitivity to gastrin. *Journal of Physiology* **2005**, 564, (Pt 3), 895-905.
- [4] Kitano, M.; Norlen, P.; Hakanson, R., Gastric submucosal microdialysis: a method to study gastrin- and food-evoked mobilization of ECL-cell histamine in conscious rats. *Regulatory Peptides* **2000**, 86, (1-3), 113-123.
- [5] Takagi, K.; Okabe, S.; Saziki, R., A new method for the production of chronic gastric ulcer in rats and the effect of several drugs on its healing. *Japanese Journal of Pharmacology* **1969**, 19, (3), 418-426.
- [6] Domenech, J.; Alba, M.; Morera, J. M.; Obach, R.; Pla Delfina, J. M., Gastric, intestinal and colonic absorption of metoprolol in the rat. *British Journal of Clinical Pharmacology* **1985**, 19 Suppl 2, 85S-89S.
- [7] Schanker, L. S.; Shore, P. A.; Brodie, B. B.; Hogben, C. A. M., Absorption of drugs from the stomach I. The rat. *Journal of Pharmacology and Experimental Therapeutics* **1957**, 120, (4), 528-539.